MATMOS Test-bed OCS cell spectra from 2012-04-11

MATMOS Test-bed Team
Jet Propulsion Laboratory
California Institute of Technology
May 21, 2012

Measurement Conditions:

2012-04-11: Glowbar source. 0.5mm InSb detector.

EDU running at 2.0s per scan.

Raw t-domain interferograms (laser & InSb) sampled by Virtex5/AD7760-based data acquisition system (described by Bekker et al. 2008) at 625 kHz.

Acquired ~4 samples per laser wavelength.

Interferograms re-sampled, phase-corrected, and FFT'd into spectra by Jean-Francois Blavier's Fortran code.

Pairs of spectra were averaged and used in subsequent plots.

EDU installed in MATMOS Test-Bed at JPL

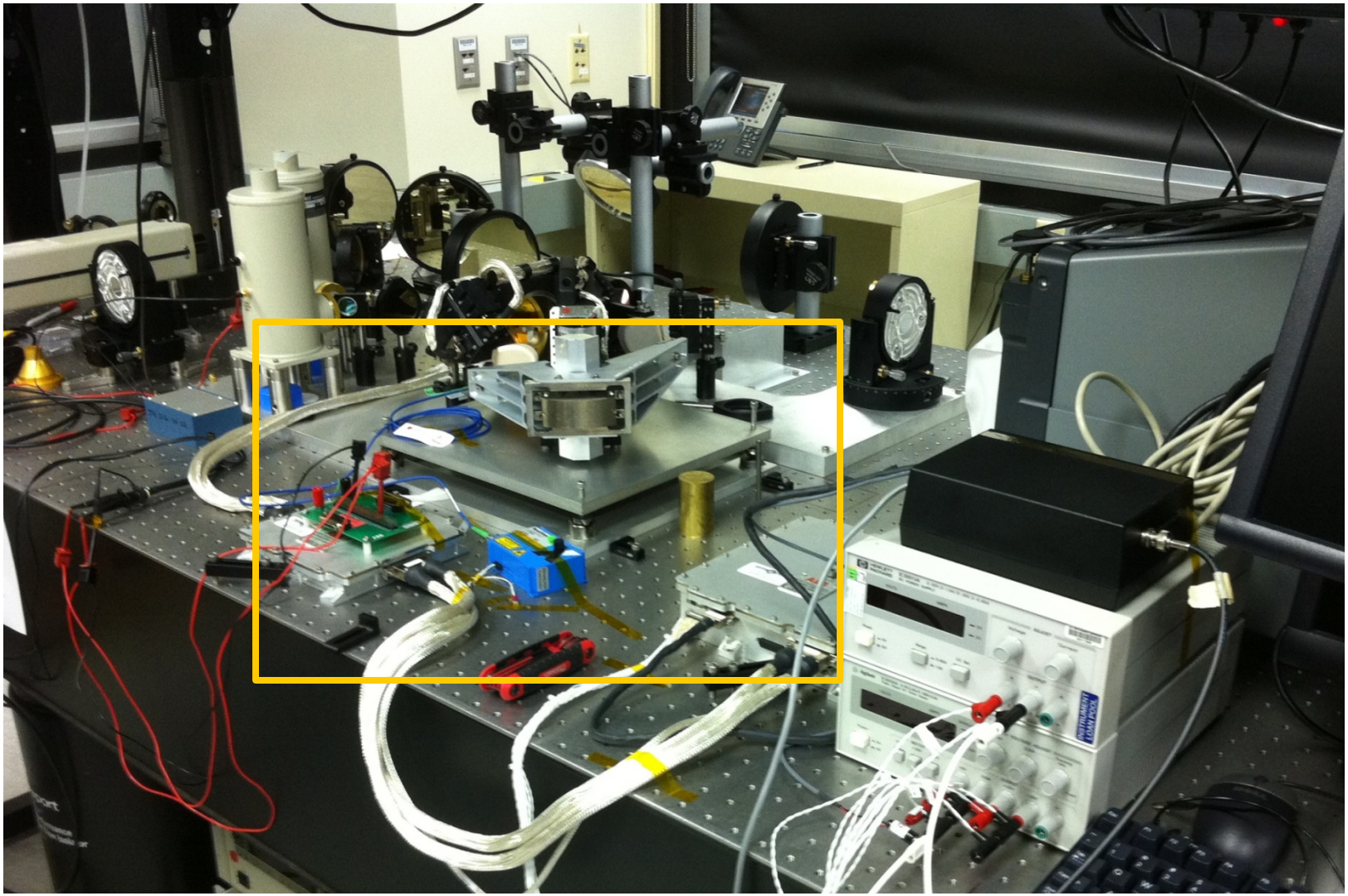

EDU built by ABB Bomem, is a non-flight version of the MATMOS interferometer

InSb Interferogram

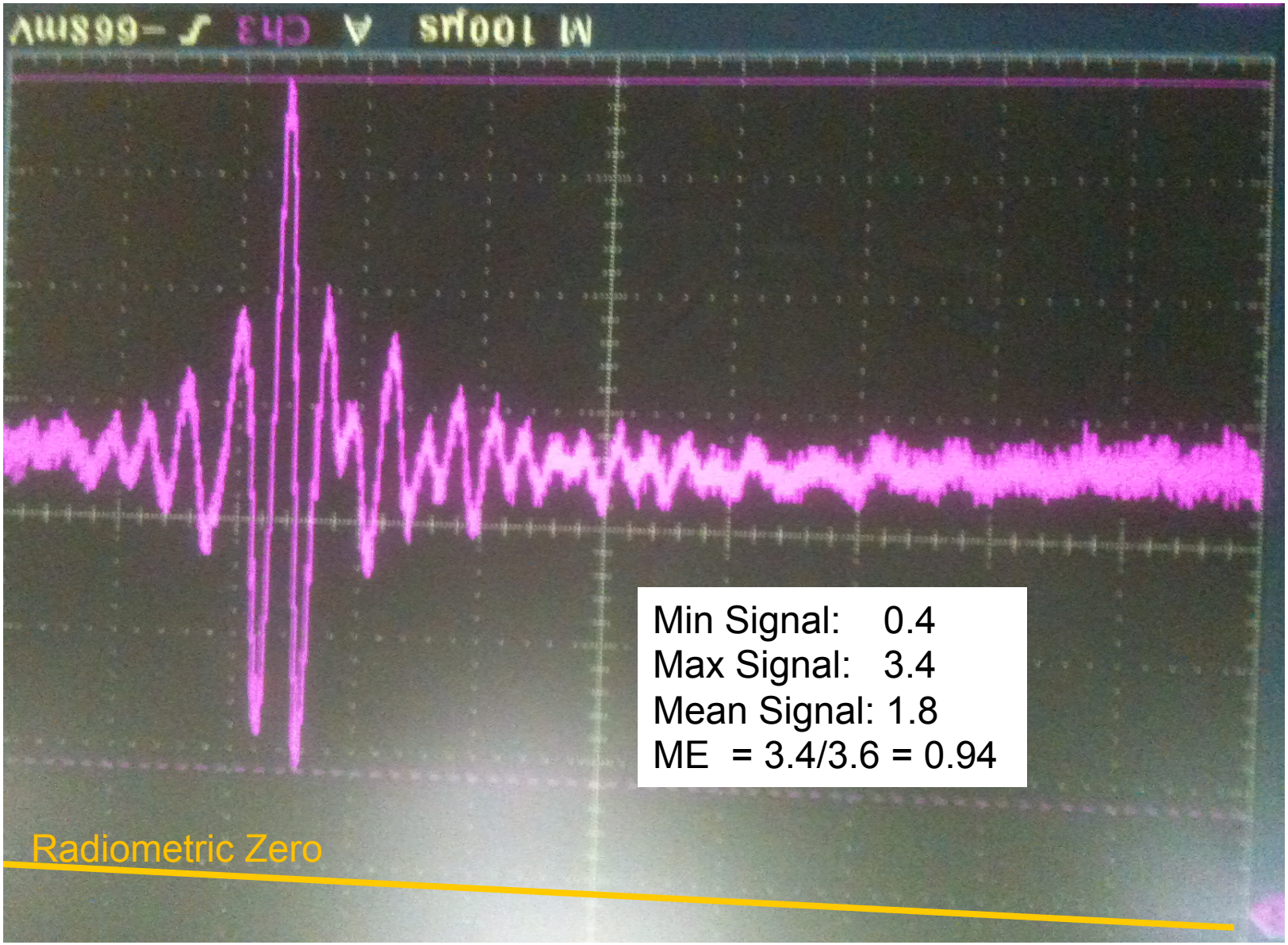

Glowbar Spectra measured 2012-04-11

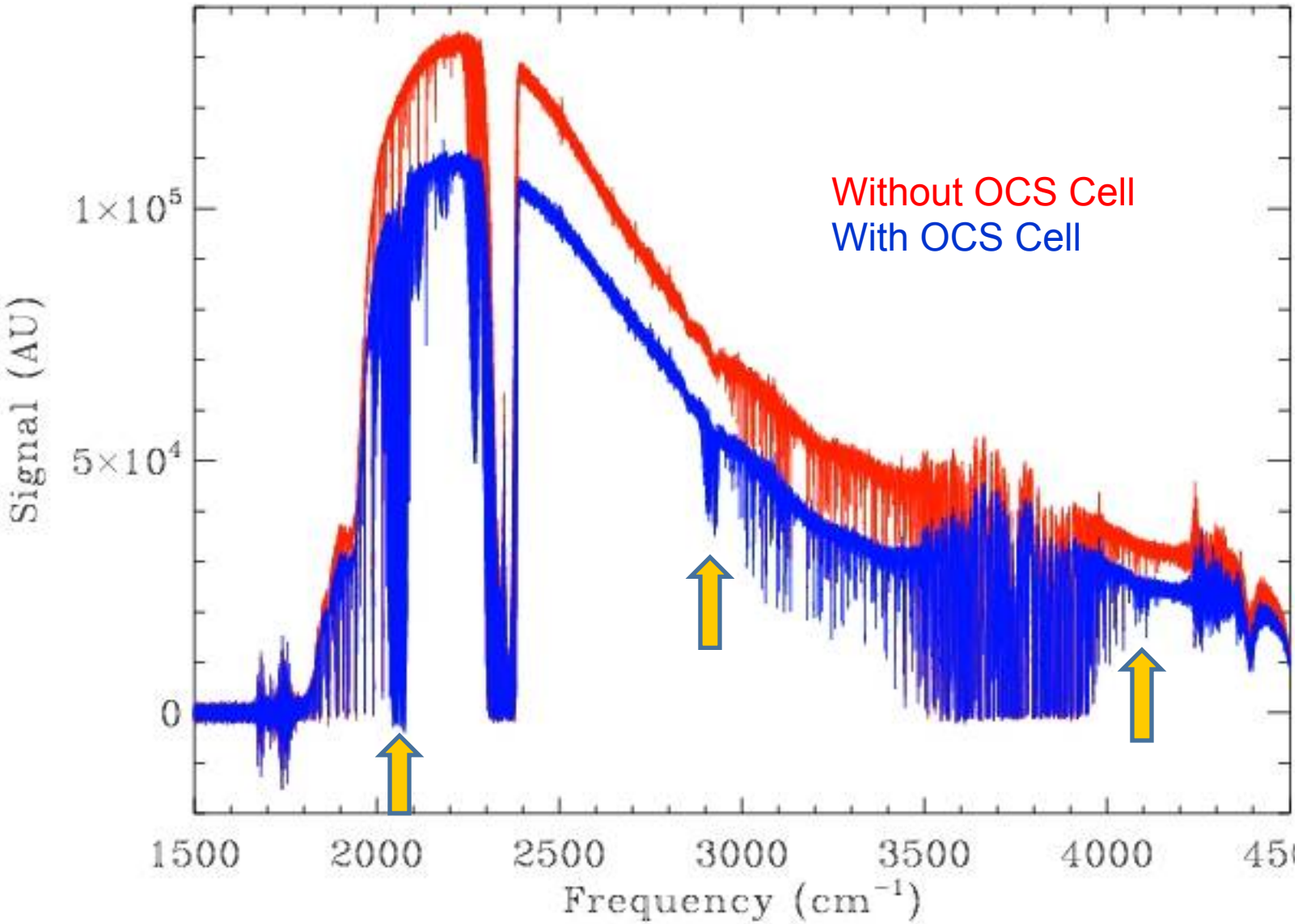

Cell OCS absorption 1980-2120 cm^{-1}

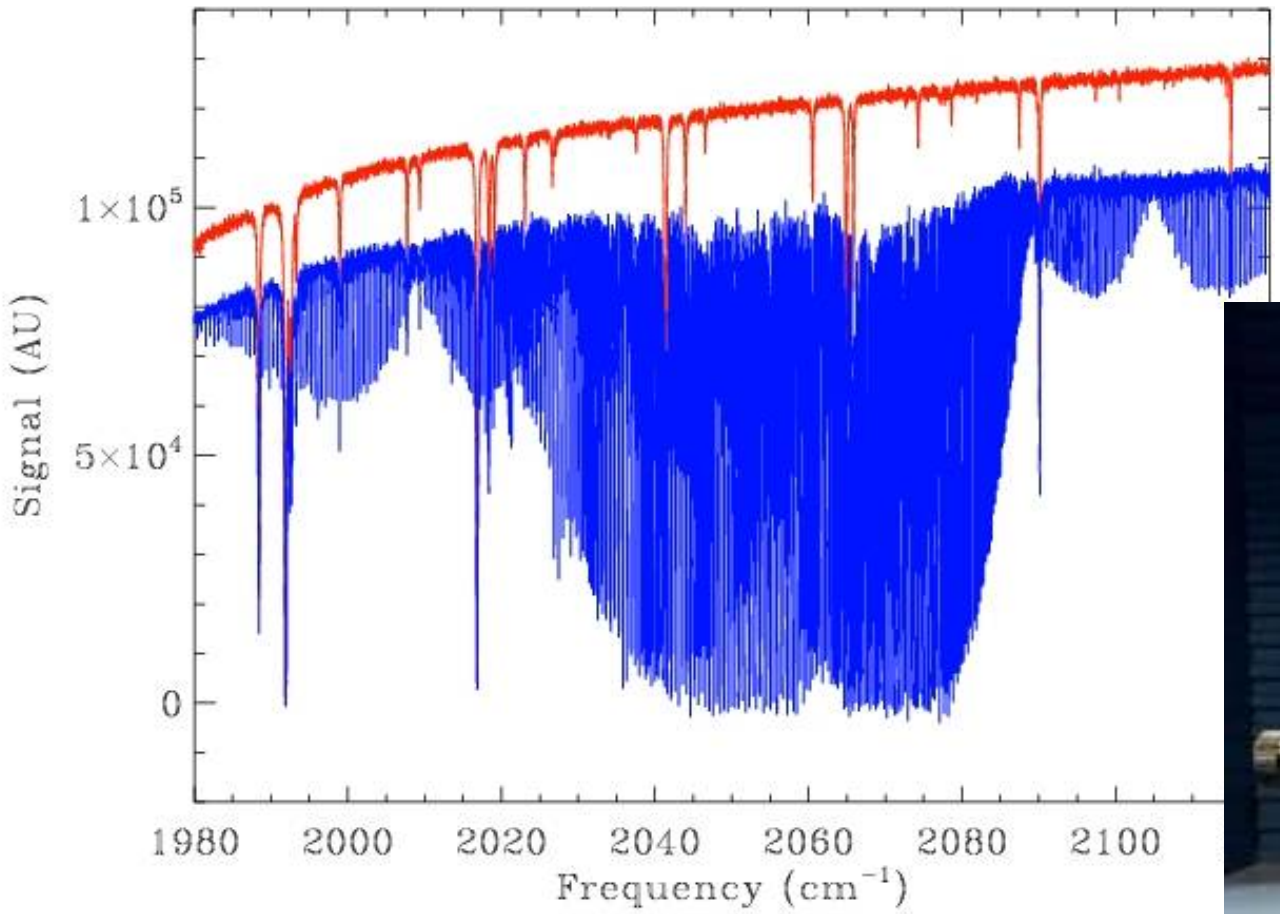

MATMOS OCS cell is 20 cm long at 10 cm in diameter.
It is shown alongside the NDACC HBr cell (2cm x 2cm).
It's large size allows it to be mounted outside telescope.

More OCS absorption bands

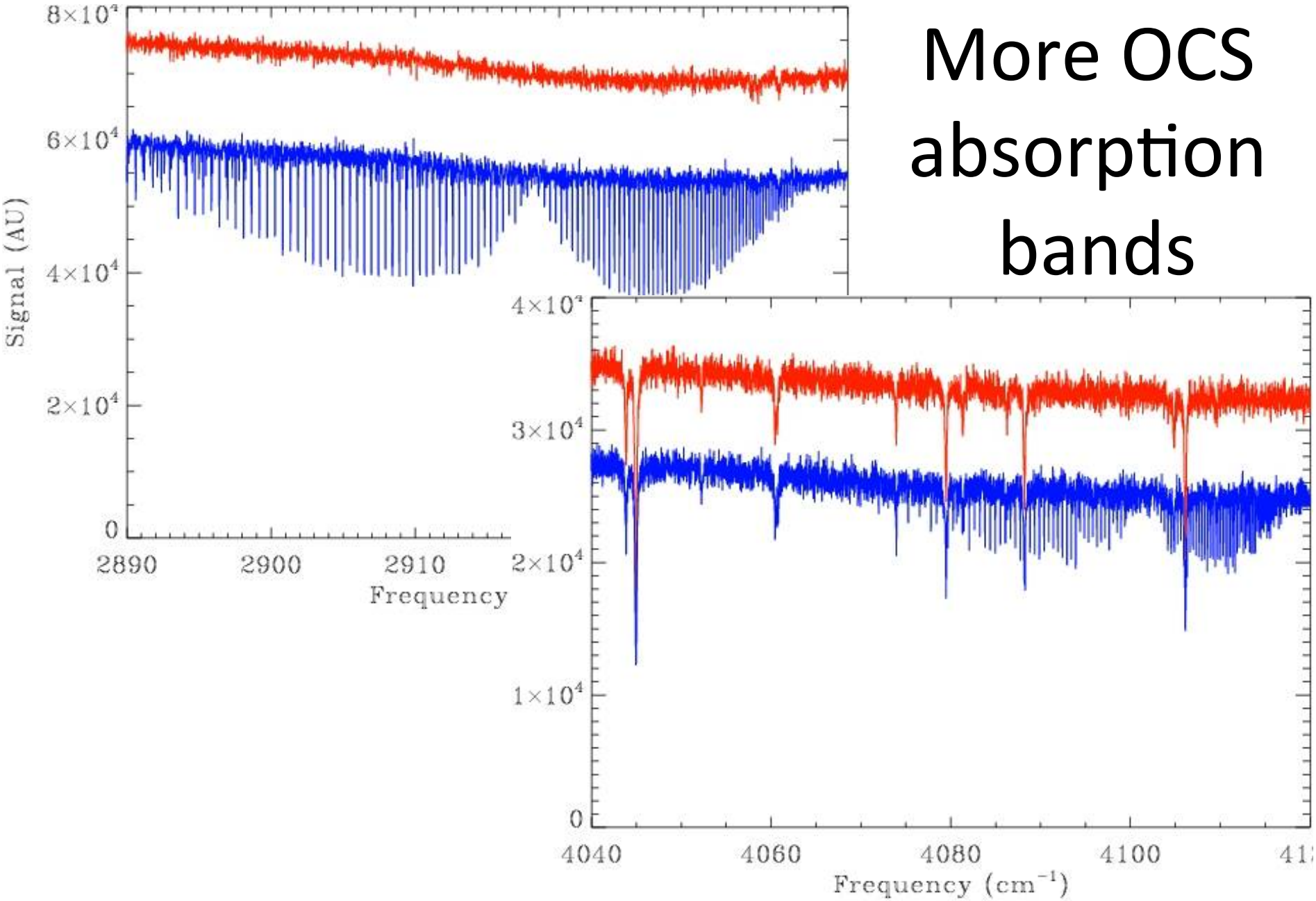

Quantitative Analysis of Gas Absorptions

Spectral absorptions were fitted using GFIT algorithm in various spectral regions:

- HITRAN 2008 spectroscopic database used in analysis
- For OCS the July 2009 update was supplemented by an empirical linelist
- Air path between glowbar and detectors assumed to be 4.2 m.
- Temperature assumed to be 297K, Pressure assumed to be 972 mbar
- ILS calculated from 25.3 cm Max OPD and 6.25 mrad internal FOV

In subsequent plots,
Large lower panel show the measured (black points) and calculated spectra (black line). The colored lines show the contributions of the various gases.
Narrow upper panel shows the residuals: (measured – calculated)

Absorption by lab CO and H_2O

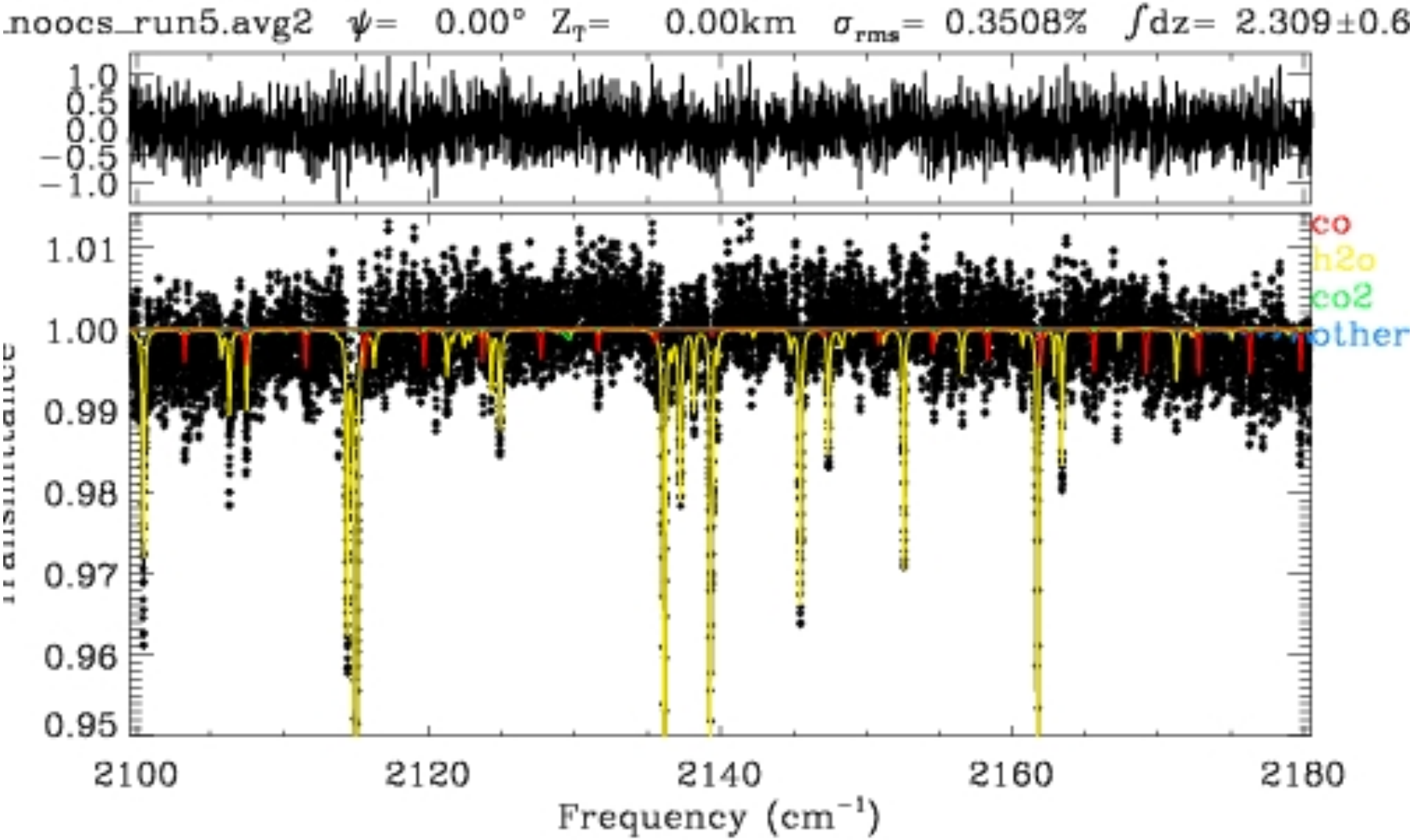

Fits showing absorption by lab N_2O

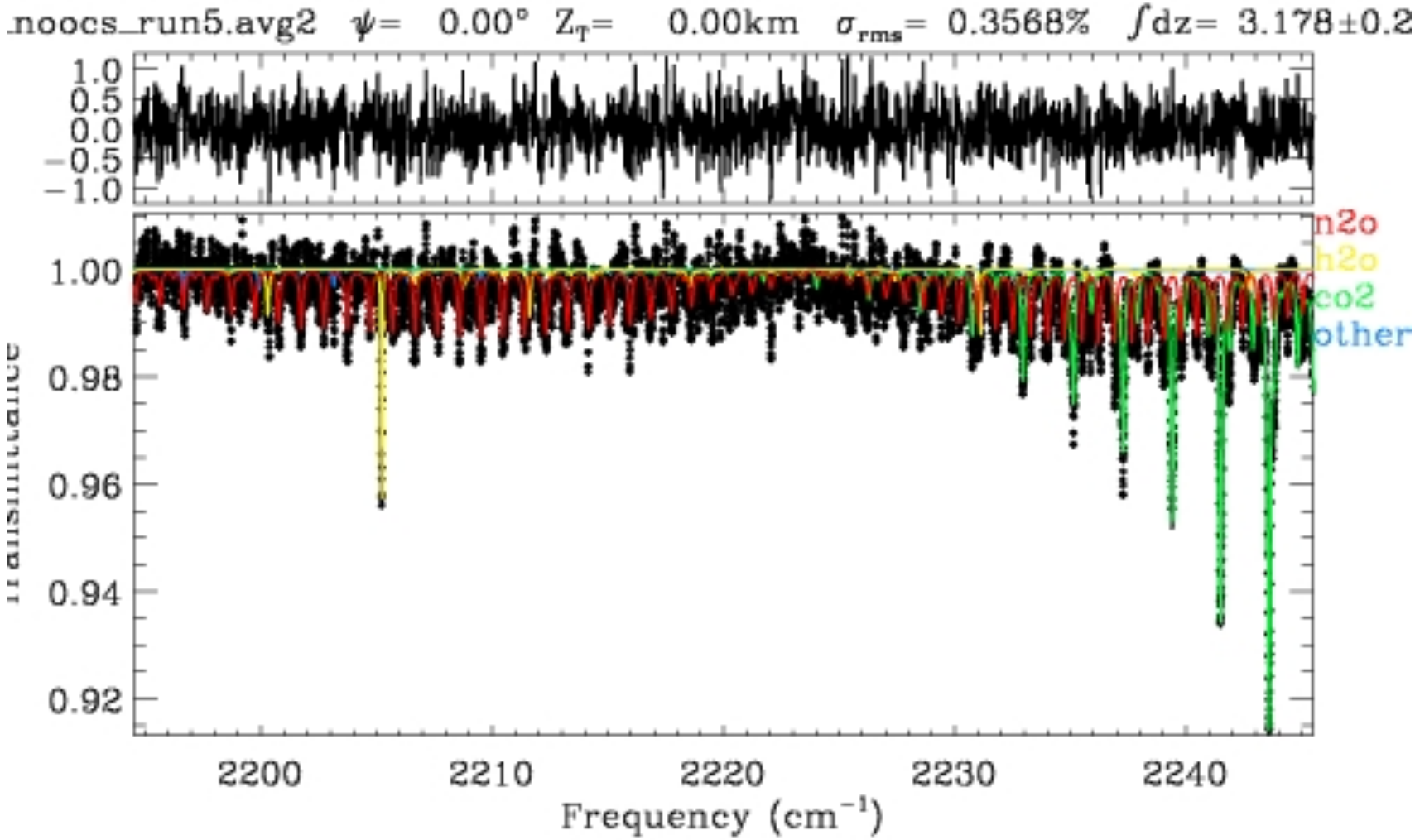

Fits showing absorption by lab $^{13}CO_2$

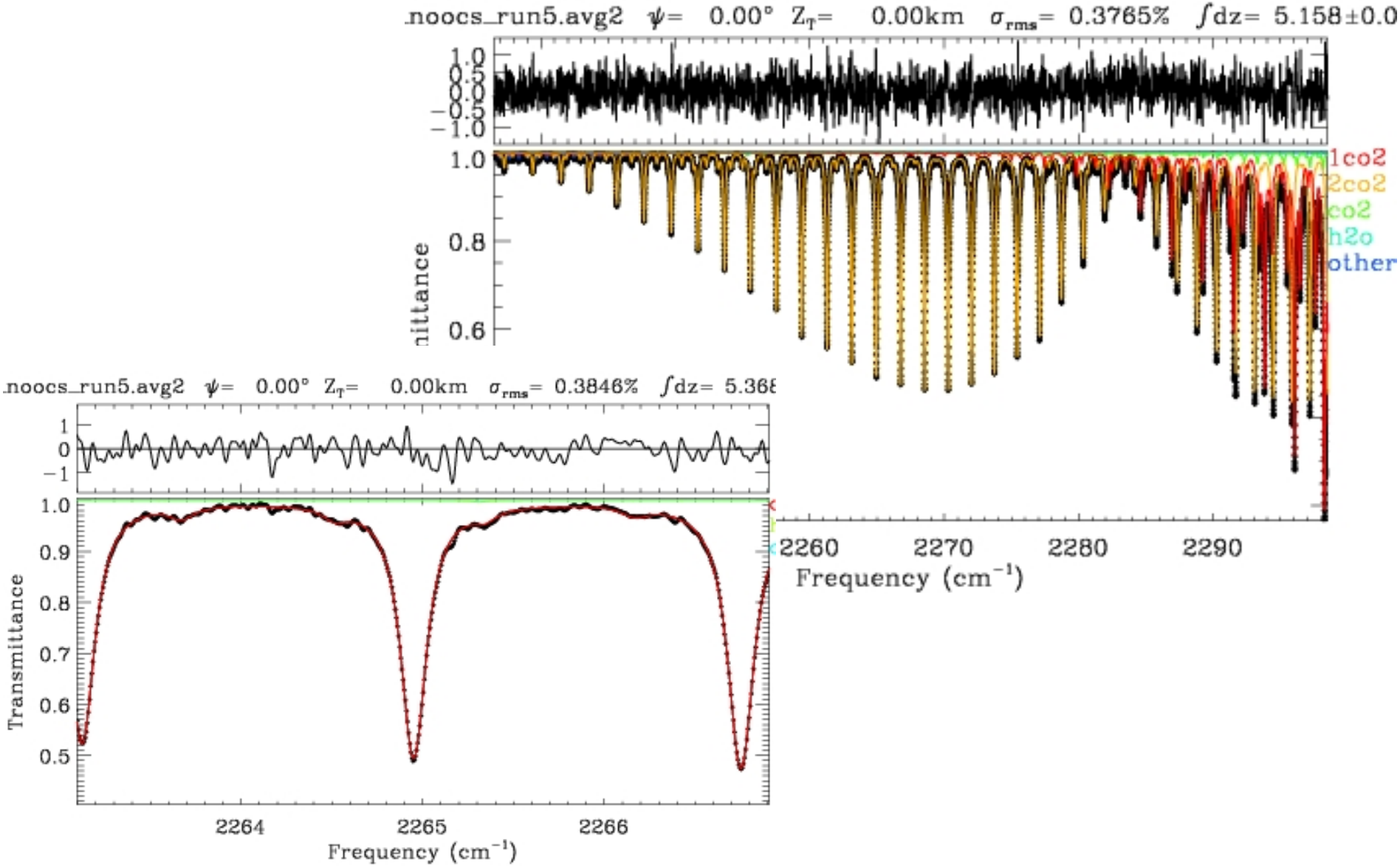

Fits showing Absorption by lab CH_4

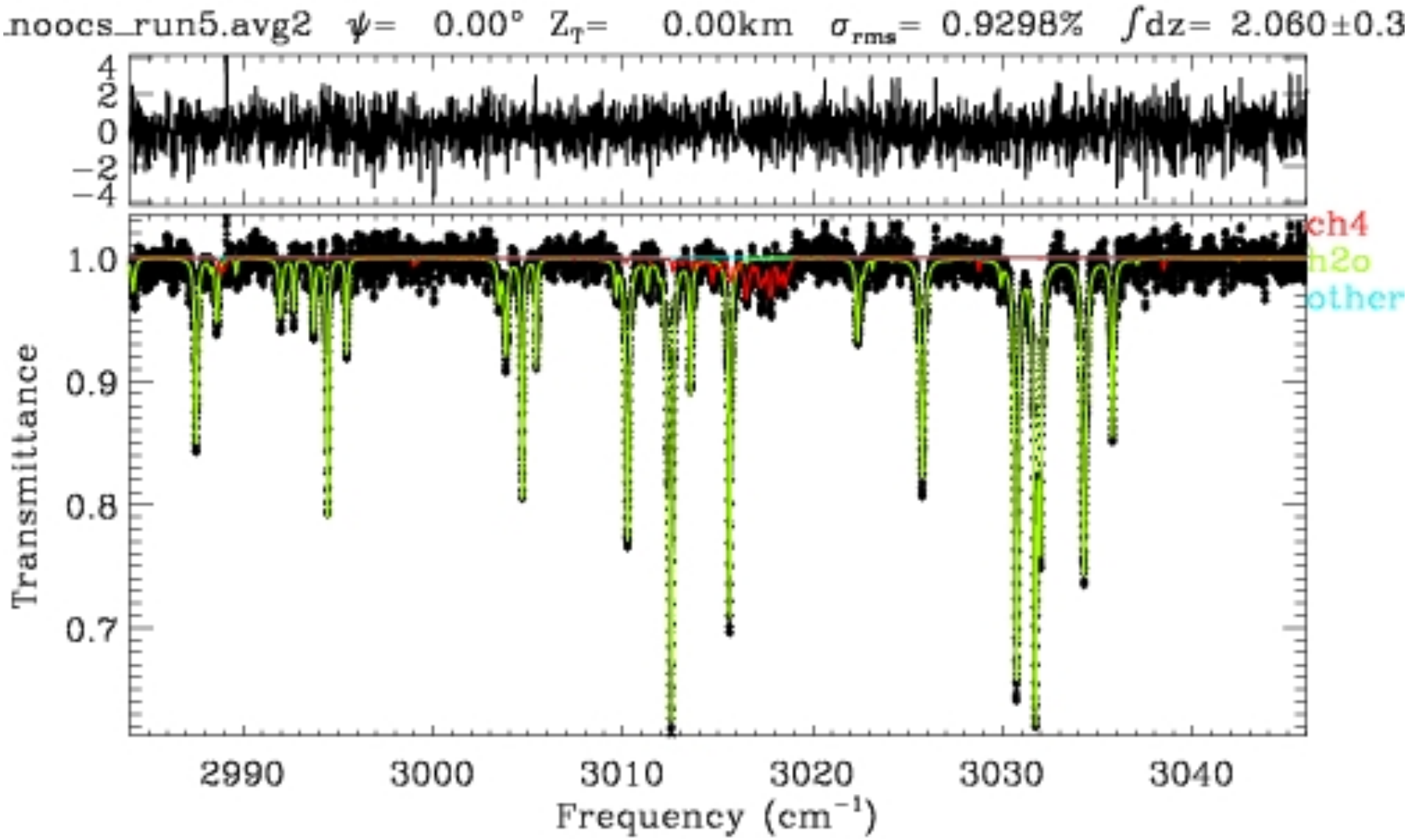

Fits showing absorption by lab $^{12}CO_2$

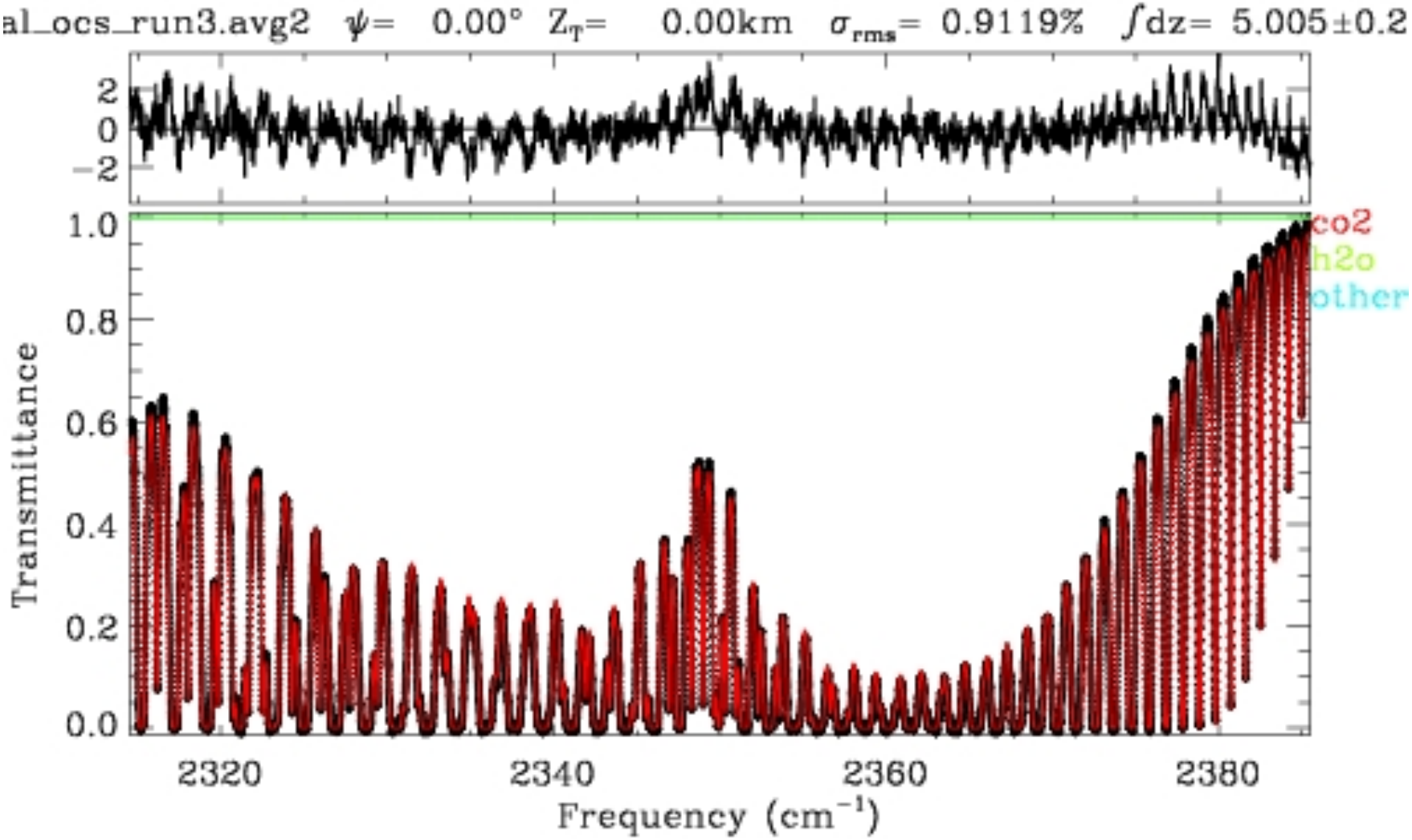

OCS fitted assuming nominal cell pressure

2 Torr was the fill pressure.

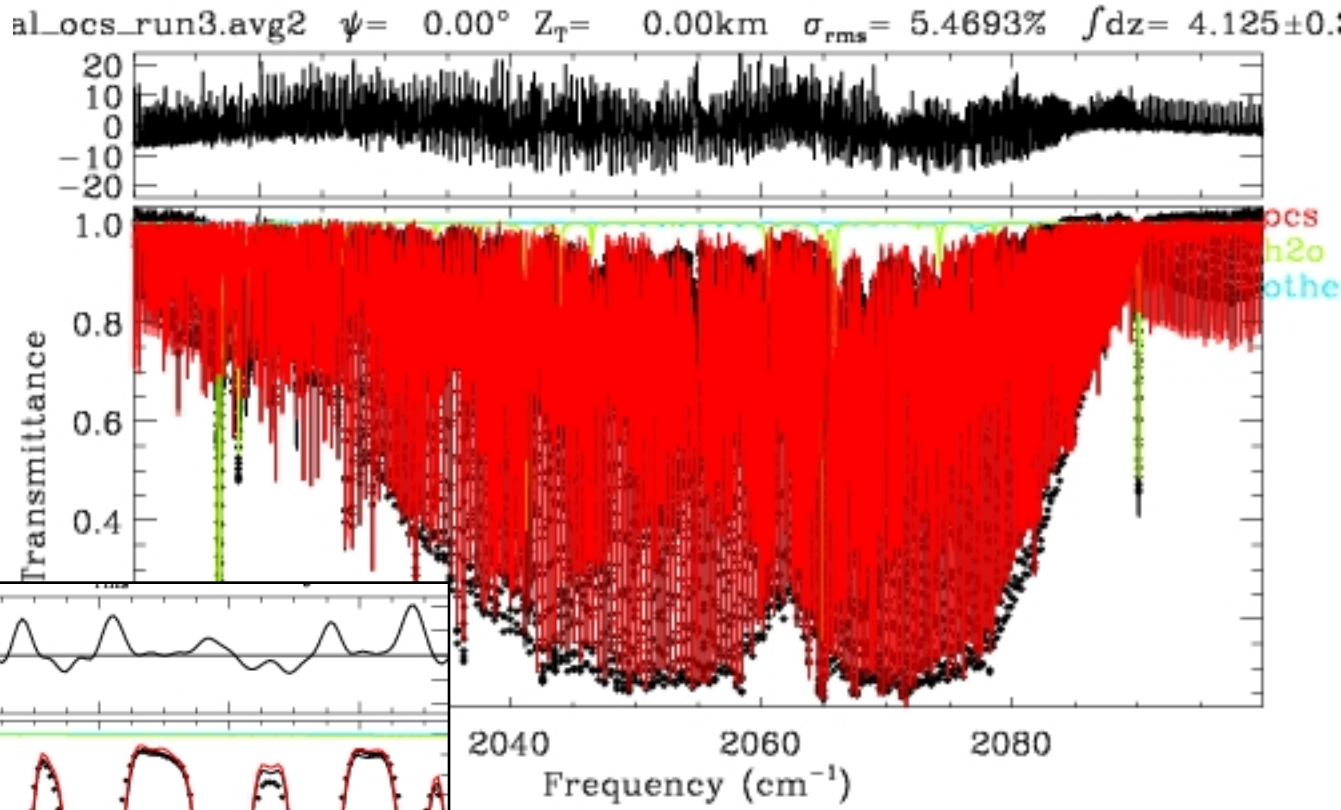

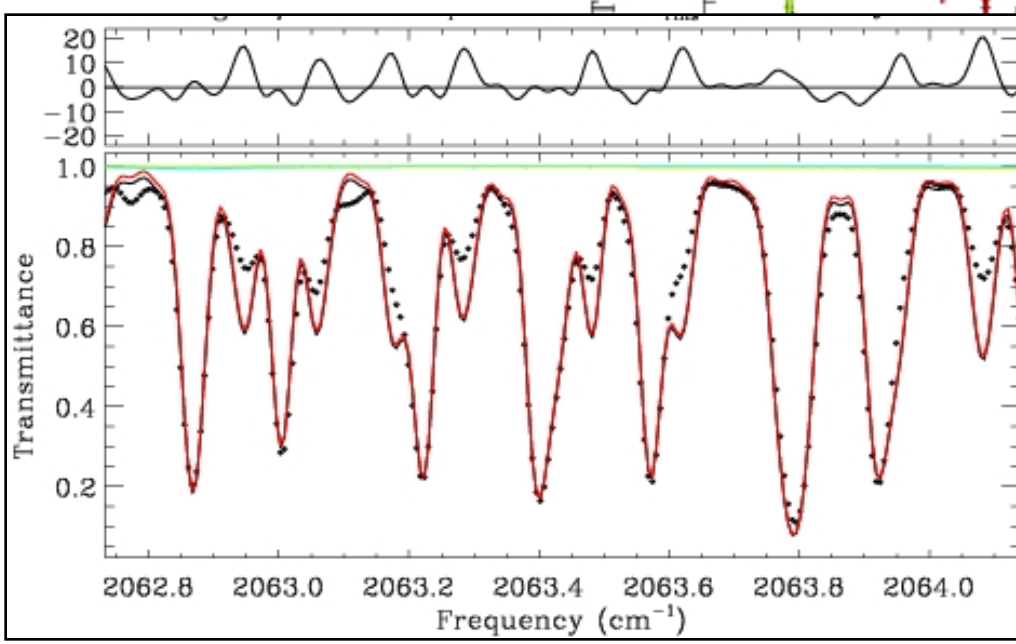

Large residuals caused by weakly absorbing lines being inconsistent with the stronger lines.

Absorption of weak lines is over-estimated in calculation.

Determination of True Cell Pressure

Assumed Cell Pressure (mbar/Torr)	RMS Fitting Residual (%)
2.66 / 2.0	5.442
10.0 / 7.6	2.224
16.0 / 12.0	1.078
19.2 / 14.6	0.807
20.1 / 15.0	0.791
21.0 / 16.0	0.802
25.0 / 19.0	1.072

The assumed cell pressure was adjusted and the OCS v3 band was re-fitted.

The OCS vmr inside the cell was also adjusted to be consistent with an air leak. i.e.

$$VMR = 2\ Torr / P_{CELL\ (Torr)}$$

Fitting the entire ν_3 OCS region, the RMS fitting residuals are quite sensitive to the cell pressure, even though the MATMOS ILS is much broader than the lines.

25% error in the cell pressure causes a 35% increase in the rms residual.

High sensitivity due to wide range of line strengths in different parts of their curve of growth.

After correcting pressure to 15 Torr

RMS residuals reduced by factor 7. Weak lines are now consistent with strong lines.

RMS is surprisingly sensitive to assumed cell pressure

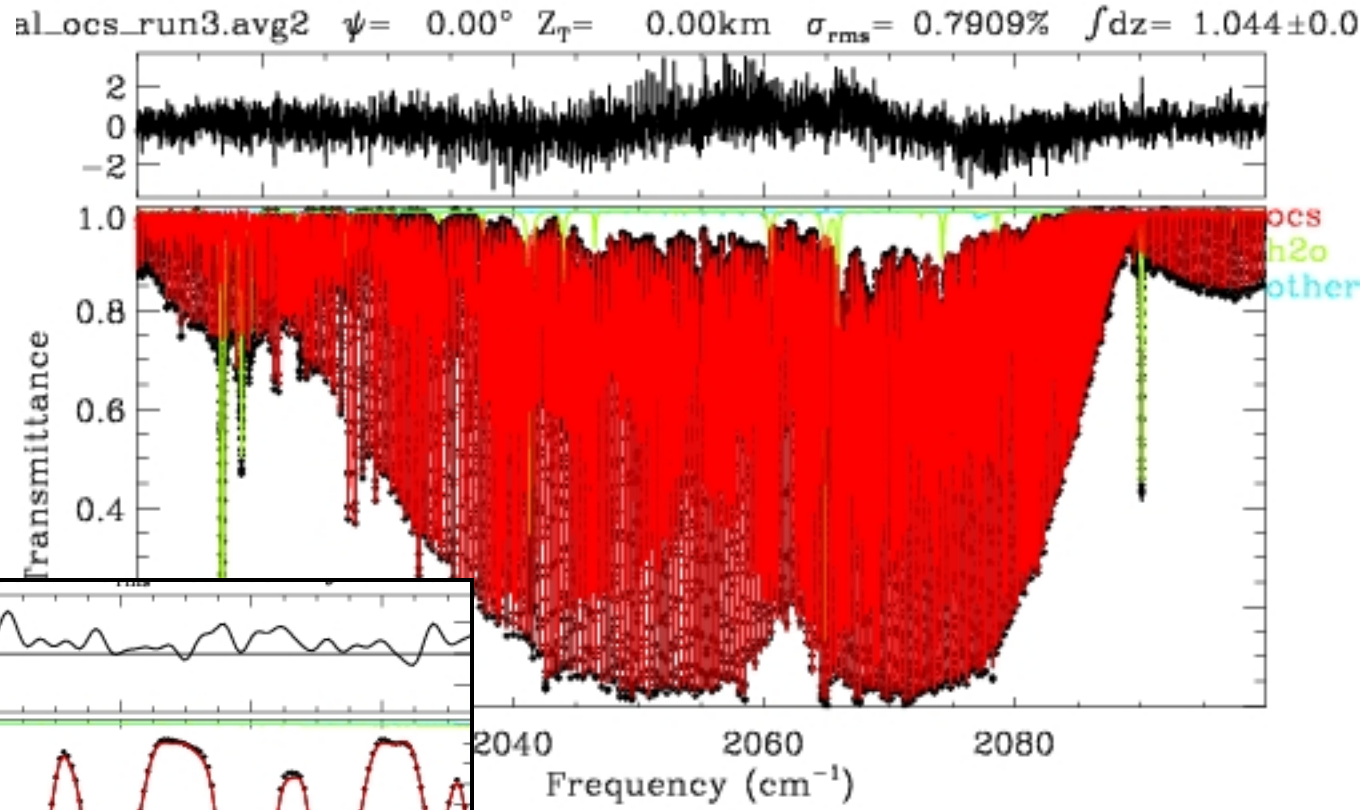

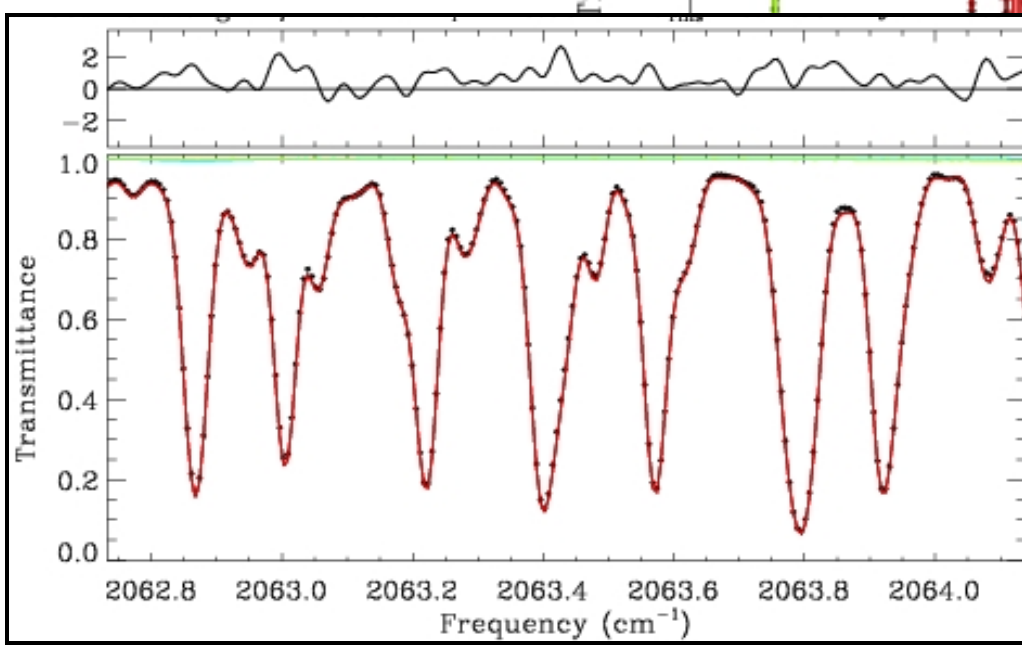

The OCS data can now be used to determine the ILS, without fear of bias.

Fit using theoretical ILS (25.3 cm OPD; 6.25 mrad FOVI). No Apodization

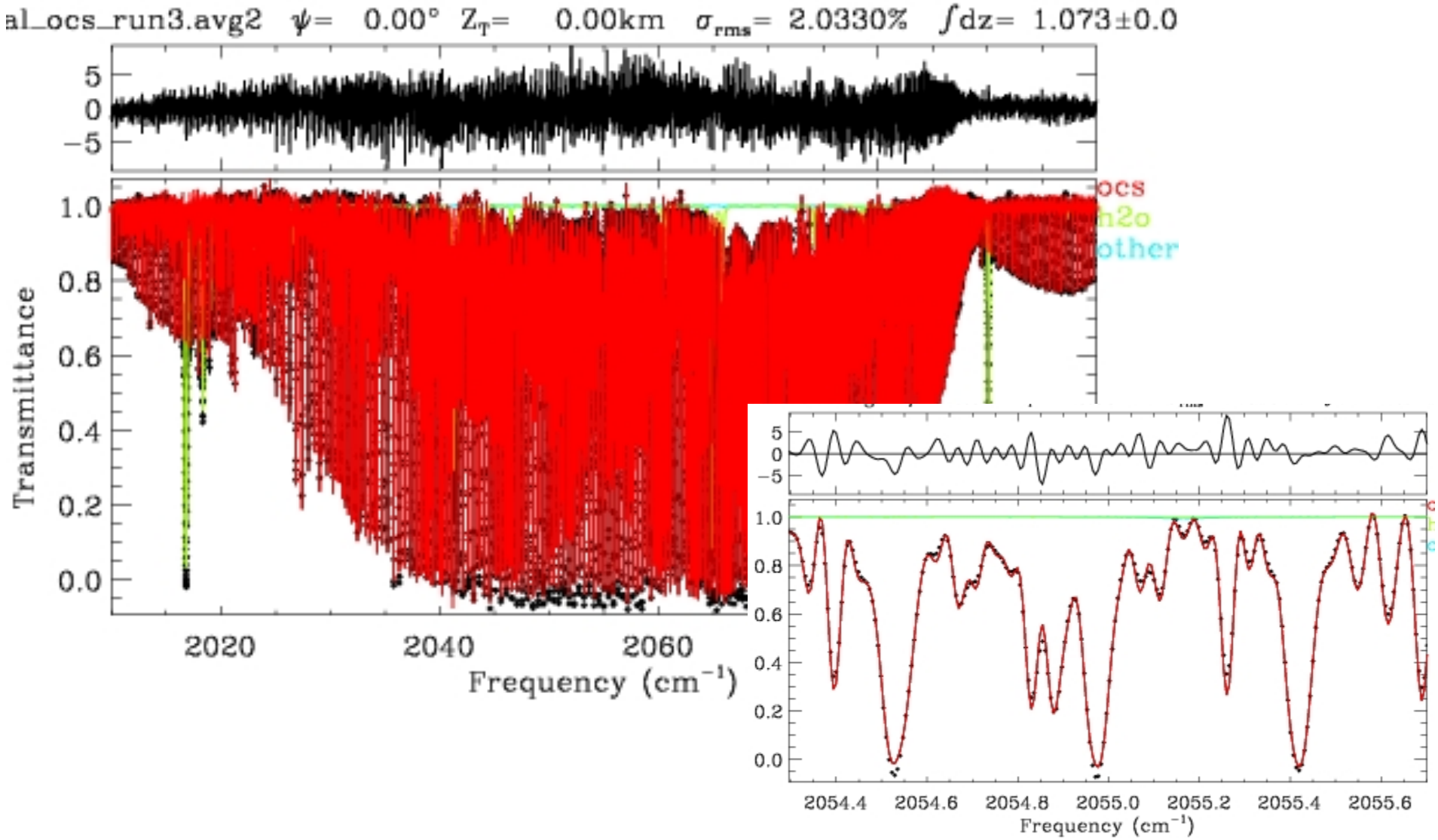

Fit using tweaked ILS (AMAL=6.5 mrad). No apodization

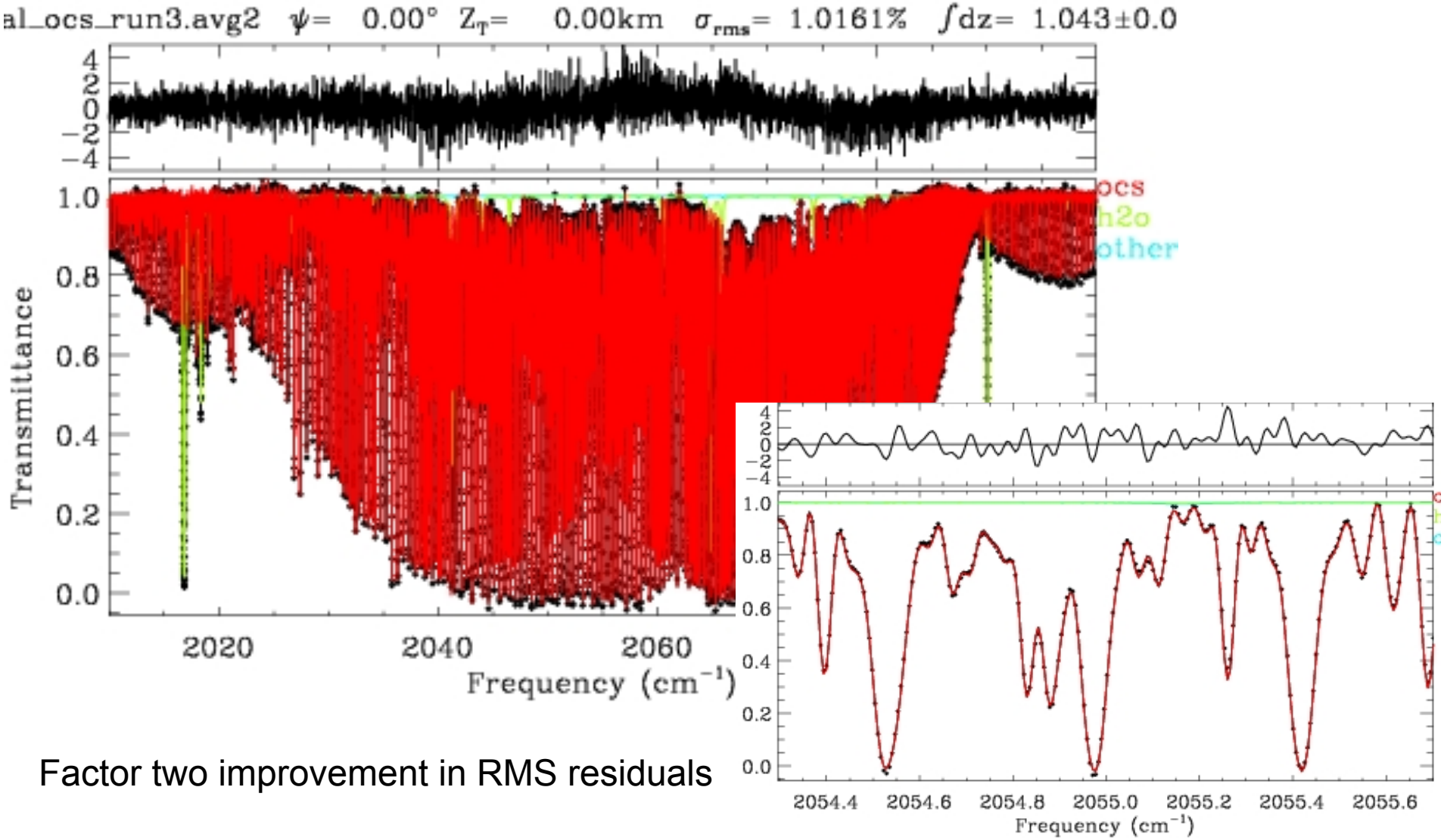

Factor two improvement in RMS residuals

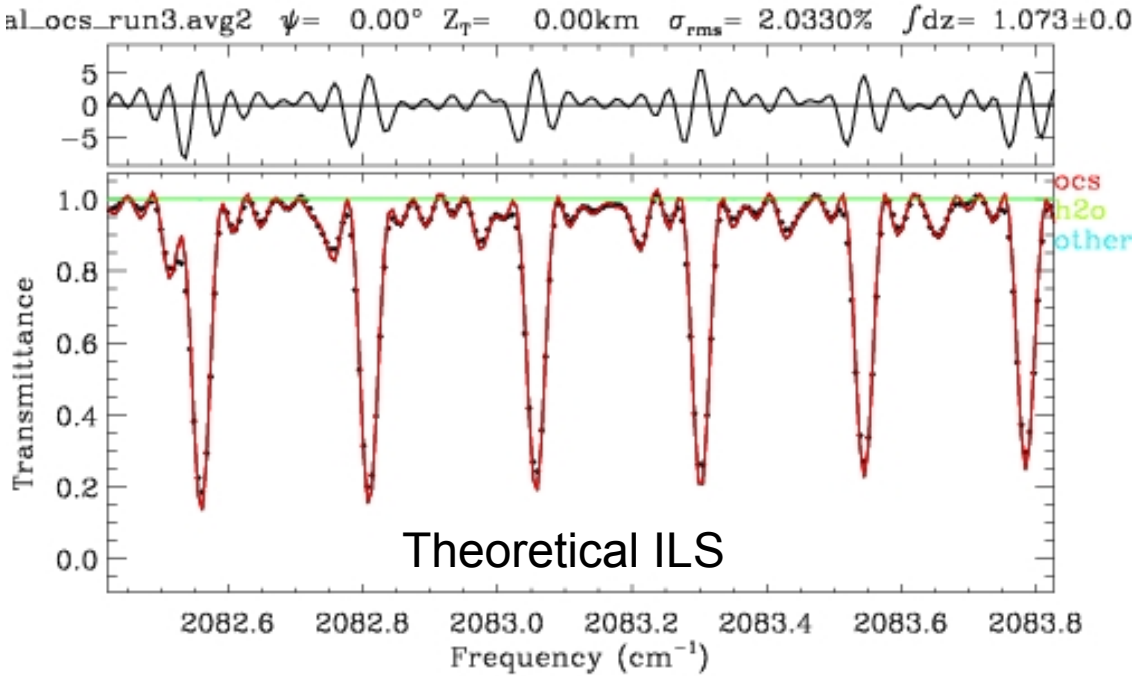

W-shaped residuals imply that measured ILS is broader than the theoretical calculation.

Negative residuals are lower on left of line than on right, Implying misalignment .

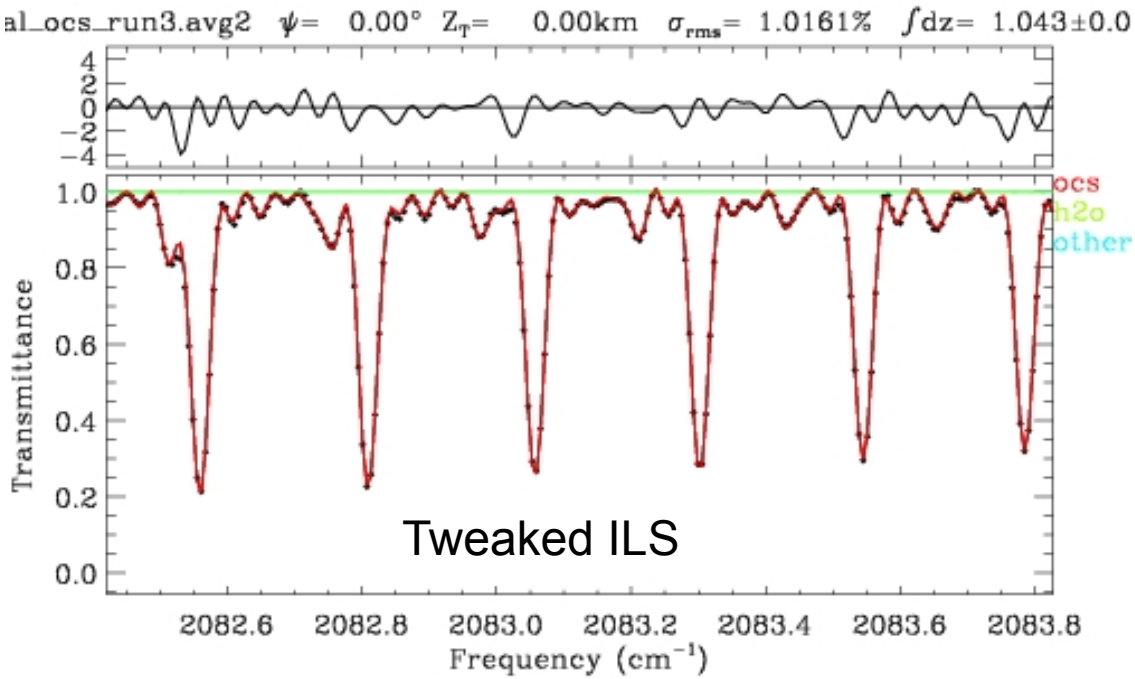

Tweaked ILS is broader but still symmetrical. It produces much better residuals (factor 2)

Low pressure OCS gas cell 2900 cm^{-1}

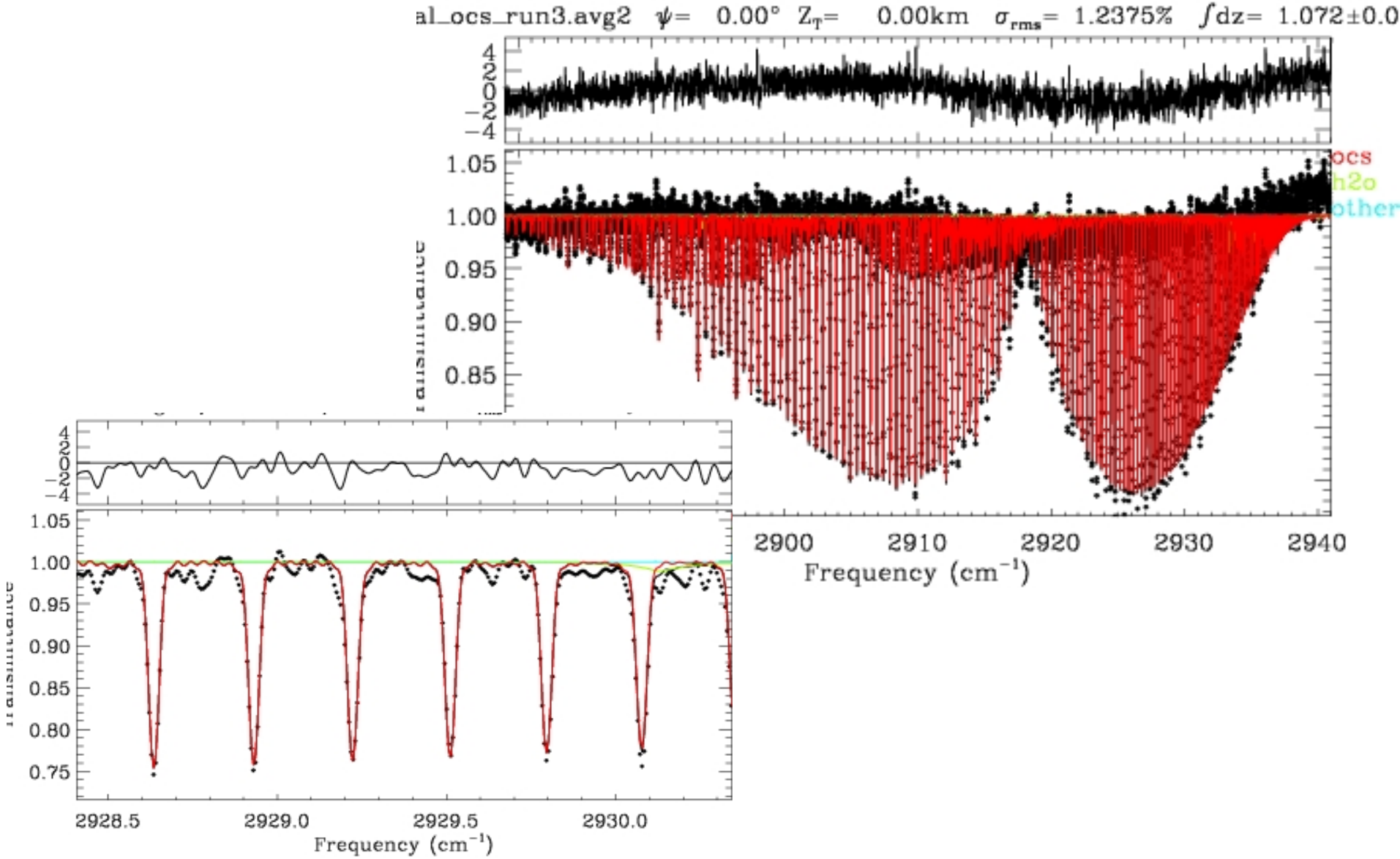

Low pressure OCS gas cell 4100 cm^{-1}

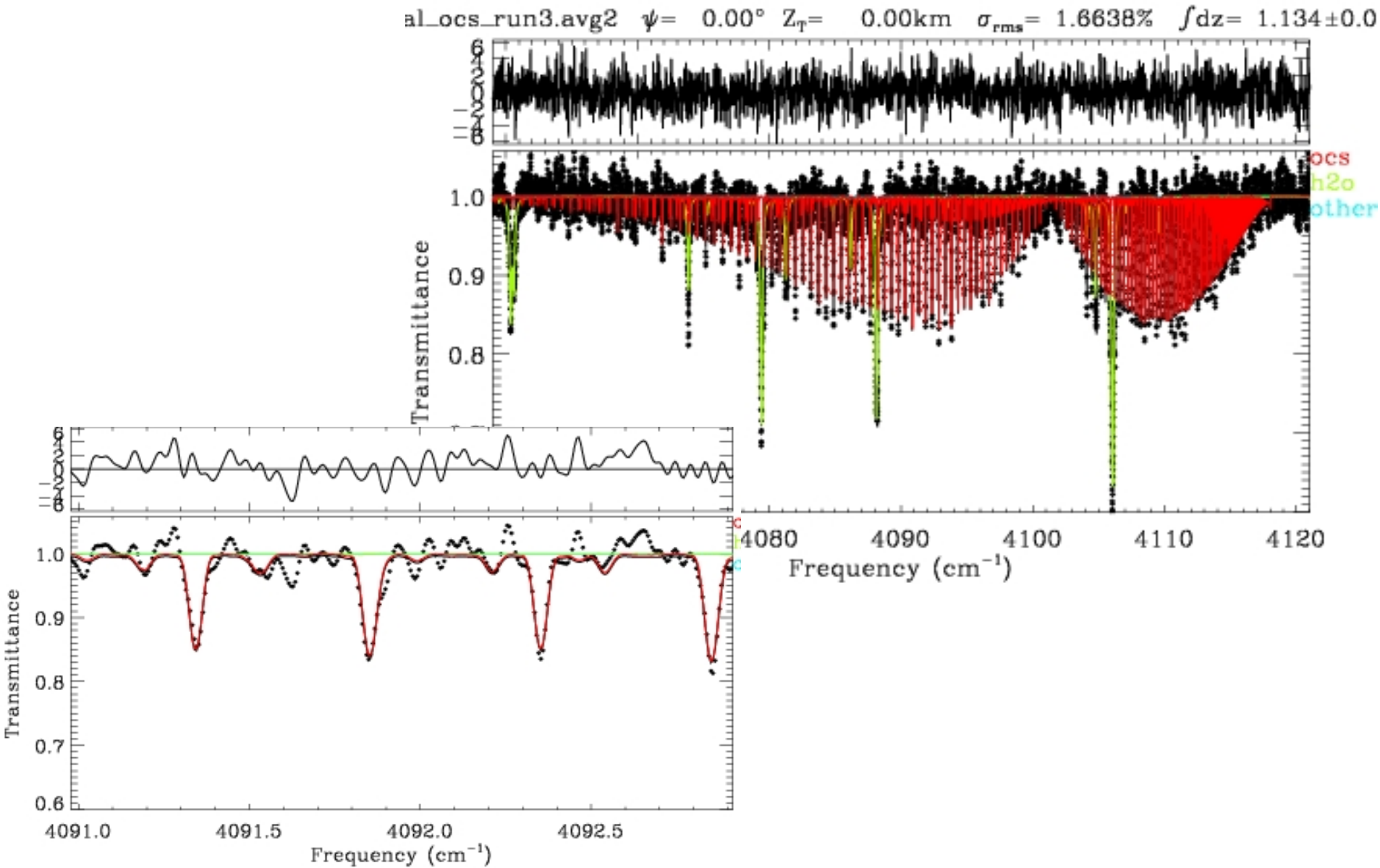

Conclusions

MATMOS is difficult to align because transmission of visible radiation is very small. So you can't "see" the Haidinger interference fringes.

There has been a marked improvement in the quality of InSb spectra from the MATMOS EDU measured on 2012-04-11. They have a higher SNR and spectral resolving power than those acquired previously.

For 4s of scanning, we now achieve a SNR of over 300:1 at 2000-2500 cm^{-1} decreasing to 80:1 at 4100 cm^{-1} due to the glowbar source.

The rectangular component of the ILS is ~ 45% wider than theoretical and is slightly asymmetrical, suggesting a remaining mis-alignment.

The total ILS width (Sinc + Rectangle) is only 10% wider than theoretical at 2050 cm^{-1}. Previously it was more than double.

The pressure in the OCS cell is 15 Torr, not the nominal 2 Torr. Total OCS slant column is consistent with filling to 2 Torr, implying that air has leaked into the cell.

Fitting the strong v_3 OCS band provides an excellent check on the cell pressure, even for instruments that cannot directly resolve the line broadening.

Future

NASA withdrew from the ExoMars TGO 2016 collaboration with ESA.

No new funds are anticipated for MATMOS in FY' 13.

Work will continue at JPL with test-bed/EDU until Sept 2012.

The EDU will then be returned to Canada.

We hope that MATMOS will be re-activated for a 2018 or 2020 Mars mission.

Over the next 4 months tests at JPL will continue to:

- Demonstrate RAD-750 based data acquisition from the 24-bit ADCs and on-board processing of raw interferogram data into spectra
- Identify cause of low signal in the HgCdTe detector
- Measure sensitivity to low levels of vibration
- Acquire spectra of 3.39 um HeNe laser to measure ME and look for ghosts
- Identify causes of remaining spikes/glitches in the spectrum

Investigating Non-Linearity in ACE interferograms

Geoff Toon
MATMOS Instrument Scientist
Jet Propulsion Laboratory
Dec 14, 2011

To help inform the MATMOS detector requirements, I looked at ACE interferograms to try to quantify the degree of non-linearity in the ACE detectors:

- HgCdTe : PV, 780 um diameter, 750 cm^{-1} cut-on
- InSb : PV, 1000 um diameter, 1850 cm^{-1} cut-on

ACE interferograms differ from MATMOS interferograms in three main respects:

- Sampled in equal steps of OPD not time (which is irrelevant for this work)
- AC coupled (MATMOS is DC coupled)
- HgCdTe cut off wavelength is longer (750 cm^{-1})

Effect of Non-Linearity on Interferograms

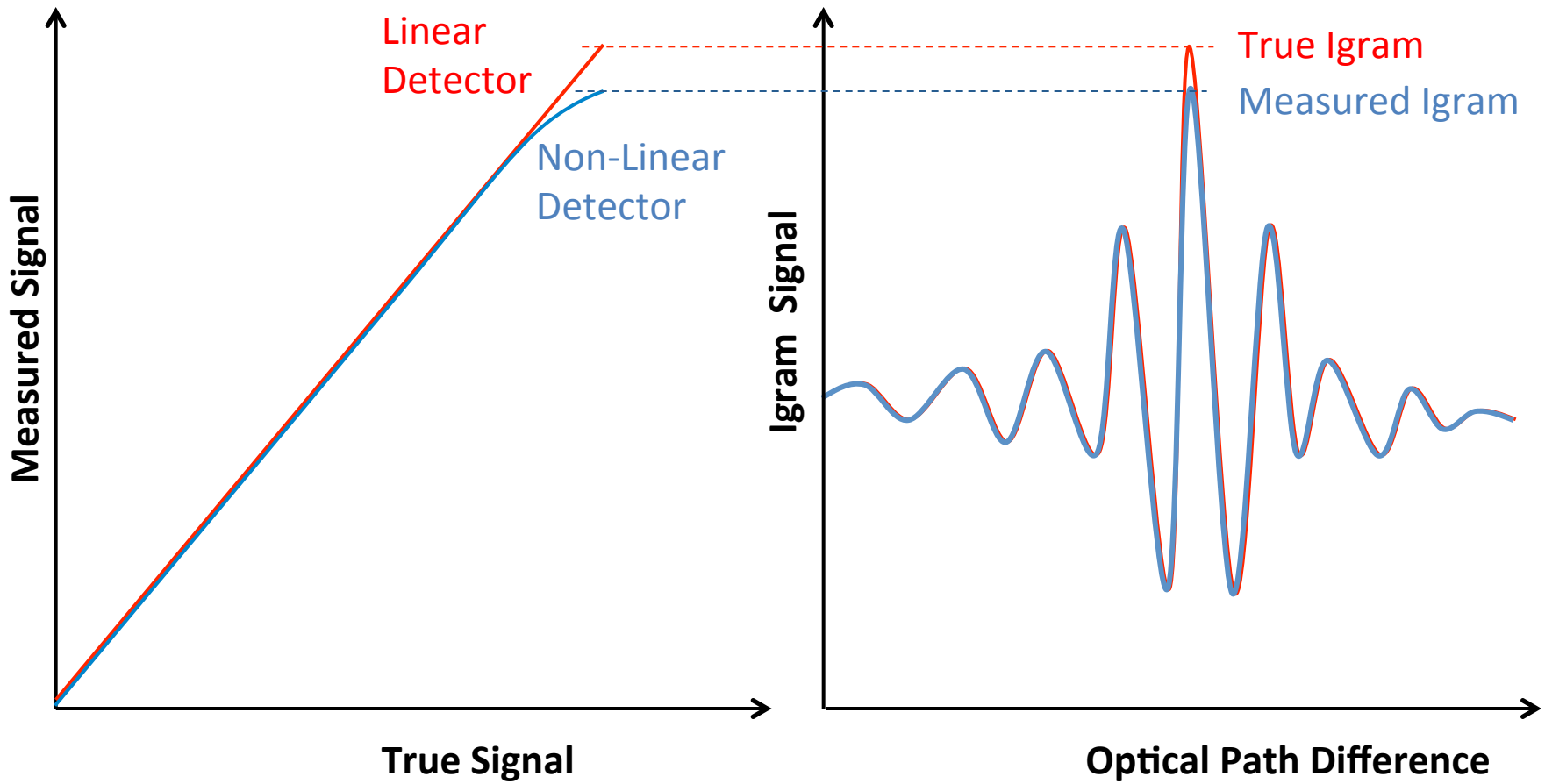

Only points very close to ZPD are affected by non-linearity

Smoothing removes interferometric modulation

Interferograms are a super-position of cosine waves, of different wavelengths, all of which are in-phase at ZPD.

When you smooth a cosine wave, it collapses into a straight line.

When you smooth a superposition of cosine waves, it should also collapse into a straight line.

If the smoothed igram has a dip at ZPD, the superposition wasn't done linearly.

This forms the basis of a method of quantifying detection non-linearity, as suggested by Keppel-Aleks et al., [2007].

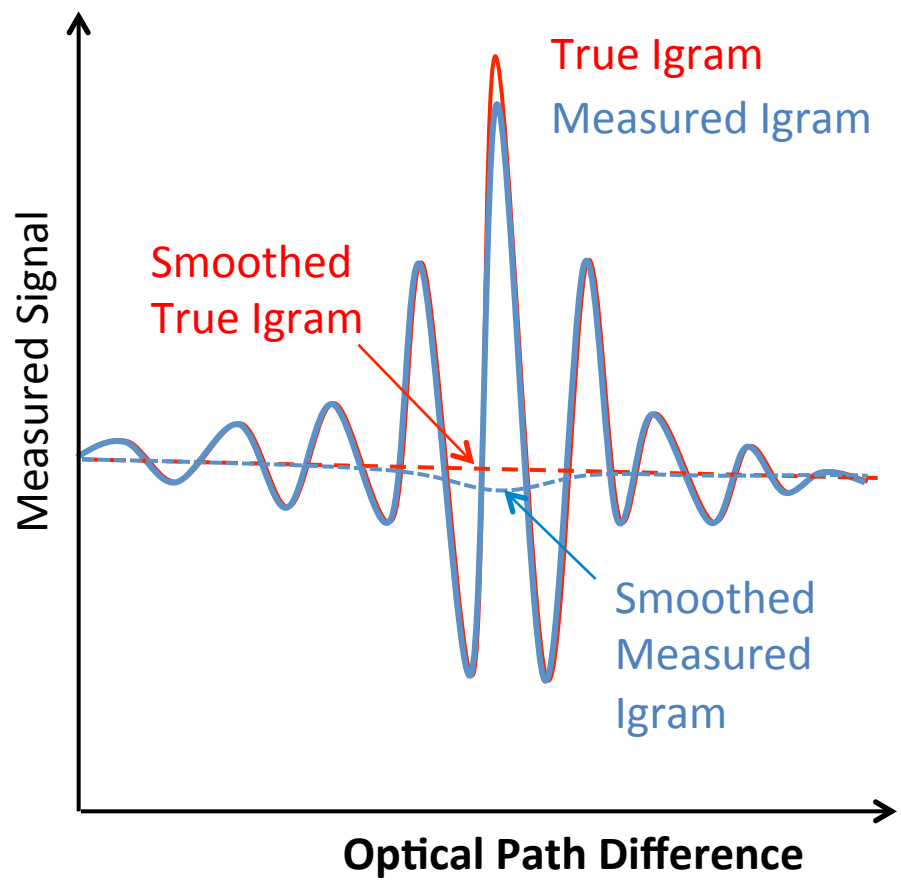

ACE Interferograms

Selected 8 consecutive bright-sun ACE interferograms covering 40-60 km altitude:

XXX-COMBINED-1269187725.750
XXX-COMBINED-1269187727.816
XXX-COMBINED-1269187729.887
XXX-COMBINED-1269187731.953
XXX-COMBINED-1269187734.020
XXX-COMBINED-1269187736.086
XXX-COMBINED-1269187738.152
XXX-COMBINED-1269187740.219

where XXX = MCT or InSb

MCT interferograms are sampled every 1.545 um (metrology laser wavelength)
InSb interferograms are sampled every 0.772 um (half laser wavelength)

The ZPD regions of these interferograms were digitally smoothed with the narrowest possible filter that still removed the fringes.

The ZPD regions of the interferograms, **raw** and **smoothed**, are shown in subsequent plots. ACE igram are sorted in OPD, not time. So in the forward scans (left panels) time increases, in the reverse scans (right panels) time decreases.

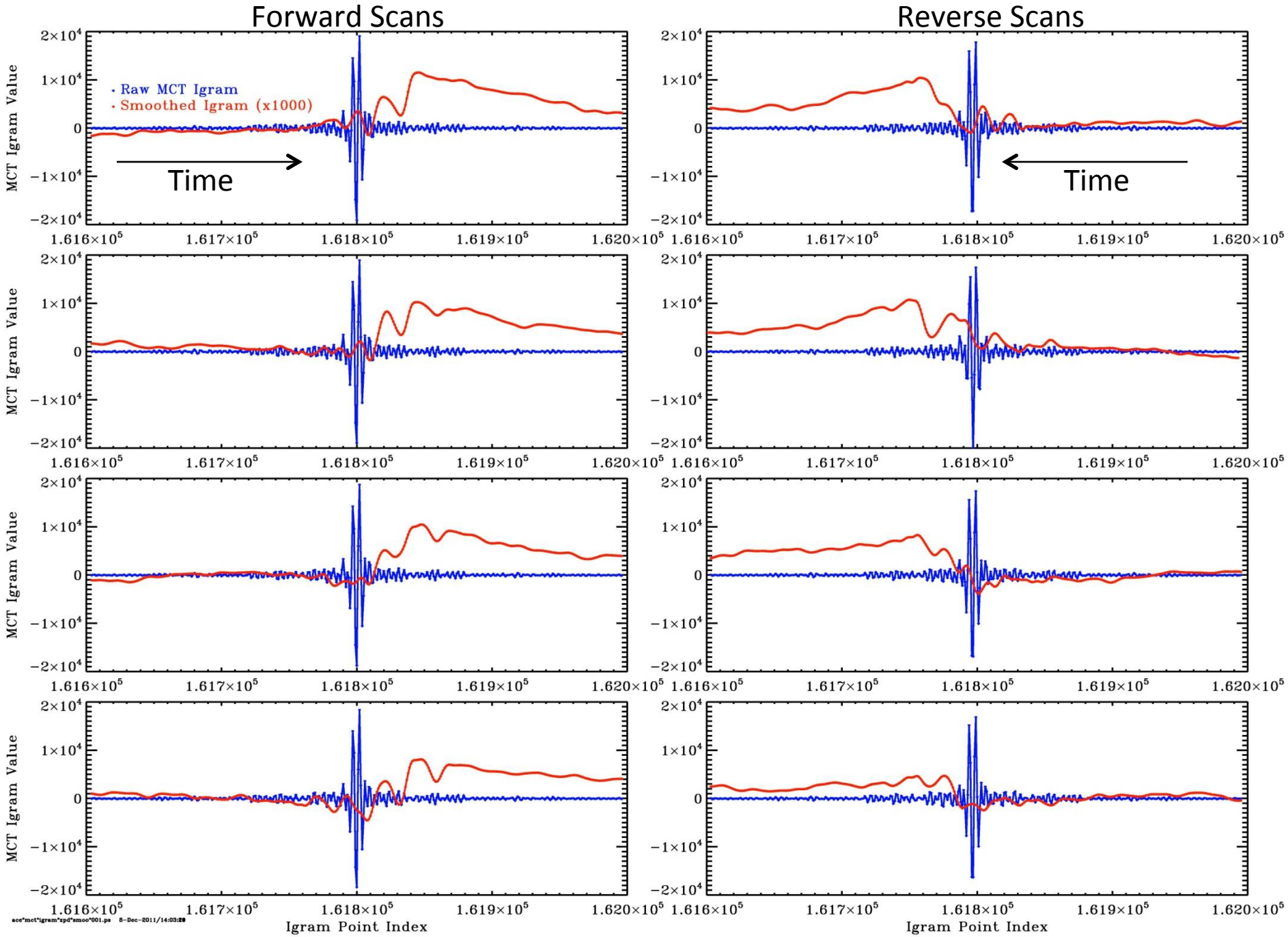
Forward Scans
Reverse Scans
Raw MCT Igram
Smoothed Igram (x1000)
Time
Time
MCT Igram Value
Igram Point Index
2×10^4
1×10^4
0
−1×10^4
−2×10^4
1.616×10^5
1.617×10^5
1.618×10^5
1.619×10^5
1.620×10^5

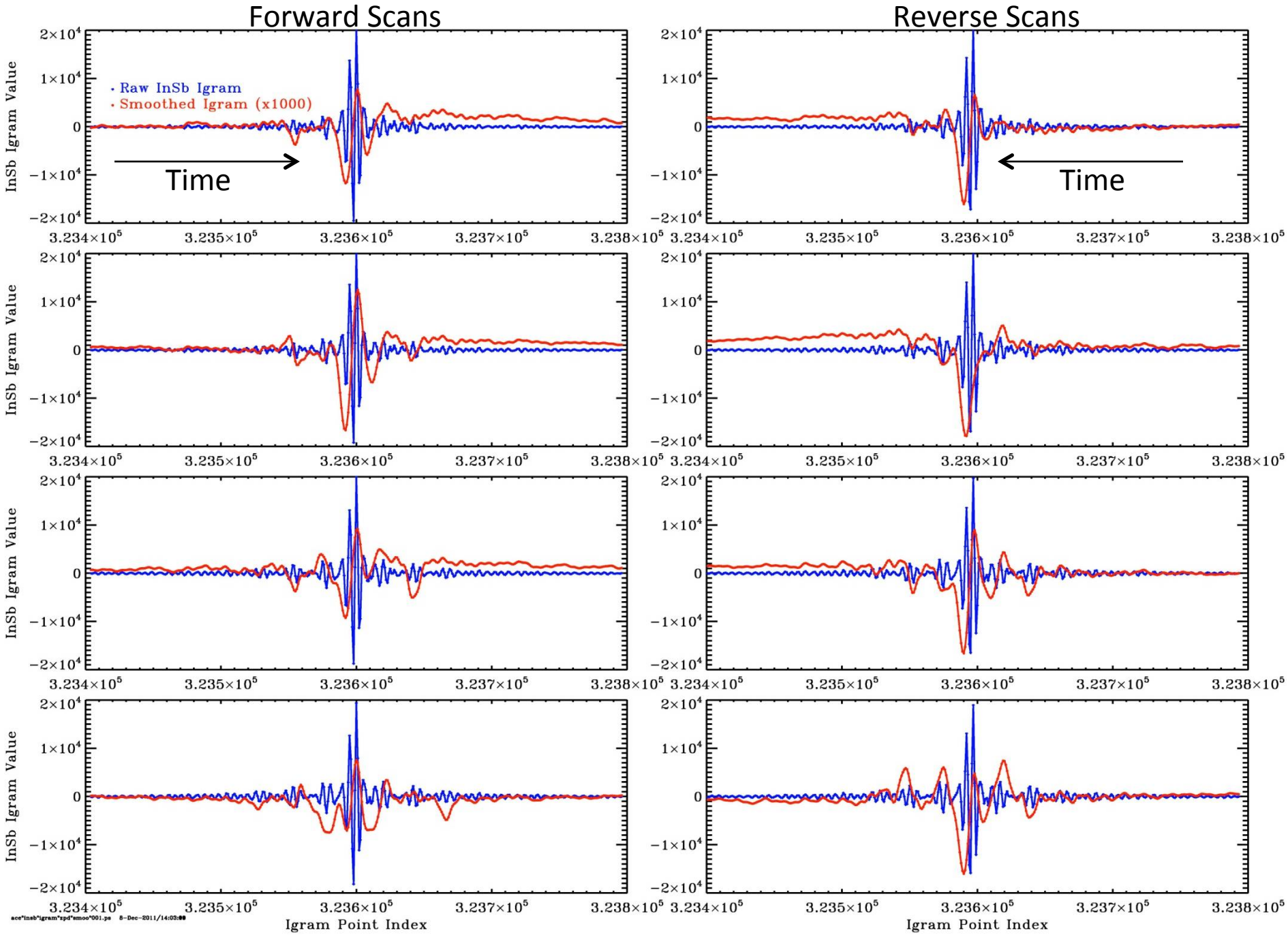
Forward Scans
Reverse Scans
Raw InSb Igram
Smoothed Igram (x1000)
Time
Time
InSb Igram Value
Igram Point Index
2×10^4
1×10^4
0
−1×10^4
−2×10^4
3.234×10^5
3.235×10^5
3.236×10^5
3.237×10^5
3.238×10^5

Summary/Conclusions – Interferogram ZPD dips

ZPD dips in the smoothed ACE interferogram signals are very small (<0.1%)

This means one or more of the following is true:

- ACE detectors are highly linear
- AC coupling has removed the low-frequency component of the dip
- Interferograms have already been correction for detector non-linearity

While these results are consistent with the ACE detectors being highly linear, they are not conclusive.

ACE Spectra

To try to obtain a more conclusive confirmation of the high linearity of the ACE detectors, the previously-shown interferograms were phase corrected and Fourier transformed into spectra.

The effect of non-linearity (anywhere in the signal chain) is to create sum and difference frequencies, whose amplitude depends on the amount of non-linearity.

For a broad-band source, the totality of these sum/difference frequencies varies very slowly with wavenumber (it is the convolution of the spectrum with itself)

The sum/difference frequencies cause a zero level offset in the spectrum.

This is most apparent in spectral regions where we know that there is no signal, e.g. wavenumbers below the detector cut-on.

Example of ACE High-Sun Spectrum

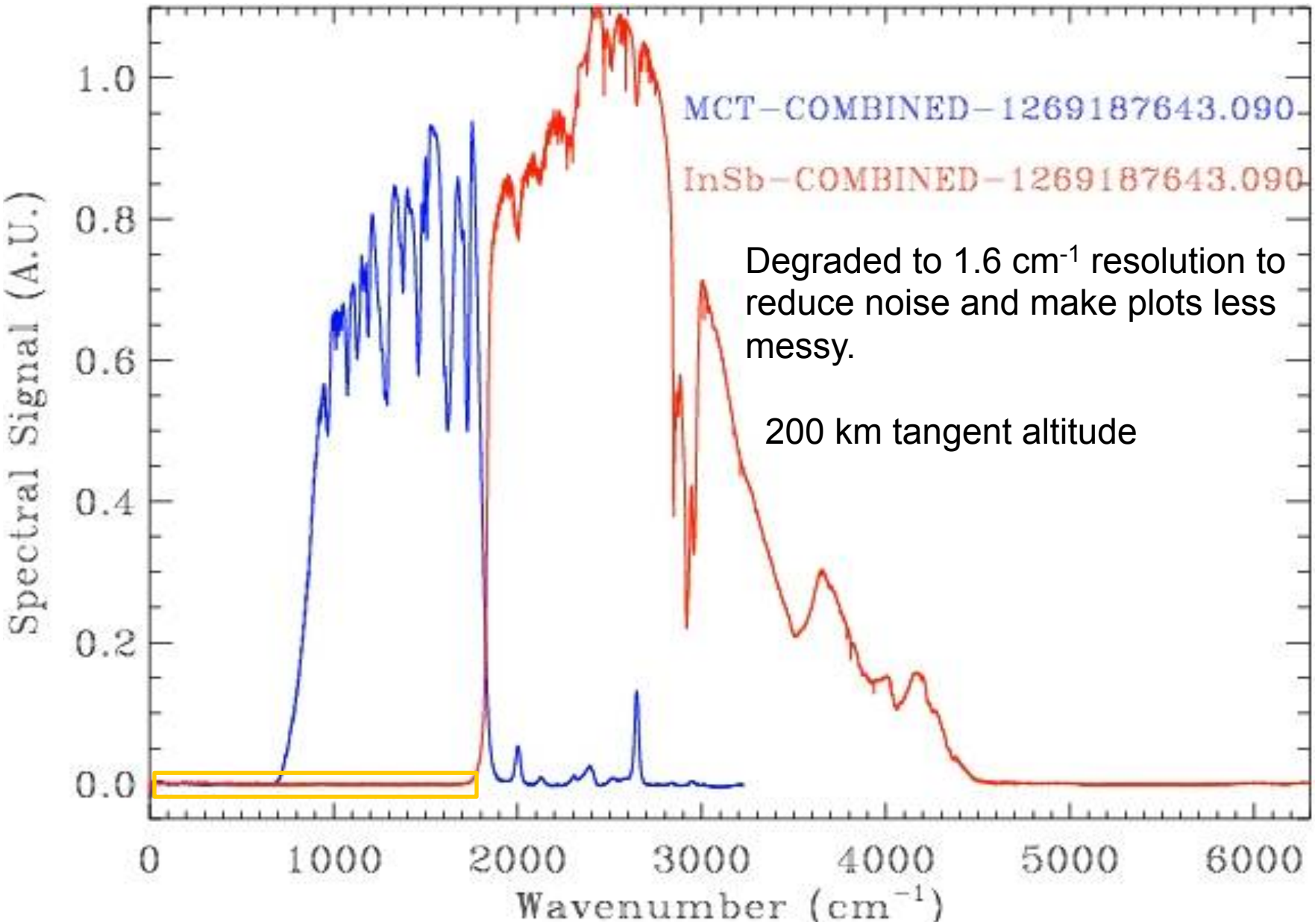

How does igram non-linearity relate to zero-offsets in the spectra?

Assume that only the largest (ZPD) interferogram point is affected by non-linearity (implicitly assumes a narrow ZPD region and a broad spectral bandwidth).

This interferogram point sets the DC level in the spectrum.

So if the largest igram point is reduced by 1% due to non-linearity, the mean spectral level will be reduced by 1%.

This will cause a zero level offset of 0.5% of the peak spectrum signal.

So to within a factor 2, the fractional zero-level offset in the spectrum is equal to the fractional non-linearity in the interferogram at ZPD.

XXXX-COMBINED-1269187643.090

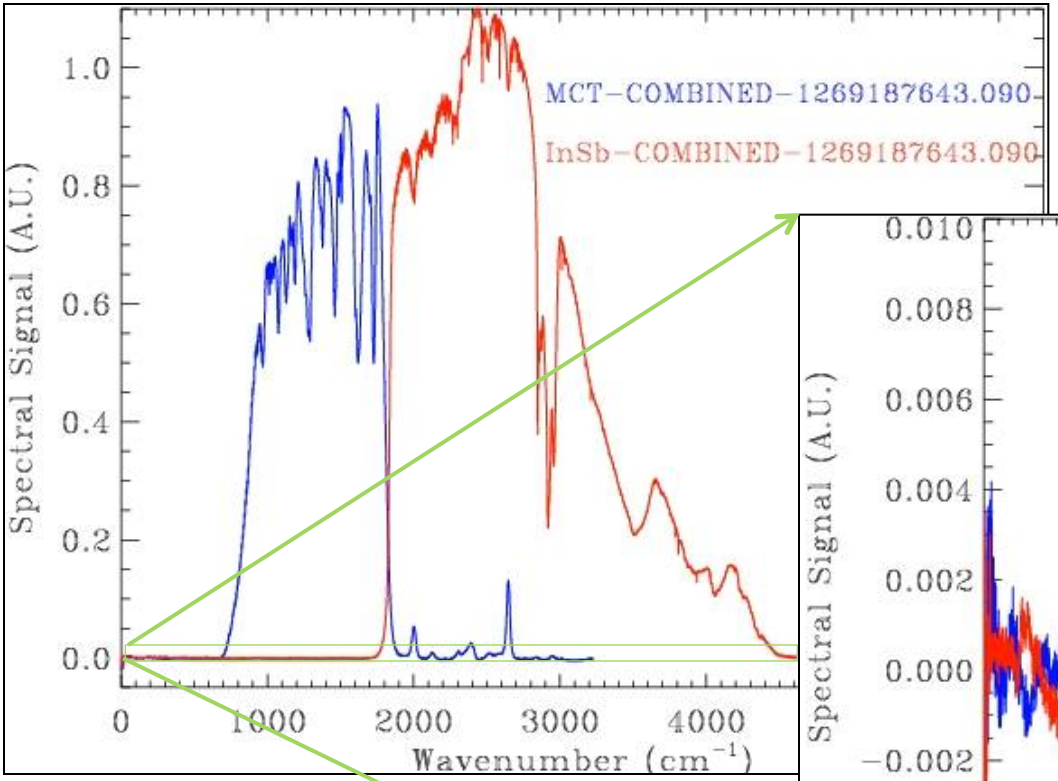

Factor 100 zoom into zero level

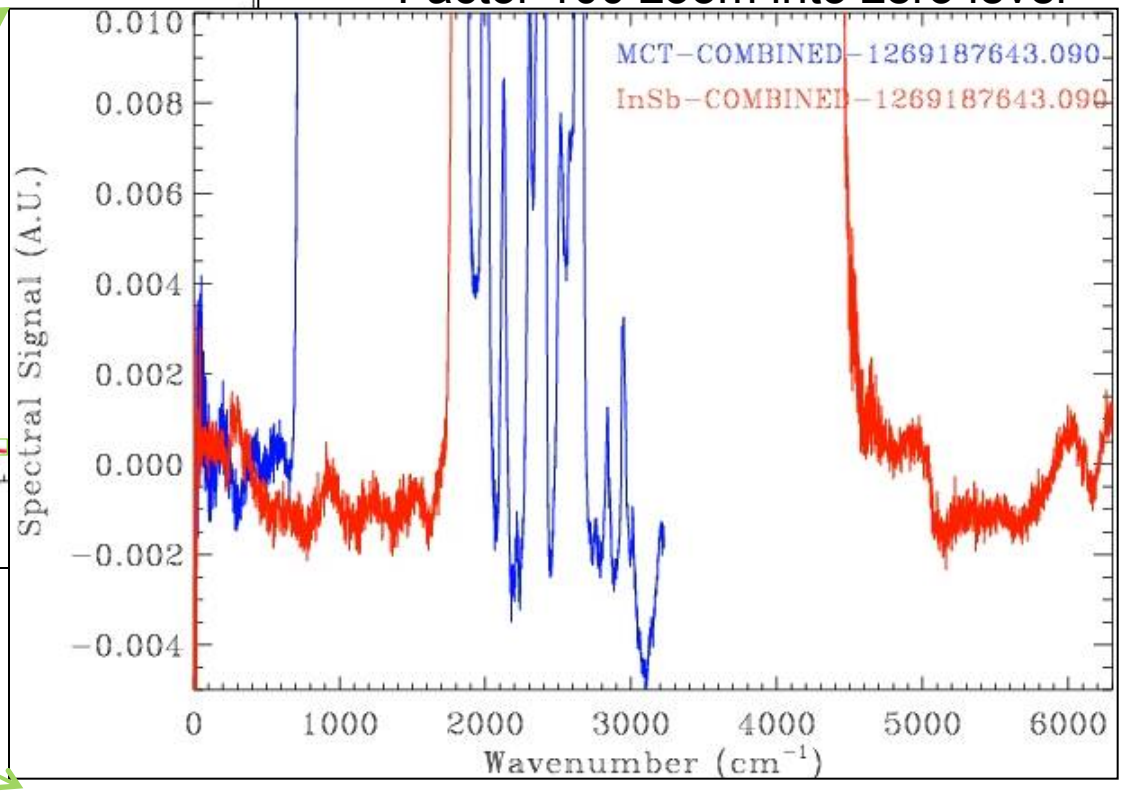

XXXX-COMBINED-1269187725.750

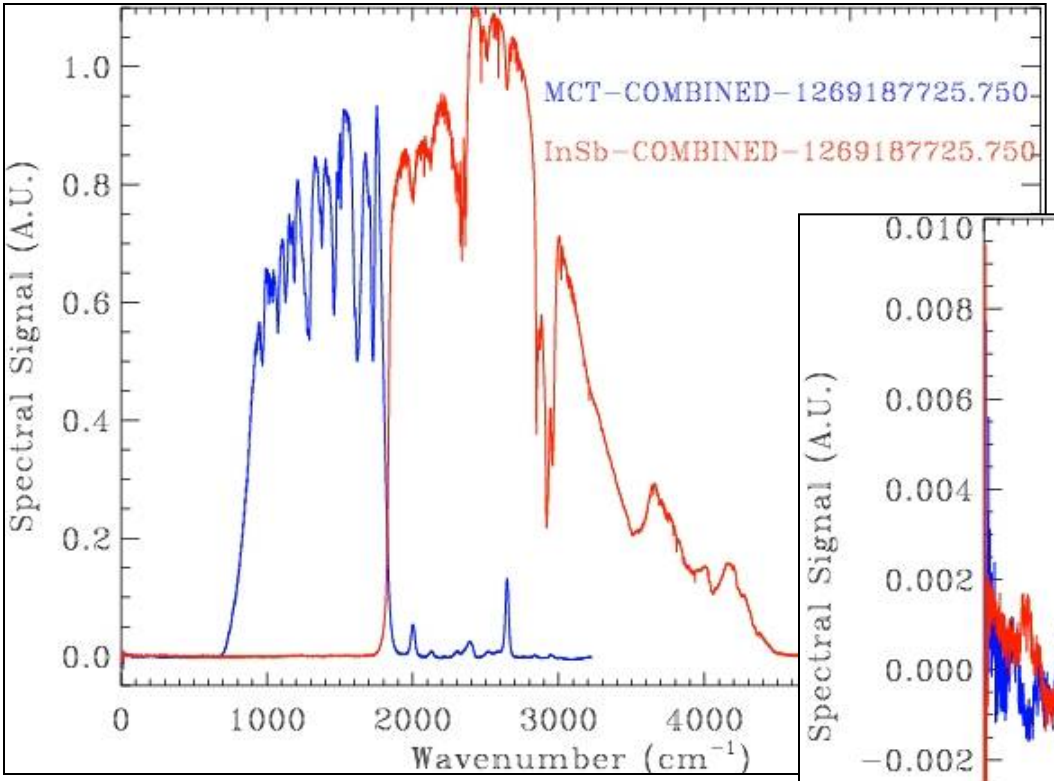

Factor 100 zoom into zero level

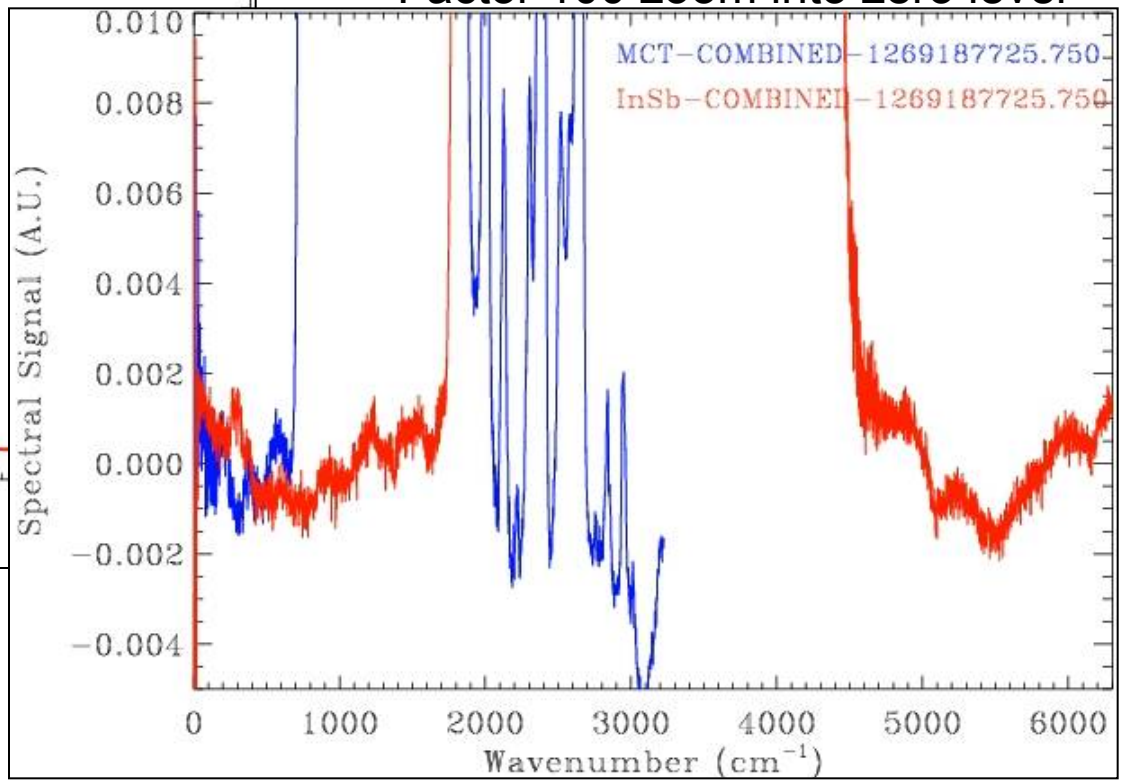

XXXX-COMBINED-1269187740.219

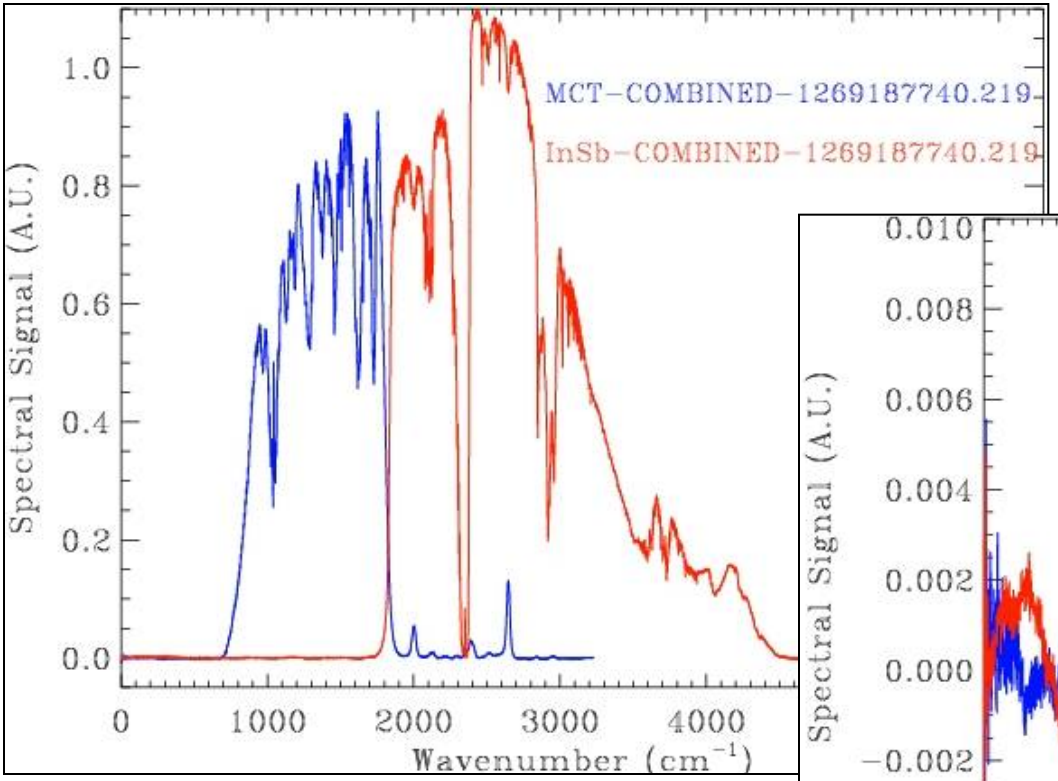

Factor 100 zoom into zero level

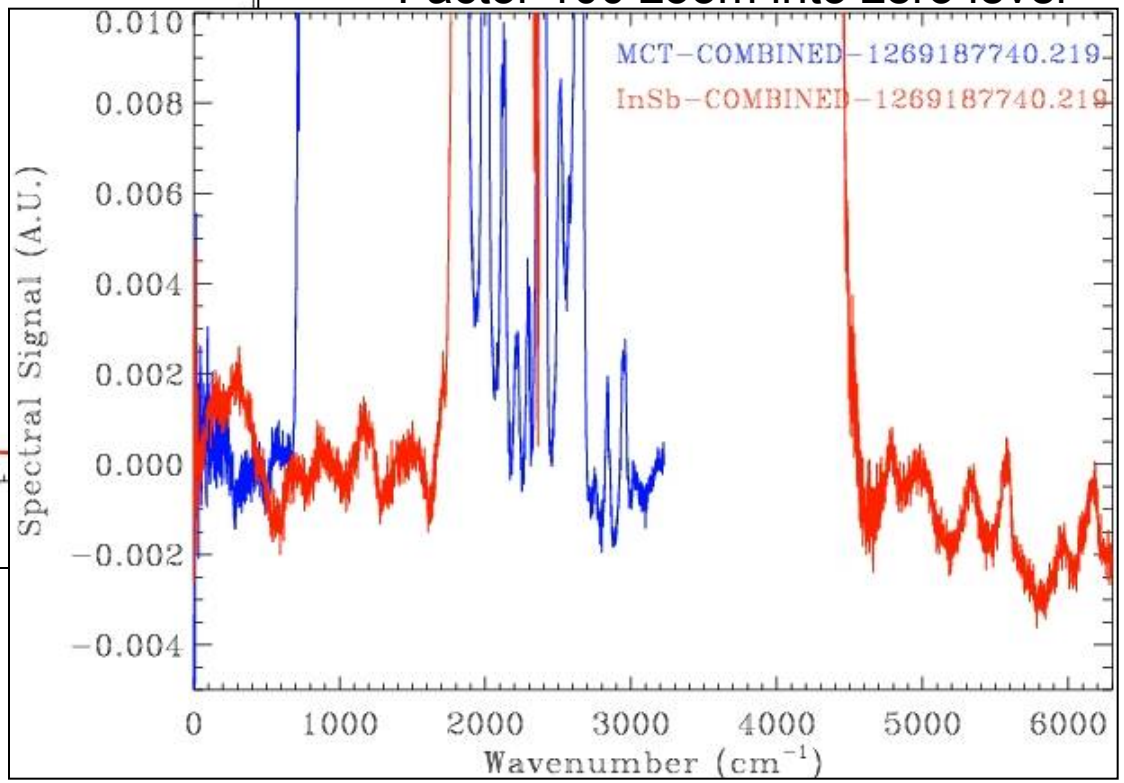

Conclusions – ACE Spectral Offsets

Examined 3 ACE spectra representing ~200 km, 60 km, 40 km altitudes.

In low wavenumber spectral regions, where we know the ACE detectors have no response, spectral offset are < 0.15%.

This implies that the non-linearity in these interferograms is < 0.3%

So at the flux levels seen from space, the ACE detectors are linear to better than 99.7%, unless:

- There is an opposite compensating non-linearity in the pre-amps (unlikely)
- The interferograms have already been corrected for non-linearity (unlikely)

CH_3Cl Linelist Evaluation

Geoffrey Toon, Linda Brown, Jet Propulsion Laboratory
Agnes Perrin, U Paris,
David Jacquemart , CNRS Jussieu

A CH_3Cl linelist has been developed by Bray, Perrin, Jacquemart, et al. See:

C. Bray, A.Perrin, D.Jacquemart, N.Lacome, The ν_1, ν_4 and $3\nu_6$ bands of methyl chloride in the 3.4-um region: Line positions and intensities, Journal of Quantitative Spectroscopy & Radiative Transfer 112 (2011) 2446–2462

C. Bray, D. Jacquemart, J. Buldyreva, N. Lacome, A. Perrin, N2-broadening coefficients of methyl chloride at room temperature, Journal of Quantitative Spectroscopy & Radiative Transfer, 2012 (in press)

This is a proper quantum-mechanically-based linelist generated by highly reputable spectroscopists (not a pseudo-linelist).

In this presentation, Kitt Peak laboratory spectra and MkIV balloon spectra are used to evaluate this new linelist.

http://vpl.astro.washington.edu

Fundamental vibrational frequencies of molecules in database (cm^{-1})

Molecule	ν_1	ν_2	ν_3	ν_4	ν_5	ν_6
Methyl chloride (CH_3Cl)	2937	1355	732	*3039*	*1452*	*1017*

Methyl chloride images from PNNL

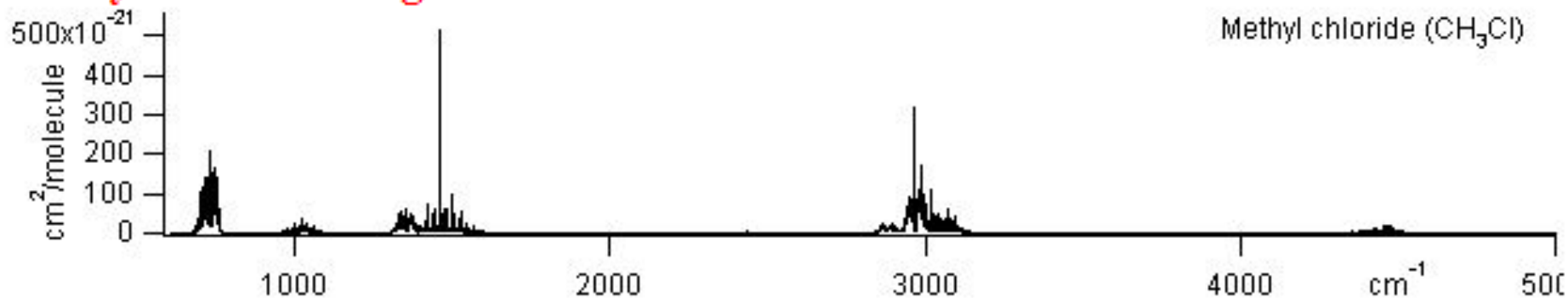

2960 cm^{-1} region does not contain the strongest IR CH_3Cl feature, but it is the best for remote sensing of the troposphere since the 1500 cm^{-1} region blacks out below 12 km.

2960 cm^{-1} region is messy due to overlap (and interaction) of ν_1, ν_4, $2\nu_5$, $2\nu_3+\nu_5$ & $3\nu_6$

Fit to MkIV balloon spectrum at 8.3 km

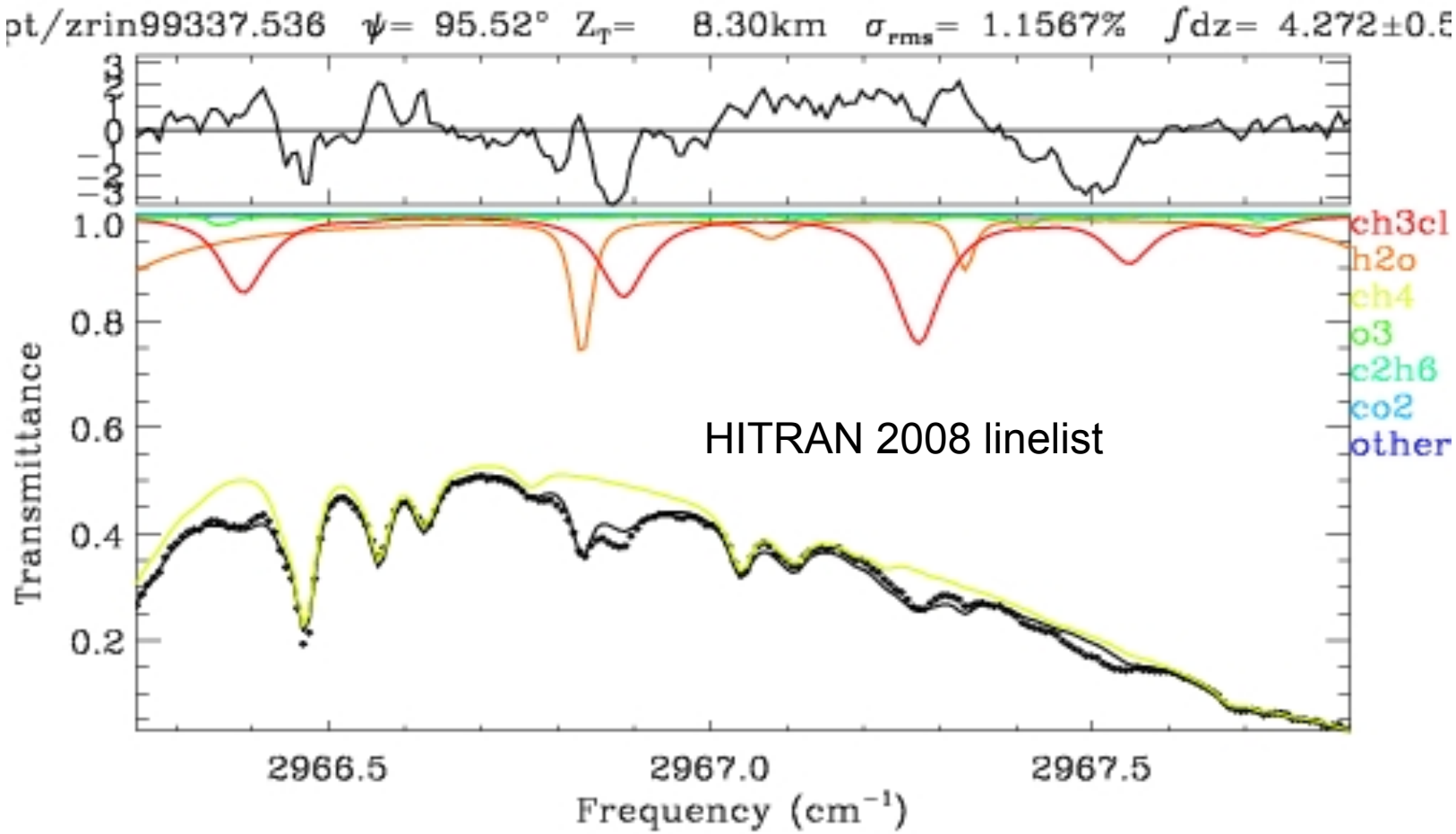

Largest residuals result from omission of C_2H_6 in this region of HITRAN_2008. Henceforth, in this presentation, a C_2H_6 pseudo-linelist (PLL) will be used, based on the work of Harrison and Bernath [2011].

Fit to same MkIV balloon spectrum

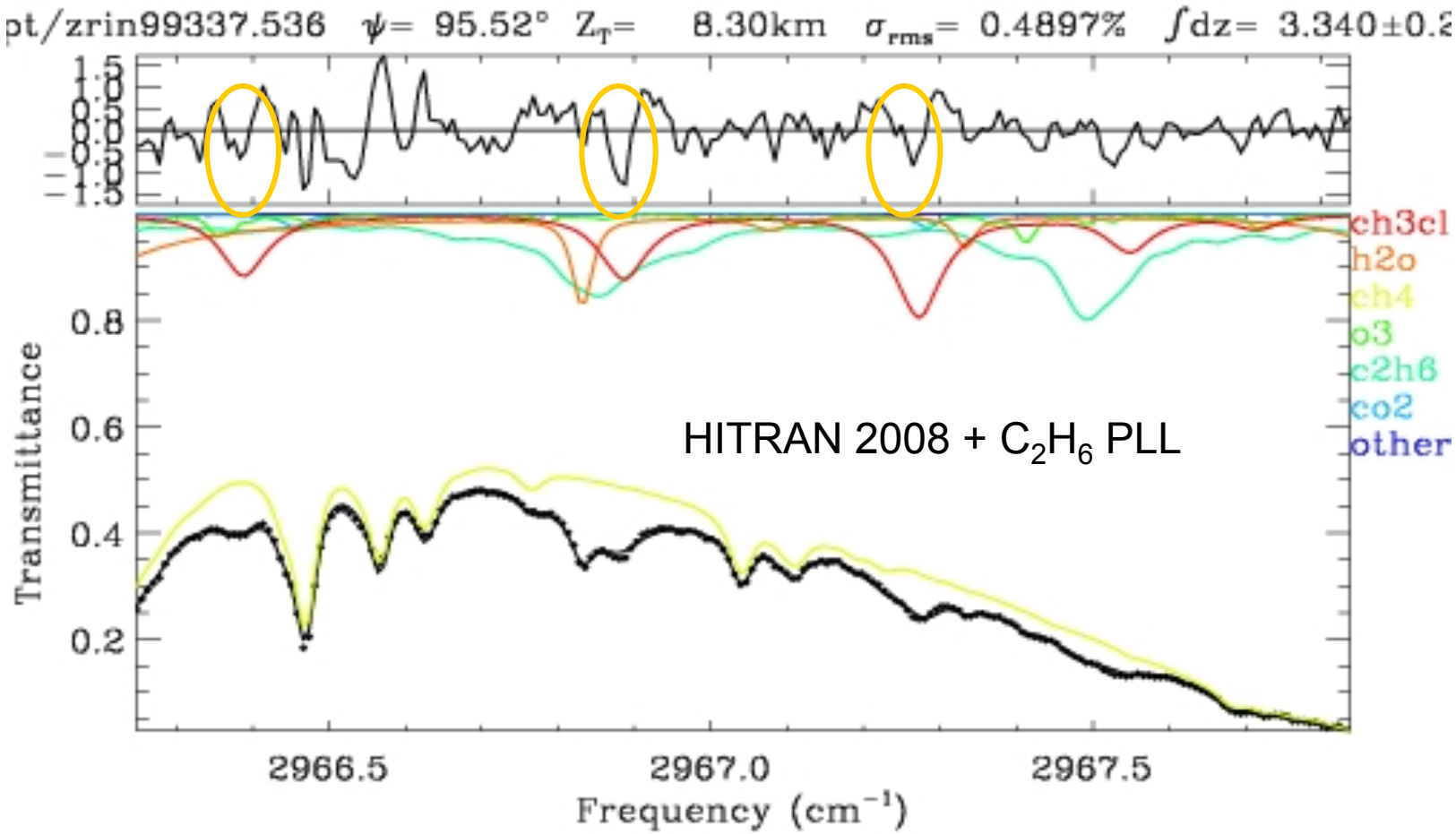

Including C_2H_6 PLL results in a factor 2-3 improvement in the residuals.
But two serious problems remain with the HITRAN CH_3Cl:
(1) Systematic "dips" in the residuals, (2) Limited spectral coverage

Lab Spectra

Look at some laboratory spectra of CH_3Cl measured by Linda Brown in 1994 at Kitt Peak. Used a 4.4m cell at 0.02 cm^{-1} spectral resolution.

Pure gas sample at 290K and 0.3 Torr
Air-broadened sample at 290K and 289 Torr

See if same systematic residuals appear in fits to the lab spectra.

Fit to Kitt Peak Lab spectrum (289 Torr)

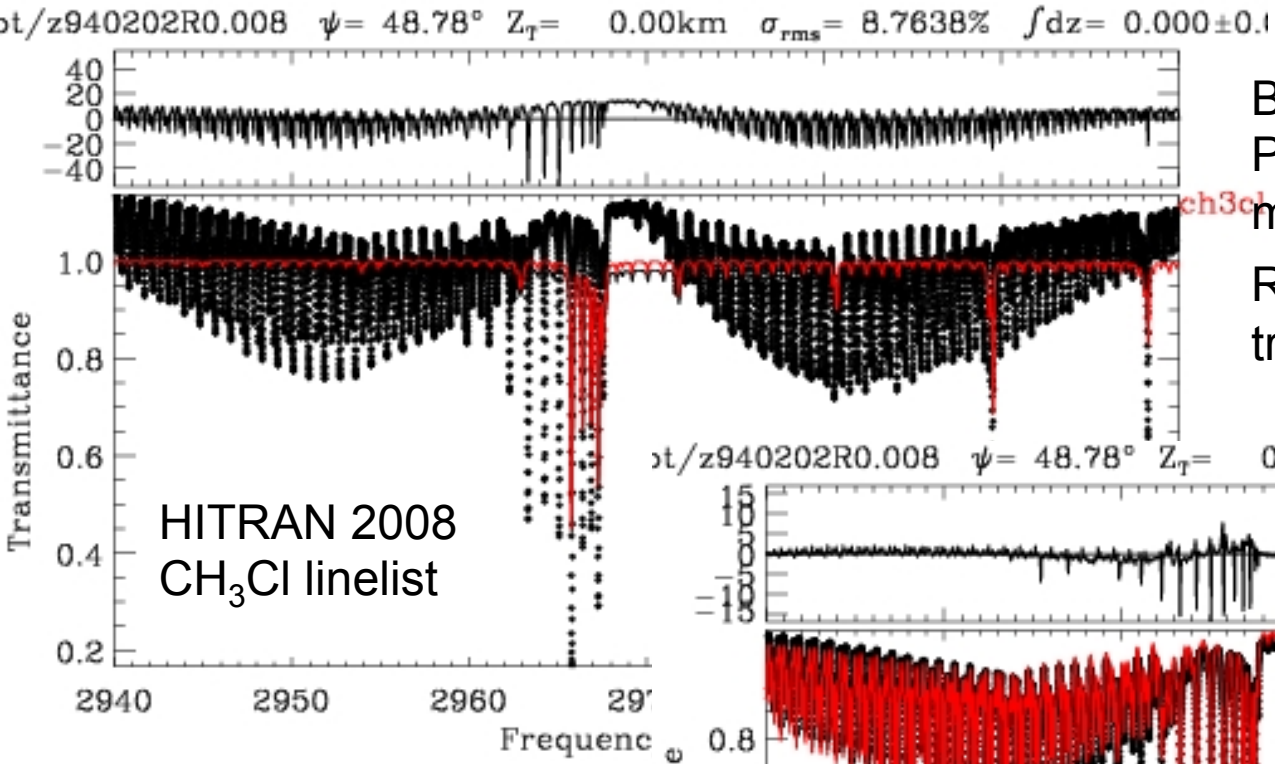

Black points: measured Kitt Peak transmittance spectra measured in 1994 (L.Brown)

Red Line: Calculated CH_3Cl transmittance

HITRAN 2008 CH_3Cl linelist

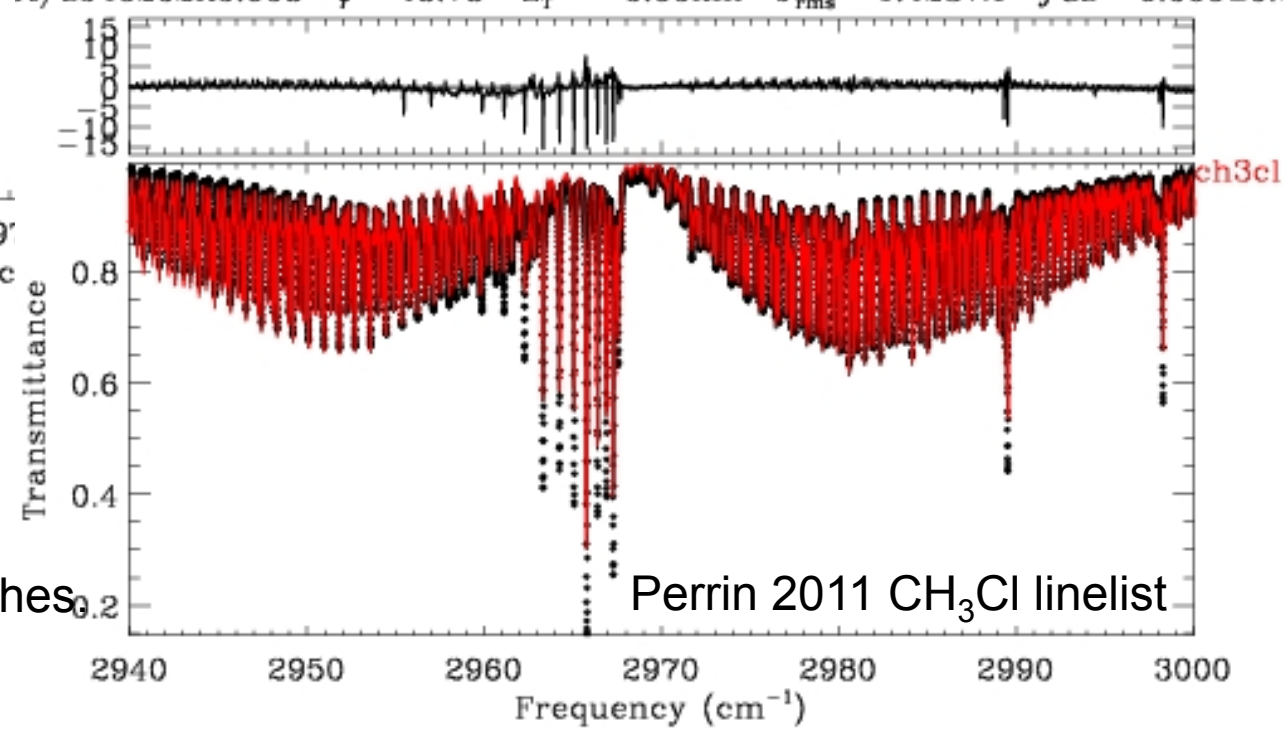

Perrin linelist is much more complete including:

- All Q-branches
- P- and R-branches

But still residuals at Q-branches. Need to investigate these.

Perrin 2011 CH_3Cl linelist

Fits to Kitt Peak Laboratory Spectra

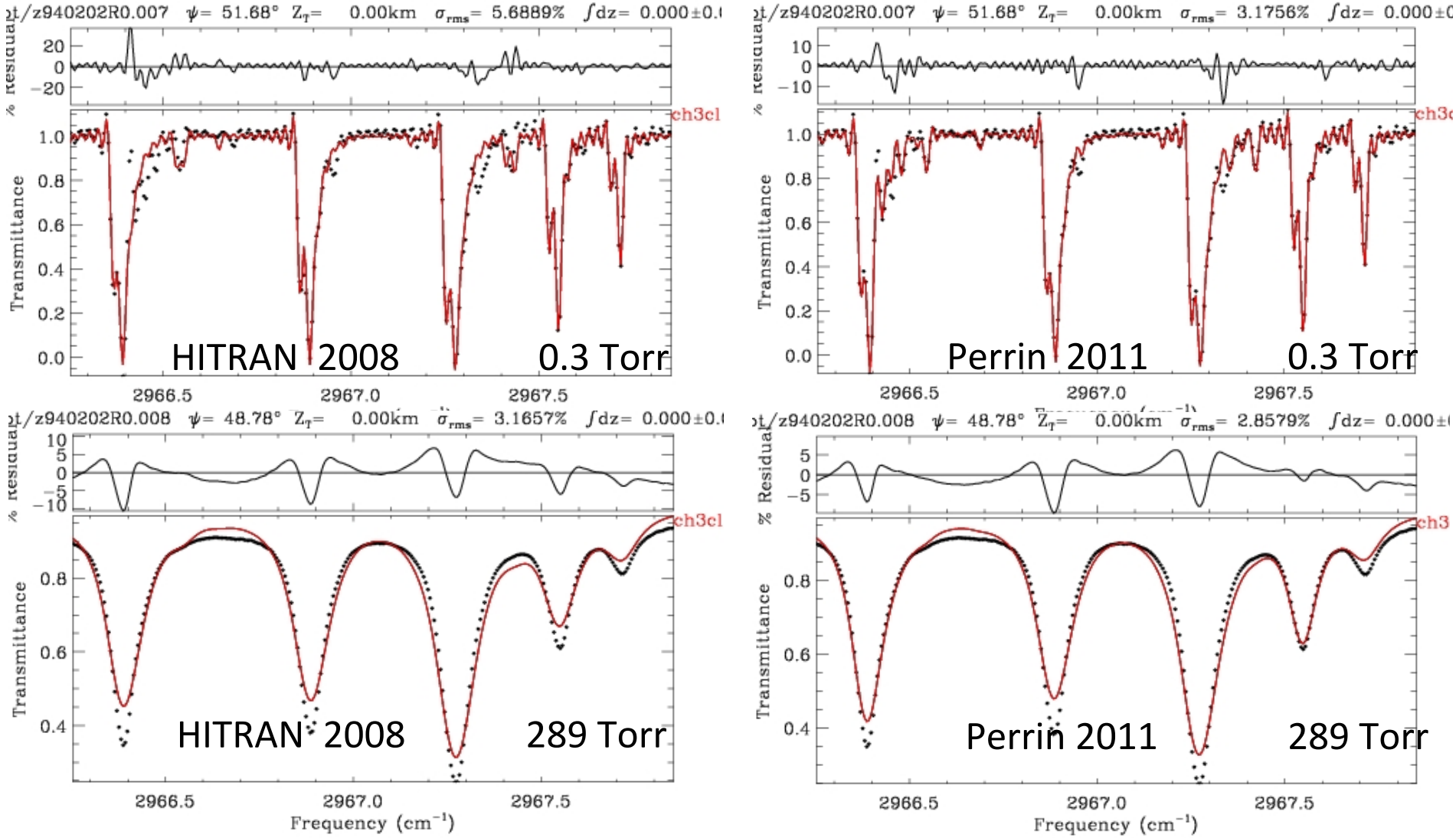

Even for the Q-branches covered by HITRAN 2008, the Perrin linelist is better, both at 0.3 Torr and at 289 Torr. But the systematic over-estimation of the widths remains.

Fits to Kitt Peak Lab spectra (289 Torr)

To understand residuals, plot the fits using different colors for P/R- & Q-branches

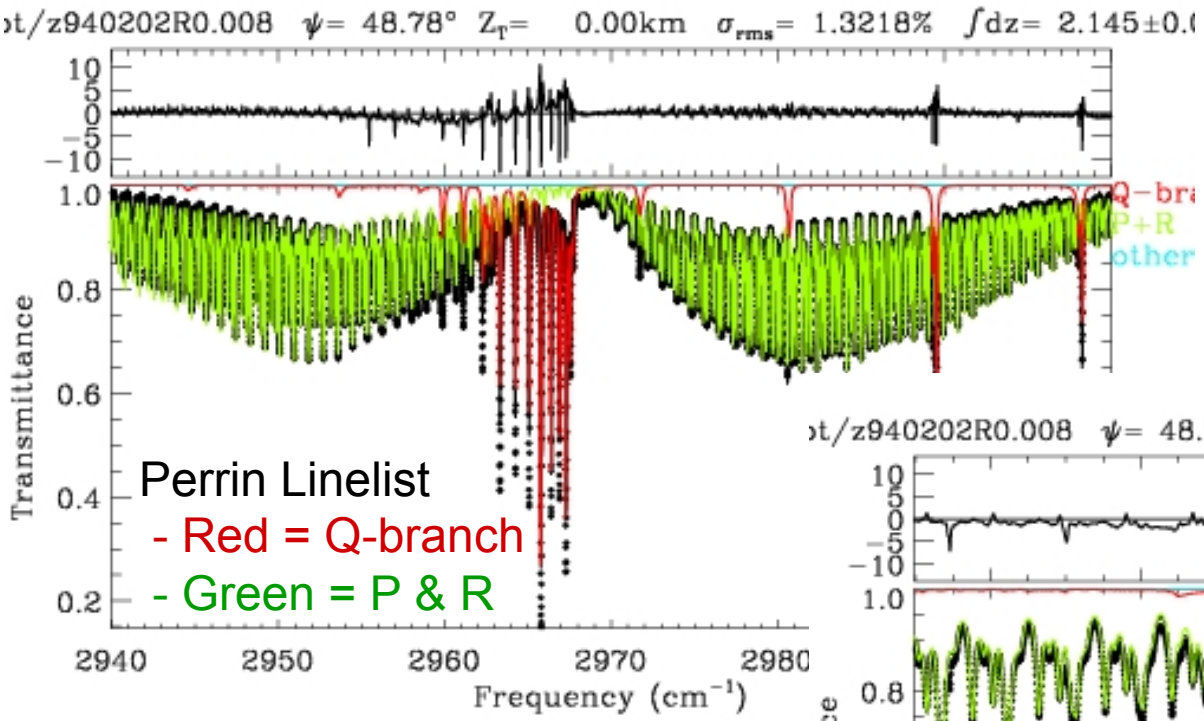

Largest residuals correspond to Q-branch absorption lines (red). P & R-branches (green) are fitted very well.

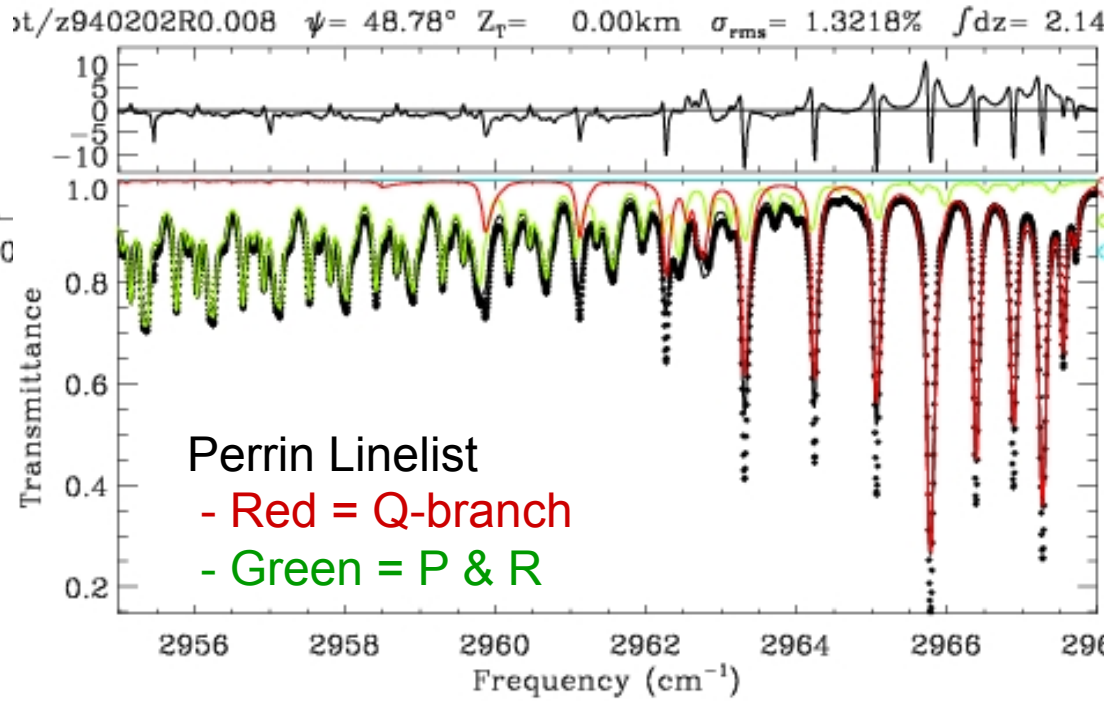

Measured Q-branches appear narrower than the calculations, causing large residuals.

Line Mixing in CH_3Cl ?

What could cause the Q-branches to be over-broadened in the Voigt calculation, but the P & R-branches fit so nicely?

The Q-branches consist of many overlapping individual lines. These would mix with each other causing the width of the feature to appear narrower than expected.

Unfortunately, I have no code to compute line-mixing in CH_3Cl. Neglecting LM not only causes poor fitting residuals, it also causes the retrieved VMR profiles to be biased high in the lower atmosphere.

So, how to take advantage of the major spectroscopic advances embodied in Perrin's CH_3Cl linelist, and not get skewed CH3Cl profiles with worse fits than previously?

Implemented a "kludge" in the line-by-line code that reads the linelist and computes the absorption coefficients: Reduces widths by 37% for CH_3Cl Q-branch lines, leaving the P & R-branch lines unchanged.

This is a temporary solution, until a proper line-mixing code is available.

New Fits to Kitt Peak Lab spectra

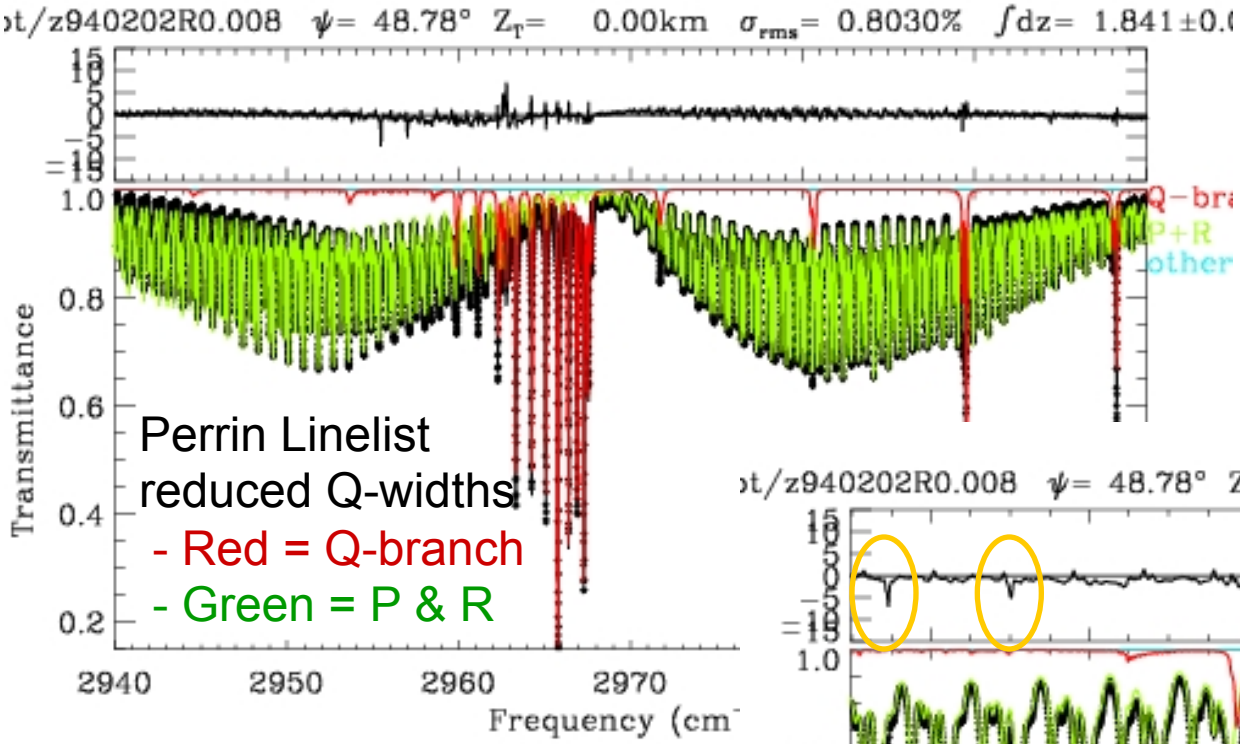

After reducing Q-branch widths, residuals improved from 1.32% to 0.80%

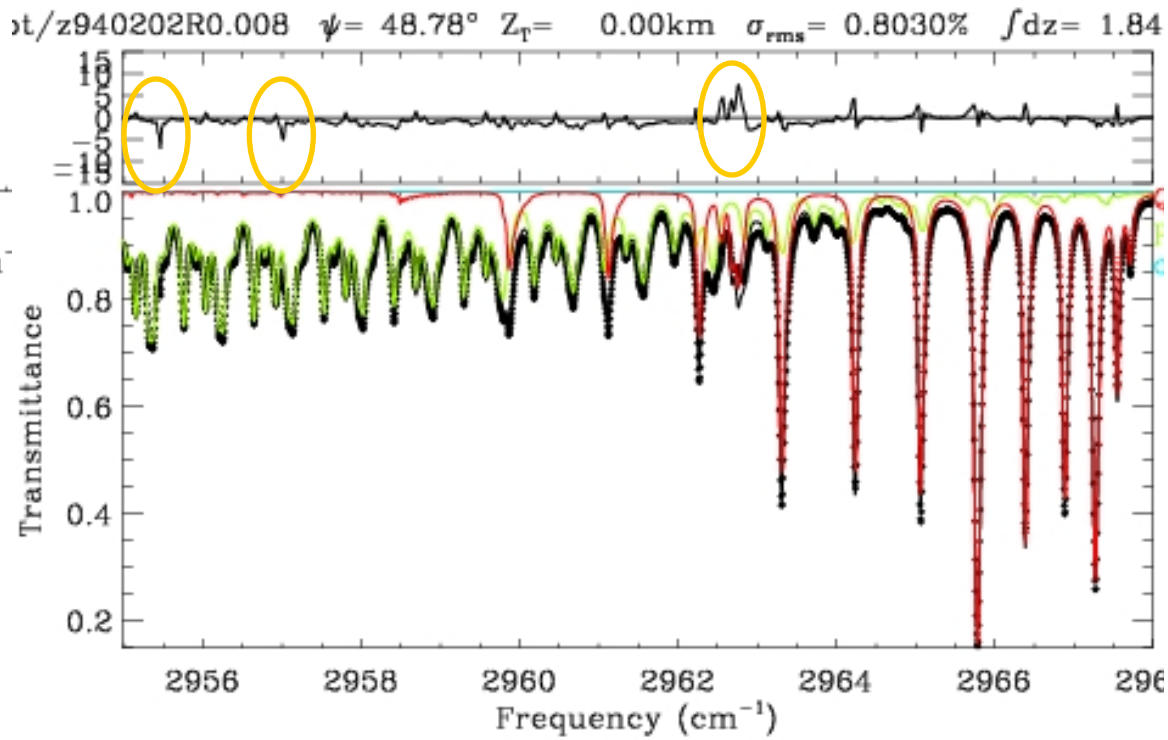

Still not perfect. Residuals now dominated by:

1) Missing Q-branches (?) at 2955.45 and 2957.0 cm^{-1}

2) Mis-shaped Q-branch at 2962.75 cm^{-1}

[See yellow circles →]

Fits to Kitt Peak Lab spectrum (289 Torr)

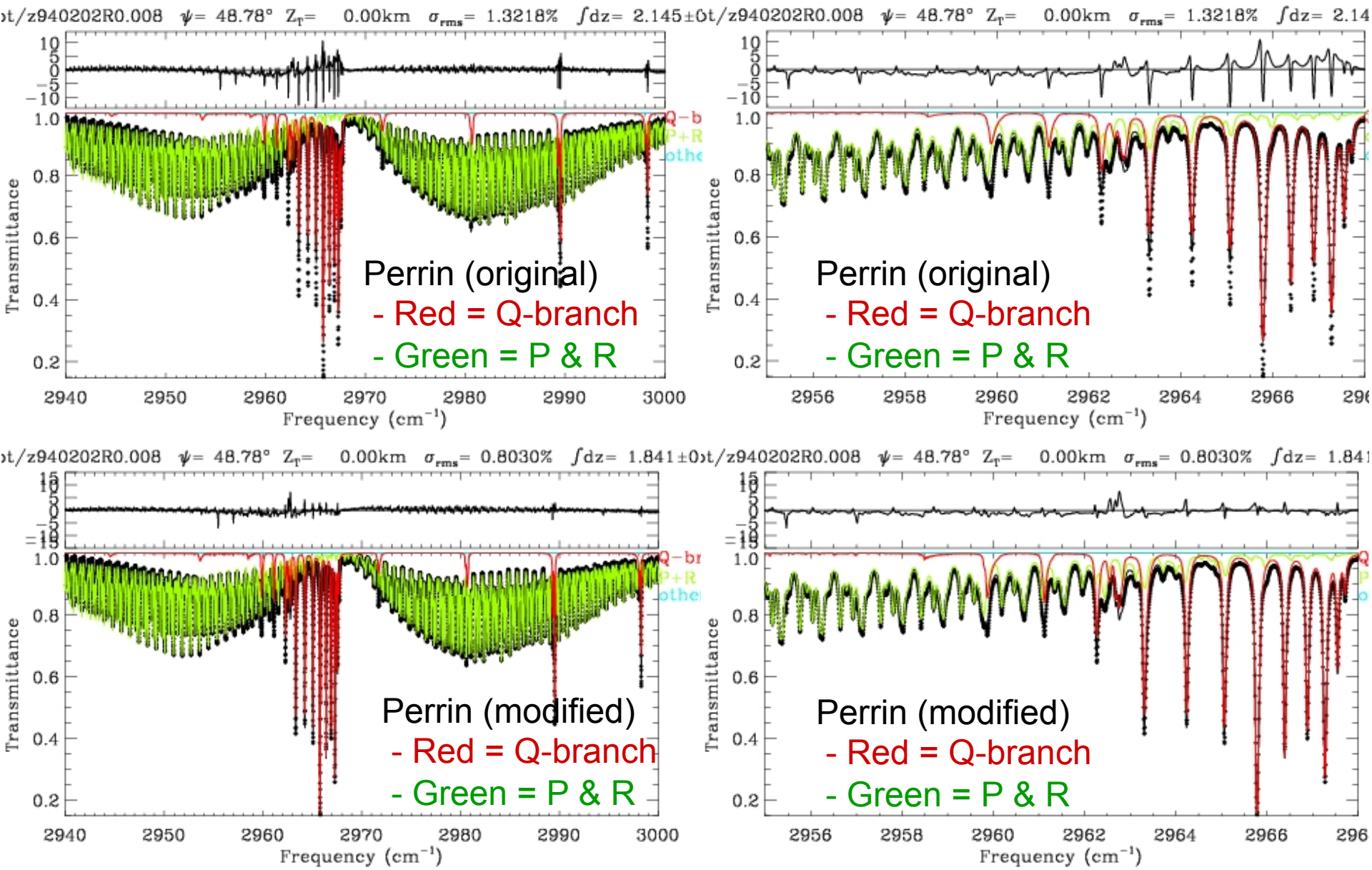

Effect on MkIV balloon retrievals

Three main advantages:

1) Better fits in the 2967.05 +/- 0.8 cm^{-1} window leading to a more accurate retrieved vmr profile
2) Enables the use of a wider CH_3Cl fitting window, which was precluded by the HITRAN CH_3Cl linelist [Some of the CH_3Cl Q-branches missing from HITRAN 2008 are 10% deep in solar occultation spectra at 8 km tangent altitude].
3) Improved retrievals of other gases whose absorptionlines are overlapped by missing CH_3Cl lines.

Fits to MkIV balloon spectra (Z_T=8.3 km)

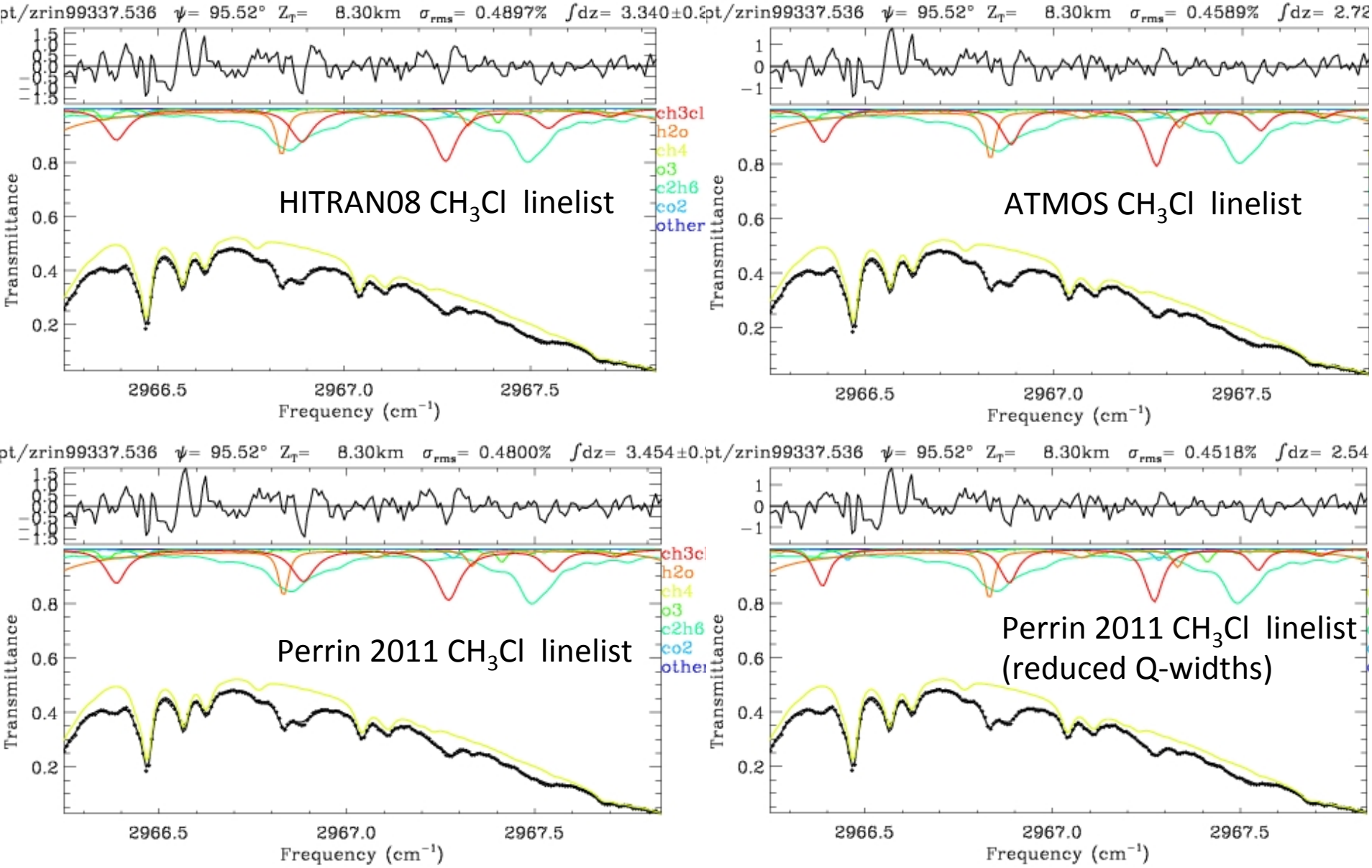

MkIV Balloon CH_3Cl profiles (1999)

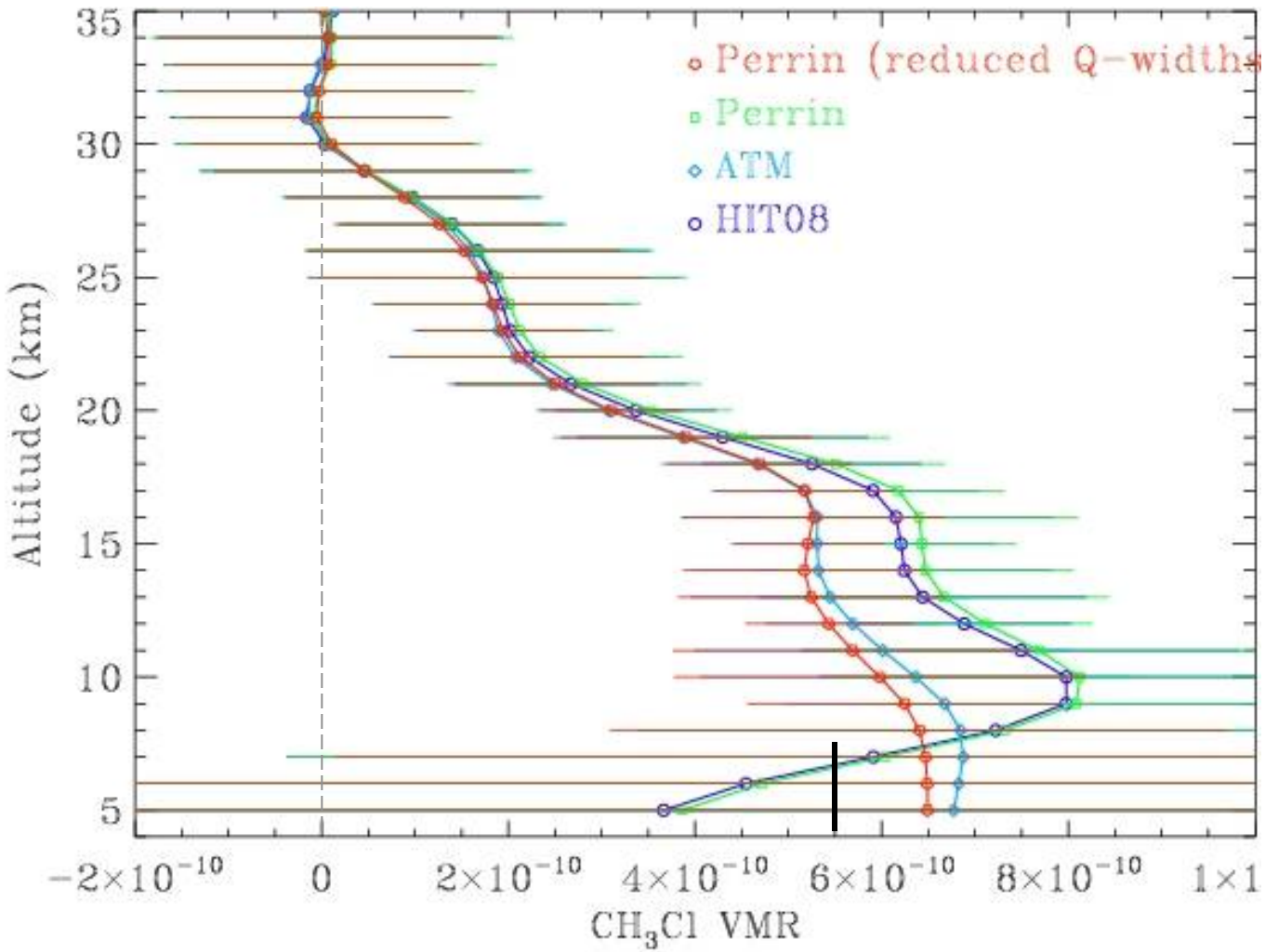

MkIV Balloon CH_3Cl Profiles (2003)

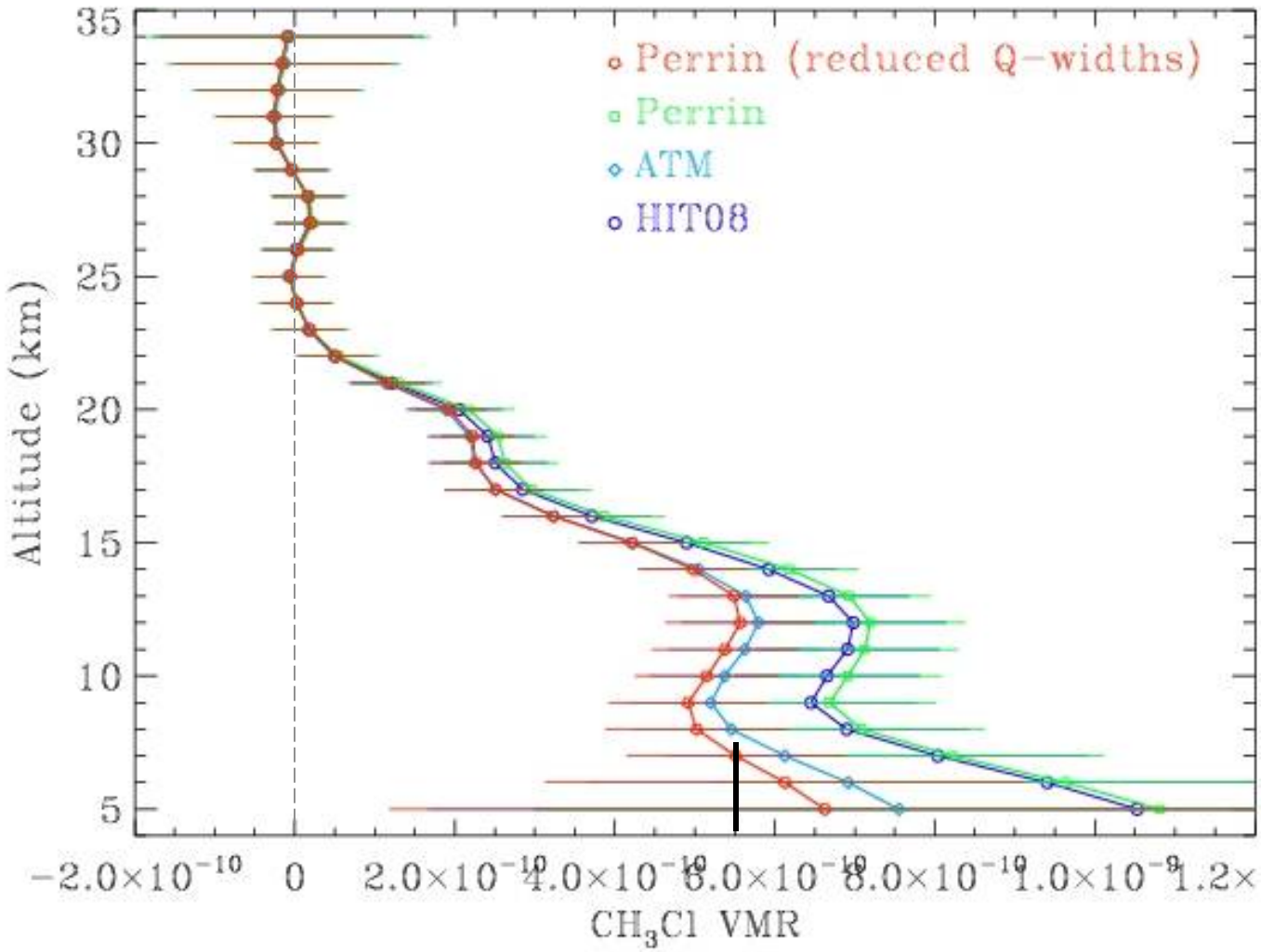

Fits to same spectrum: wider window

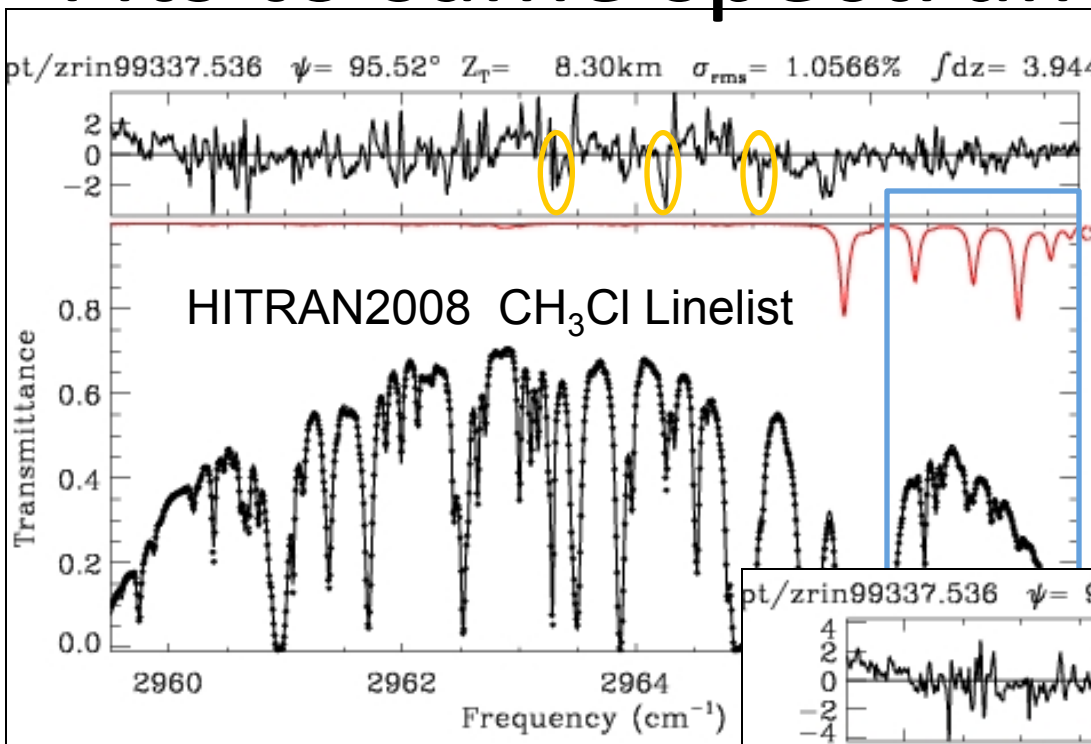

CH_3Cl Q-branches missing From HITRAN are 10% deep at 8 km tangent altitude.

Using Perrin 2011 CH_3Cl linelist improves residuals

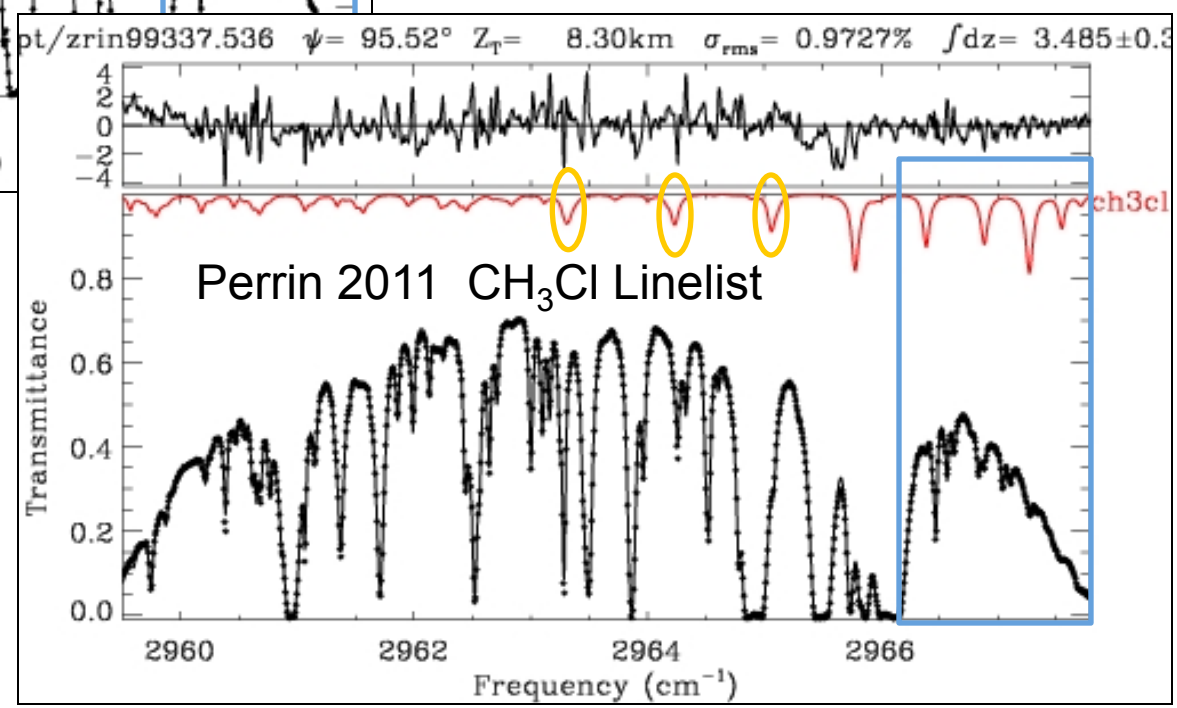

Blue rectangle shows spectral region fitted in previous plots.

In wider window, residuals dominated by poor CH_4 spectroscopy (widths).

Summary/Conclusions (1)

HITRAN 2008 CH_3Cl linelist is severely deficient:
• contains only 5/10 strongest Q-branches in the 2960-2968 cm^{-1} region.
• most of the P- and R-branch structure is missing or under-represented.

Fits to Kitt Peak Lab spectra with Perrin 2011 linelist are better than with HITRAN:
• factor of 6 times better RMS residual over entire band
• 10% better RMS residual over Q-branches represented in HITRAN 2008

Widths of the Q-branch features over-estimated in a Voigt line-by-line calculation, both in lab and atmospheric spectra. Widths of P- & R-branch features are good.

Likely that my neglect of line mixing is the cause of this over-broadening. Awaiting line-mixing parameterization from David Jacquemart.

In the absence of CH_3Cl line-mixing code, reducing the Q-branch line widths by 37% improves fits to lab and atmospheric spectra.

[To be clear, there is no problem with Perrin's widths. Reducing them is just a convenient way of representing the main effects of line-mixing]

Summary/Conclusions (2)

In fits to Lab spectra, performed with the 37% Q-branch width reduction:
- Perrin's ^{35}Cl and ^{37}Cl intensities are consistent to better than 3%
- Perrin's P-, Q- and R-branch intensities are consistent to better than 2%

In fits to MkIV atmospheric spectra:
- Retrieved CH_3Cl profiles are more realistic (closer to 550 ppt in the lower trop)
- Retrieval Uncertainties are smaller

Future Work
- Implement Line Mixing into CH_3Cl LBL calculations (instead of reducing Q-widths)
- Explore the use of wider windows for the retrieval of CH_3Cl (incl. P- & R-branch)
- Quantify effect of new CH_3Cl linelist on other gas retrievals in 2900-3100 cm^{-1} region.

This linelist should be incorporated into HITRAN at the earliest opportunity

Supplemental Material

Journal of Quantitative Spectroscopy & Radiative Transfer ▮ (▮▮▮▮) ▮▮▮–▮▮▮

Contents lists available at SciVerse ScienceDirect

Journal of Quantitative Spectroscopy & Radiative Transfer

journal homepage: www.elsevier.com/locate/jqsrt

N_2-broadening coefficients of methyl chloride at room temperature

C. Bray[a,b,*], D. Jacquemart[a,b], J. Buldyreva[c], N. Lacome[a,b], A. Perrin[d]

[a] Laboratoire de Dynamique, Interactions et Réactivité, UPMC Univ Paris 06, UMR 7075, Case Courrier 49, 4 Place Jussieu, 75252 Paris Cedex 05, France
[b] Laboratoire de Dynamique, Interactions et Réactivité, CNRS, UMR 7075, Case Courrier 49, 4 Place Jussieu, 75252 Paris Cedex 05, France
[c] Institut UTINAM, UMR CNRS 6213, Université de Franche-Comté, 16 Route de Gray, 25030 Besançon Cedex, France
[d] Laboratoire Interuniversitaire des Systèmes Atmosphériques, LISA-UMR7583, CNRS and Universités Paris Est Créteil (UPEC) and Paris Diderot- Paris 7, 1 avenue du Général de Gaulle, 94010 Créteil Cedex, France

ARTICLE INFO

Keywords:
Methyl chloride
ν_1 band
Pure rotational band
High-resolution Fourier transform spectra
N_2-broadening coefficients
Room temperature
J and *K* dependences
Semi-classical approach

ABSTRACT

Methyl chloride is of interest for atmospheric applications, since this molecule is directly involved in the catalytic destruction of ozone in the lower stratosphere. In a previous work [Bray et al. JQSRT 2011;112:2446], lines positions and intensities of self-perturbed $^{12}CH_3^{35}Cl$ and $^{12}CH_3^{37}Cl$ have been studied into details for the 3.4 μm spectral region. The present work is focused on measurement and calculation of N_2-broadening coefficients of the $^{12}CH_3^{35}Cl$ and $^{12}CH_3^{37}Cl$ isotopologues. High-resolution Fourier Transform spectra of CH_3Cl–N_2 mixtures at room-temperature have been recorded between 2800 and 3200 cm^{-1} at LADIR (using a classical source) and between 47 and 59 cm^{-1} at SOLEIL (using the synchrotron source on the AILES beamline). 612 mid-infrared transitions of the ν_1 band and 86 far-infrared transitions of the pure rotational band have been analyzed using a multispectrum fitting procedure. Average accuracy on the deduced N_2-broadening coefficients has been estimated to 5% and 10% in the mid- and far-infrared spectral regions, respectively. The *J*- and *K*-rotational dependences of these coefficients have been observed in the mid-infrared region and then a simulation has been performed using an empirical model for $0 \le J \le 50$, $K \le 9$. The $^{12}CH_3^{35}Cl$–N_2 line widths for $0 \le J \le 50$ and $K \le 10$ of the ν_1 band and for $55 \le J \le 67$ and $K \le 15$ of the pure rotational band have been computed using a semi-classical approach involving exact trajectories and a real symmetric-top geometry of the active molecule. Finally, a global

Journal of Quantitative Spectroscopy & Radiative Transfer 112 (2011) 2446–2462

Contents lists available at ScienceDirect

Journal of Quantitative Spectroscopy & Radiative Transfer

journal homepage: www.elsevier.com/locate/jqsrt

The ν_1, ν_4 and $3\nu_6$ bands of methyl chloride in the 3.4-μm region: Line positions and intensities

C. Bray [a,b], A. Perrin [c,*], D. Jacquemart [a,b], N. Lacome [a,b]

[a] UPMC Univ Paris 06, Laboratoire de Dynamique, Interactions et Réactivité, UMR 7075, Case Courrier 49, 4 Place Jussieu, 75252 Paris Cedex 05, France
[b] CNRS, UMR 7075, Laboratoire de Dynamique, Interactions et Réactivité, Case Courrier 49, 4 Place Jussieu, 75252 Paris Cedex 05, France
[c] Laboratoire Interuniversitaire des Systèmes Atmosphériques, LISA-UMR7583, CNRS and Universités Paris Est Créteil (UPEC) and Paris Diderot-Paris 7, 61 avenue du Général de Gaulle, 94010 Créteil Cedex, France

ARTICLE INFO

Article history:
Received 29 April 2011
Received in revised form
17 June 2011
Accepted 27 June 2011
Available online 3 July 2011

Keywords:
Methyl chloride
CH_3Cl
3.4 μm
High-resolution Fourier Transform spectroscopy
Effective Hamiltonian
Interacting states
Line positions
Line intensities

ABSTRACT

Methyl chloride (CH_3Cl) is one of the most abundant chlorine-containing molecules in the atmosphere. For this reason a recent update was performed in HITRAN in the 640–2600 cm^{-1} region based on the line parameters generated in Nikitin et al. [Nikitin A, Champion JP, Bürger H. J Mol Spectrosc 2005;230:174–84] with the intensities scaled to existing experimental data. CH_3Cl has a rather strong signature around 3000 cm^{-1} which was used recently by the Atmospheric Chemistry Experiment (ACE) satellite mission to produce the first study of the global distribution of methyl chloride in the upper troposphere and stratosphere. However, it was mentioned that the CH_3Cl line positions and intensities spectroscopic parameters are of very low quality in this spectral region in the public access HITRAN or GEISA databases. We present a complete update of the line positions and line intensities for the ν_1, ν_4, $3\nu_6$ bands of $CH_3\,^{35}Cl$ and $CH_3\,^{37}Cl$ in the 3.4 μm region. For this task, Fourier transform spectra have been recorded at high resolution at the Laboratoire de Dynamique, Interactions et Réactivité in France. Measurements of line positions and line intensities have been retrieved for both isotopologues $^{12}CH_3\,^{35}Cl$ and $^{12}CH_3\,^{37}Cl$ in the ν_1, ν_4, $3\nu_6$ bands. The theoretical model accounts for the interactions coupling the ($\nu_1=1$; $\ell=0$), ($\nu_4=1$; $\ell=\pm1$) and ($\nu_6=3$; $\ell=\pm1$) energy levels, together with additional resonances involving several

Validating A Priori VMR profiles

Geoff Toon
Jet Propulsion Laboratory,
California Institute of Technology
2011-12-13

The GGG retrieval code uses an empirical model to generate a priori trace gas profiles. Includes effects due to:

- Age of air
- Secular trends
- Inter-hemispheric differences
- Seasonal cycle

Model has been tweaked to optimize agreement with in-situ profiles from:

- TCCON aircraft over-flights (CO_2, CH_4, CO, N_2O)
- Air-Core (CO_2, CH_4)
- IMECC (CO_2, CH_4, CO)
- OMS Balloon

Main motivation is to support ground-based measurements (e.g., TCCON)

Recent Model Improvements

Model was improved in 2011 to better represent inter-hemispheric differences of CO, CH4, and CO_2.
Especially important for SH sites measuring CO, CH4, and CO_2.
Previous profiles were optimized for Northern Hemisphere.

Model inputs: Time, Latitude, Tropopause Altitude
Model Outputs: A VMR profile for each different gases.

In the following slides results from the 2009 and 2011 model predictions are compared with in situ profiles:

- Blue Points: In Situ data
- Green Points: 2009 A priori profiles
- Red Points: Dec 2011 A priori profiles

Bias tables computed by the program: compare_with_insitu_profiles.f
Plots made with the script: tccon_insitu_gas_profiles.log

N_2O Comparison Table

#	Site/Date/Gas	2010 Priors	2011 Priors
1	start08_parkfalls_20080512_N2O.atm	0.9927 +- 0.0082	0.9991 +- 0.0082
2	hippo_lauder_20090121_N2O.atm	0.9988 +- 0.0114	1.0034 +- 0.0098
3	hippo_lamont_20090130_N2O.atm	0.9979 +- 0.0092	1.0035 +- 0.0067
4	learjet_lamont_20090731_N2O.atm	0.9928 +- 0.0008	1.0003 +- 0.0008
5	learjet_lamont_20090802_N2O.atm	0.9920 +- 0.0013	0.9996 +- 0.0013
6	learjet_lamont_20090803_N2O.atm	0.9915 +- 0.0012	0.9991 +- 0.0012
7	hippo_wgong_descent_20091115_N2O.atm	0.9913 +- 0.0023	0.9988 +- 0.0023
8	hippo_wgong_ascent_20091115_N2O.atm	0.9897 +- 0.0015	0.9971 +- 0.0015
	Overall	**0.9924 +- 0.0035**	**0.9998 +- 0.0029**

First value is the ratio: Prior/Measurement averaged over the profile
Second value is the standard deviation (SD) of the bias over the profile(s)
A small SD implies that the *shape* of the model profile is good.

The 2011 Priors are better:
- smaller bias
- smaller SD

In subsequent tables you will see that this is true for all gases.

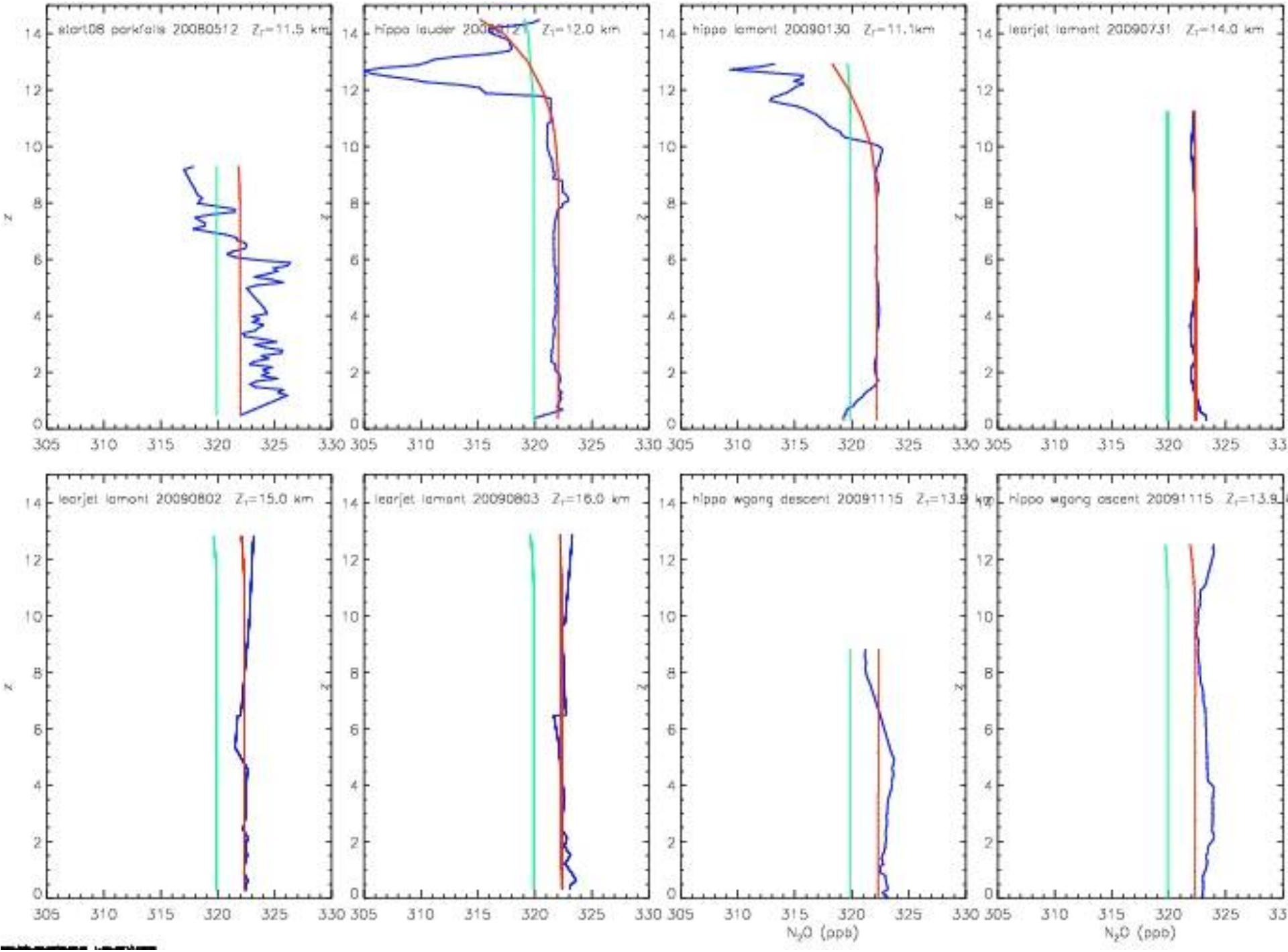
start08 parkfalls 20080512 Z_T=11.5 km
hippo lauder 20080512 Z_T=12.0 km
hippo lamont 20090130 Z_T=11.1km
learjet lamont 20090731 Z_T=14.0 km
learjet lamont 20090802 Z_T=15.0 km
learjet lamont 20090803 Z_T=16.0 km
hippo wgong descent 20091115 Z_T=13.9 km
hippo wgong ascent 20091115 Z_T=13.9
Z
N2O (ppb)

CO_2 Comparison Table (1)

#	Site/Date/Gas	2010 Priors	Dec 2011 Priors
1	beechcraft_tsukuba_20090115_CO2.atm	0.9961 +- 0.0065	0.9986 +- 0.0045
2	cobra_parkfalls_20040715_CO2.atm	1.0138 +- 0.0084	1.0001 +- 0.0078
3	cobra_parkfalls_20040814_CO2.atm	1.0235 +- 0.0059	1.0093 +- 0.0059
4	cobra_parkfalls_20040815_CO2.atm	1.0243 +- 0.0092	1.0108 +- 0.0126
5	hippo_lamont_20090130_CO2.atm	1.0002 +- 0.0038	1.0030 +- 0.0022
6	hippo_lauder_20090121_CO2.atm	1.0050 +- 0.0017	1.0006 +- 0.0014
7	hippo_wgong_ascent_20091115_CO2.atm	1.0057 +- 0.0012	1.0000 +- 0.0014
8	hippo_wgong_descent_20091115_CO2.atm	1.0069 +- 0.0021	1.0011 +- 0.0023
9	intex_parkfalls_20040712_CO2.atm	1.0098 +- 0.0035	0.9957 +- 0.0047
10	intex_parkfalls_20040715_pm_CO2.atm	1.0122 +- 0.0060	0.9989 +- 0.0065
11	intex_parkfalls_20040715_am_CO2.atm	1.0154 +- 0.0102	1.0019 +- 0.0101
12	learjet_lamont_20090731_CO2.atm	1.0127 +- 0.0043	1.0056 +- 0.0067
13	learjet_lamont_20090802_CO2.atm	1.0094 +- 0.0039	1.0021 +- 0.0059
14	learjet_lamont_20090803_CO2.atm	1.0024 +- 0.0117	0.9949 +- 0.0089
15	learjet_lamont_20100718_CO2.atm	0.9998 +- 0.0072	0.9932 +- 0.0047
16	start08_parkfalls_20080512_CO2.atm	0.9999 +- 0.0019	0.9974 +- 0.0017
17	twp-ice_darwin_20060204_CO2.atm	1.0056 +- 0.0023	1.0005 +- 0.0023
18	aircore_20071027_co2.dat.head	0.9960 +- 0.0056	0.9999 +- 0.0034
19	aircore_20090509_co2.dat.head	1.0011 +- 0.0023	0.9994 +- 0.0015
20	aircore_20101016_co2.dat.head	0.9955 +- 0.0072	0.9976 +- 0.0047
21	aircore_20110312_co2.dat.head	1.0020 +- 0.0024	1.0028 +- 0.0020

CO_2 Comparison Table (2)

22	Orleans20091002.23764secUT_co2.dat	0.9986 +- 0.0057	0.9972 +- 0.0027
23	Orleans20091002.25299secUT_co2.dat	0.9958 +- 0.0031	0.9971 +- 0.0031
24	Orleans20091002.38115secUT_co2.dat	0.9988 +- 0.0054	0.9974 +- 0.0018
25	Orleans20091002.39447secUT_co2.dat	0.9964 +- 0.0042	0.9969 +- 0.0018
26	Karlsruhe20091002.34251secUT_co2.dat	0.9948 +- 0.0043	0.9953 +- 0.0056
27	Jena20091005.28541secUT_co2.dat	0.9984 +- 0.0057	0.9986 +- 0.0029
28	Jena20091005.29303secUT_co2.dat	0.9957 +- 0.0043	0.9982 +- 0.0034
29	Jena20091009.36713secUT_co2.dat	0.9984 +- 0.0056	0.9998 +- 0.0030
30	Jena20091009.38125secUT_co2.dat	0.9983 +- 0.0063	0.9997 +- 0.0029
31	Garmisch20091005.31598secUT_co2.dat	0.9988 +- 0.0058	0.9990 +- 0.0009
32	Bremen20091009.39920secUT_co2.dat	0.9990 +- 0.0068	1.0003 +- 0.0043
33	Bremen20091005.42336secUT_co2.dat	0.9988 +- 0.0060	0.9985 +- 0.0025
34	Bialystok20090930.34740secUT_co2.dat	1.0032 +- 0.0050	1.0001 +- 0.0032
35	Bialystok20090930.36217secUT_co2.dat	1.0027 +- 0.0046	1.0003 +- 0.0024
36	Bialystok20090930.49693secUT_co2.dat	1.0015 +- 0.0047	1.0005 +- 0.0036
37	Bialystok20090930.50975secUT_co2.dat	1.0020 +- 0.0043	0.9993 +- 0.0048
38	Descent_OMS19980518_co2.dat	1.0047 +- 0.0067	0.9983 +- 0.0062
39	Descent_OMS19971120_co2.dat	1.0050 +- 0.0016	0.9987 +- 0.0017
40	Descent_OMS19971111_co2.dat	1.0051 +- 0.0021	0.9986 +- 0.0020
41	Descent_OMS19970630_co2.dat	1.0086 +- 0.0027	1.0019 +- 0.0025
42	Descent_OMS19970214_co2.dat	1.0043 +- 0.0019	0.9971 +- 0.0017
43	Descent_OMS19960921_co2.dat	1.0098 +- 0.0017	0.9980 +- 0.0024
44	Ascent_OMS19980518_co2.dat	1.0061 +- 0.0039	0.9994 +- 0.0038
45	Ascent_OMS19971120_co2.dat	1.0060 +- 0.0016	0.9993 +- 0.0015
46	Ascent_OMS19970630_co2.dat	1.0097 +- 0.0021	1.0039 +- 0.0019
47	Ascent_OMS19970214_co2.dat	1.0048 +- 0.0015	0.9980 +- 0.0013
48	Ascent_OMS19960921_co2.dat	1.0096 +- 0.0022	1.0030 +- 0.0045
	Overall	**1.0042 +- 0.0074**	**1.0003 +- 0.0052**

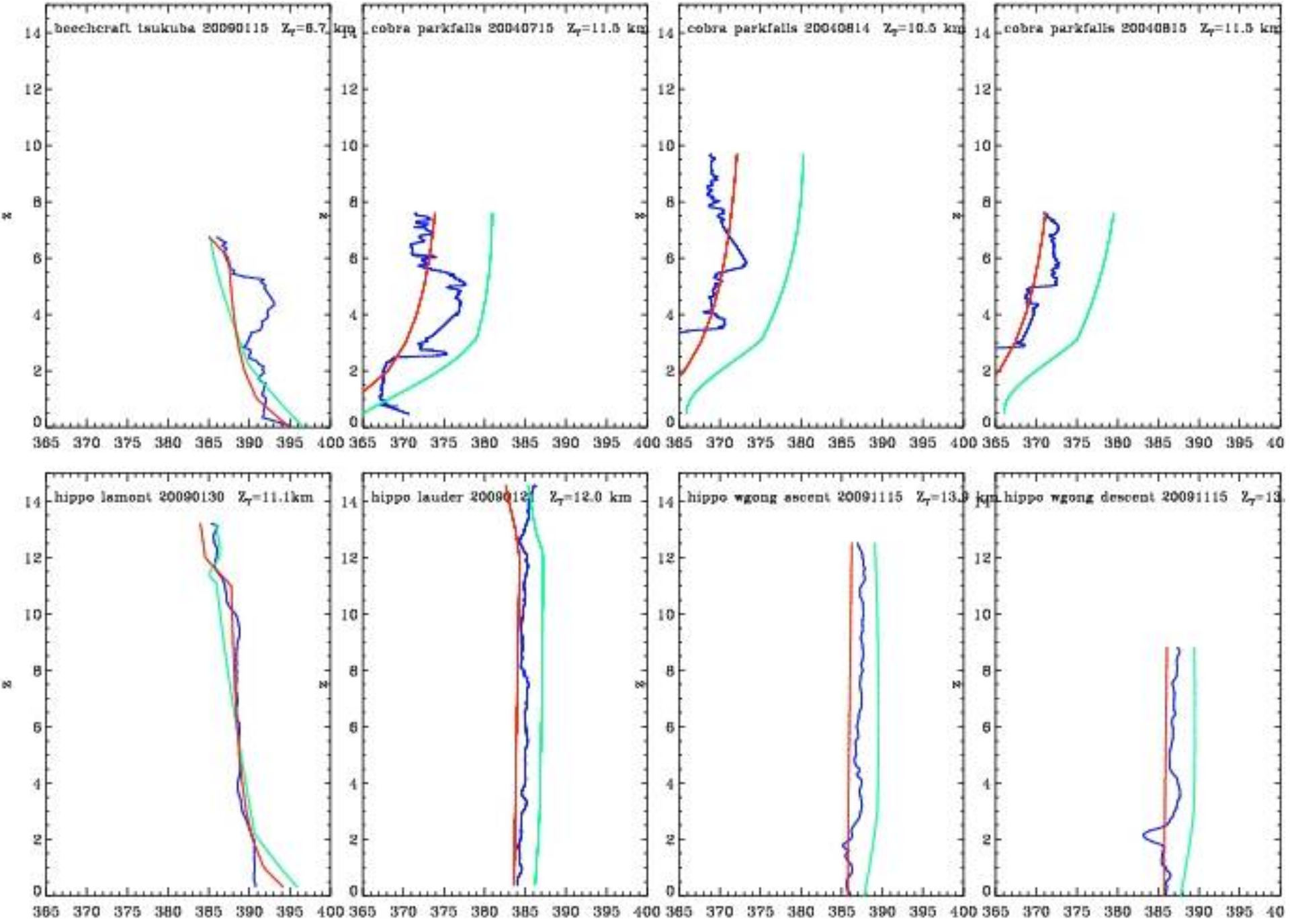
beechcraft tsukuba 20090115 Z_T=6.7 km
cobra parkfalls 20040715 Z_T=11.5 km
cobra parkfalls 20040814 Z_T=10.5 km
cobra parkfalls 20040815 Z_T=11.5 km
hippo lamont 20090130 Z_T=11.1km
hippo lauder 20090123 Z_T=12.0 km
hippo wgong ascent 20091115 Z_T=13.0 km
hippo wgong descent 20091115 Z_T=13.
z
0 2 4 6 8 10 12 14
365 370 375 380 385 390 395 400

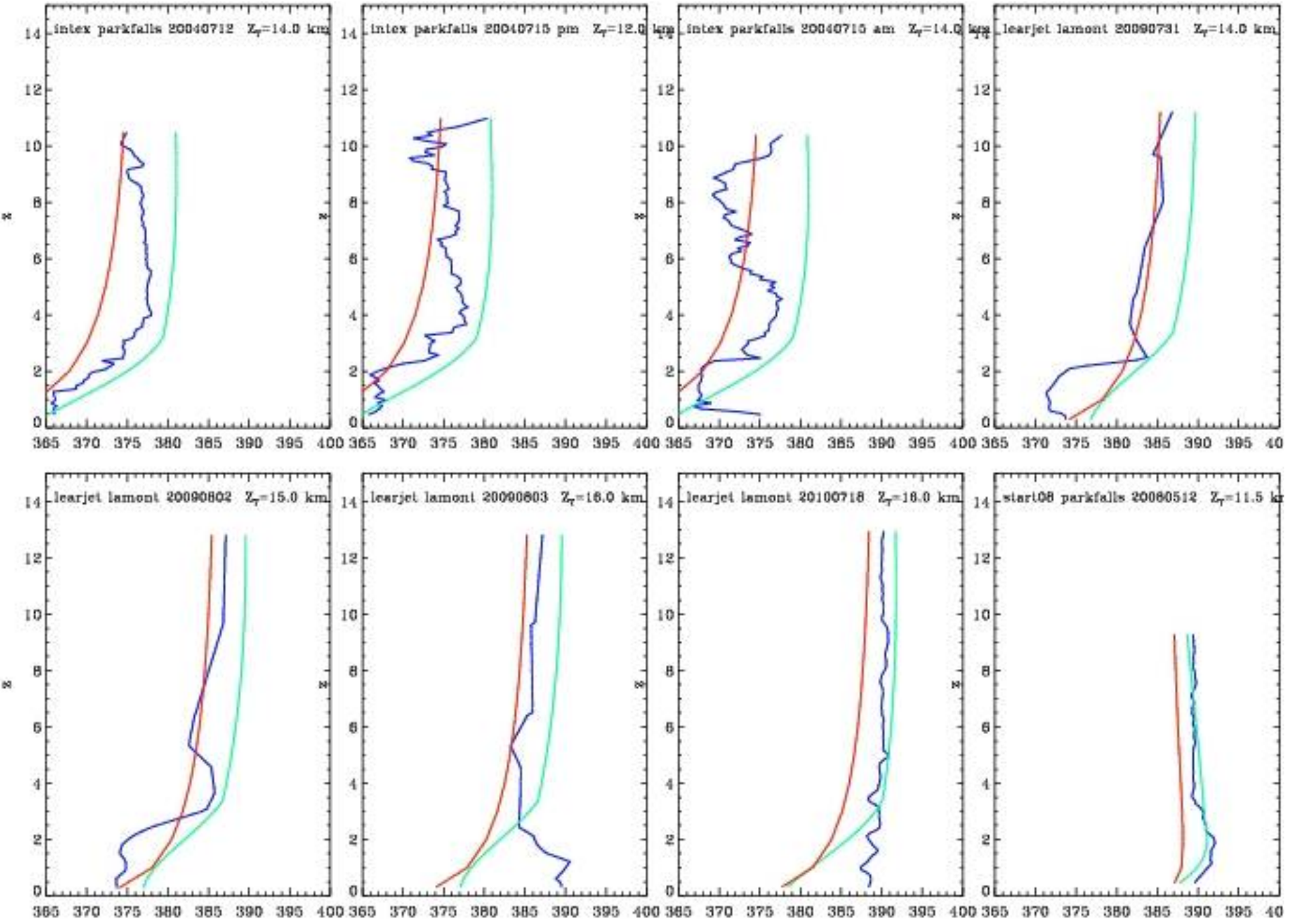
intex parkfalls 20040712 Z_T=14.0 km
intex parkfalls 20040715 pm Z_T=12.0 km
intex parkfalls 20040715 am Z_T=14.0 km
learjet lamont 20090731 Z_T=14.0 km
learjet lamont 20090802 Z_T=15.0 km
learjet lamont 20090803 Z_T=16.0 km
learjet lamont 20100718 Z_T=16.0 km
start08 parkfalls 20080512 Z_T=11.5 km
z
0 2 4 6 8 10 12 14
365 370 375 380 385 390 395 400

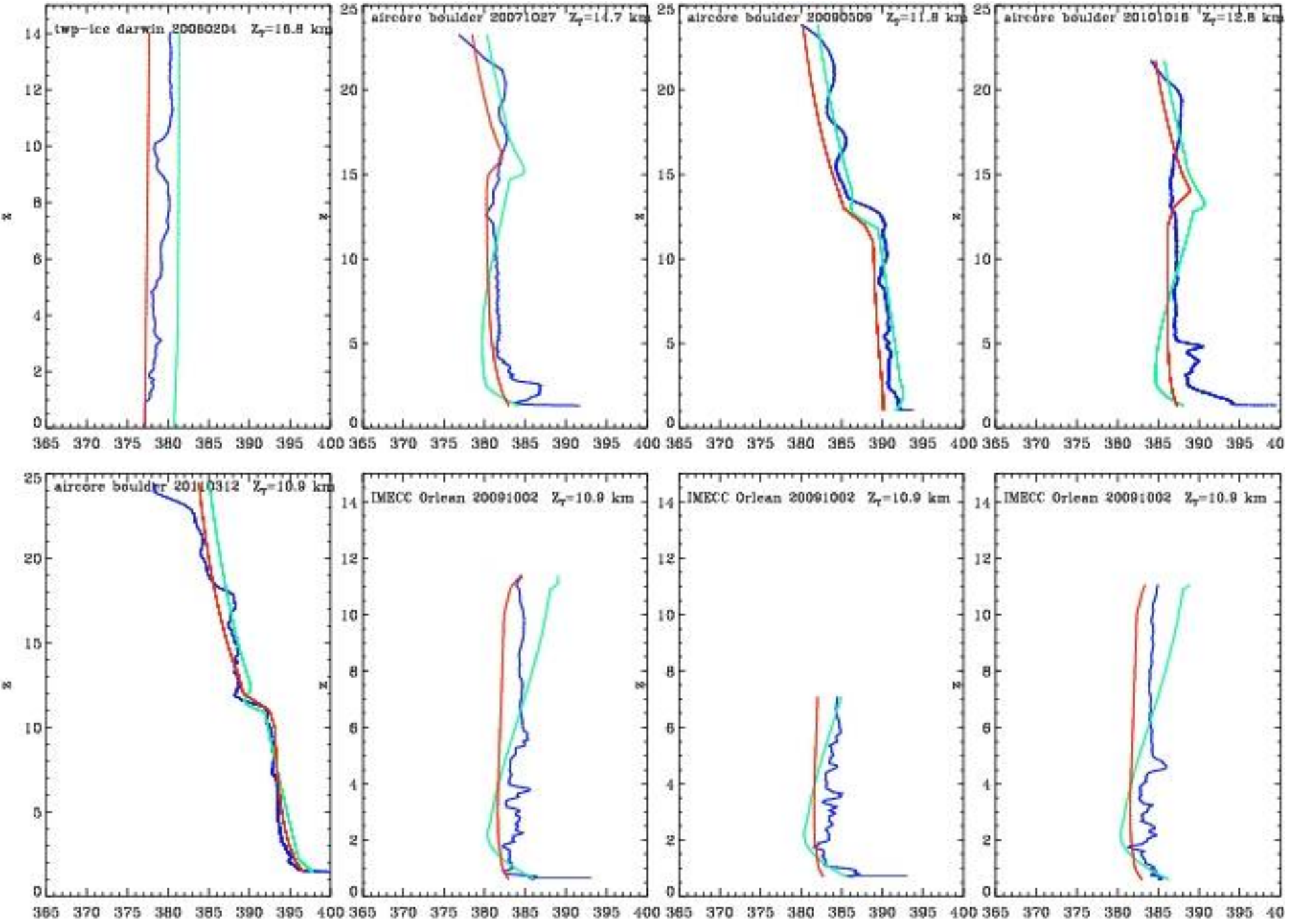
twp-ice darwin 20080204 Z_T=16.8 km
aircore boulder 20071027 Z_T=14.7 km
aircore boulder 20090509 Z_T=11.8 km
aircore boulder 20101016 Z_T=12.8 km
aircore boulder 20110312 Z_T=10.9 km
IMECC Orlean 20091002 Z_T=10.9 km
IMECC Orlean 20091002 Z_T=10.9 km
IMECC Orlean 20091002 Z_T=10.9 km
z
365 370 375 380 385 390 395 400

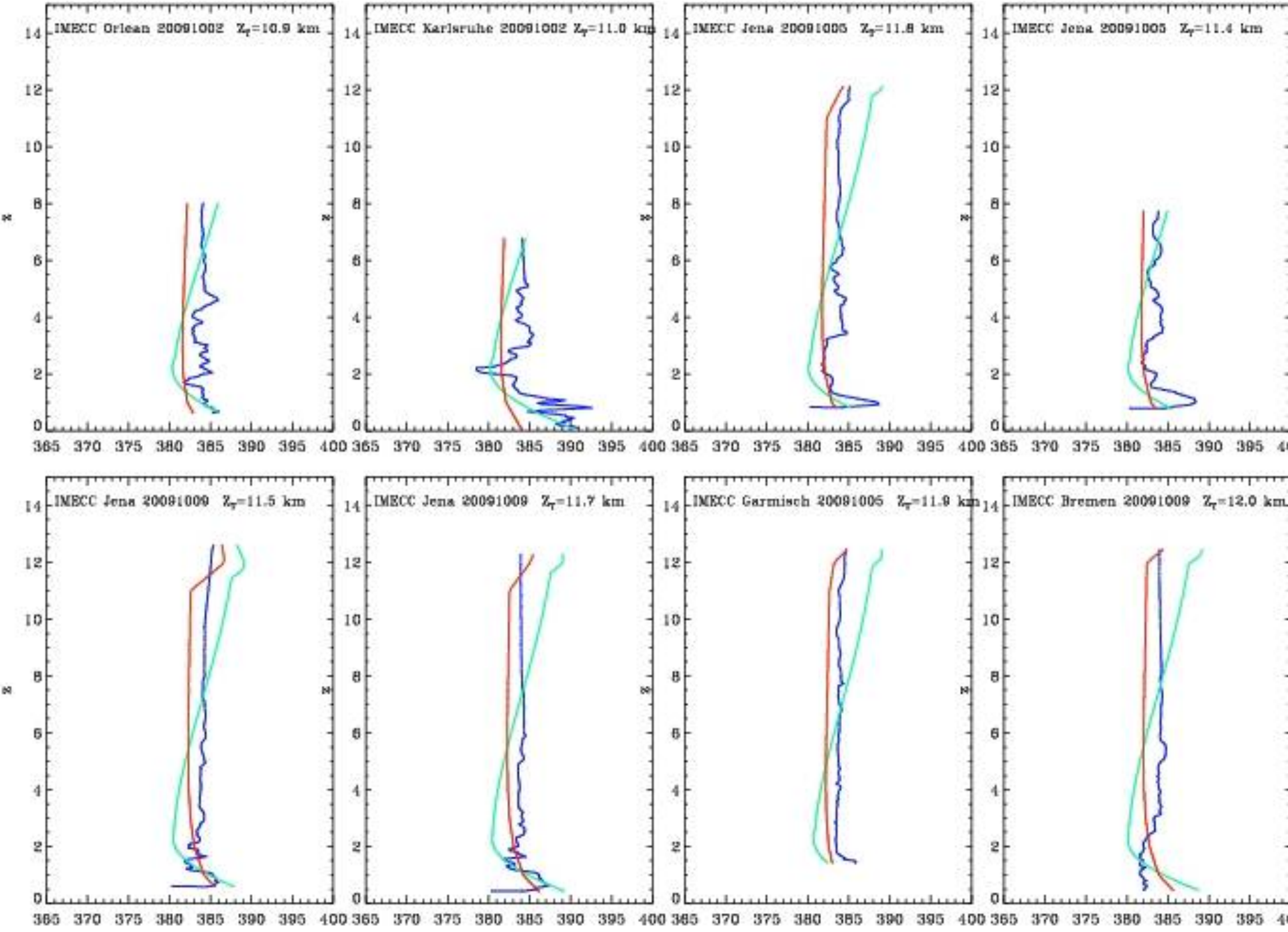
IMECC Orleans 20091002 Z_T=10.9 km
IMECC Karlsruhe 20091002 Z_T=11.0 km
IMECC Jena 20091005 Z_T=11.8 km
IMECC Jena 20091005 Z_T=11.4 km
IMECC Jena 20091009 Z_T=11.5 km
IMECC Jena 20091009 Z_T=11.7 km
IMECC Garmisch 20091005 Z_T=11.9 km
IMECC Bremen 20091009 Z_T=12.0 km
z
0 2 4 6 8 10 12 14
365 370 375 380 385 390 395 400

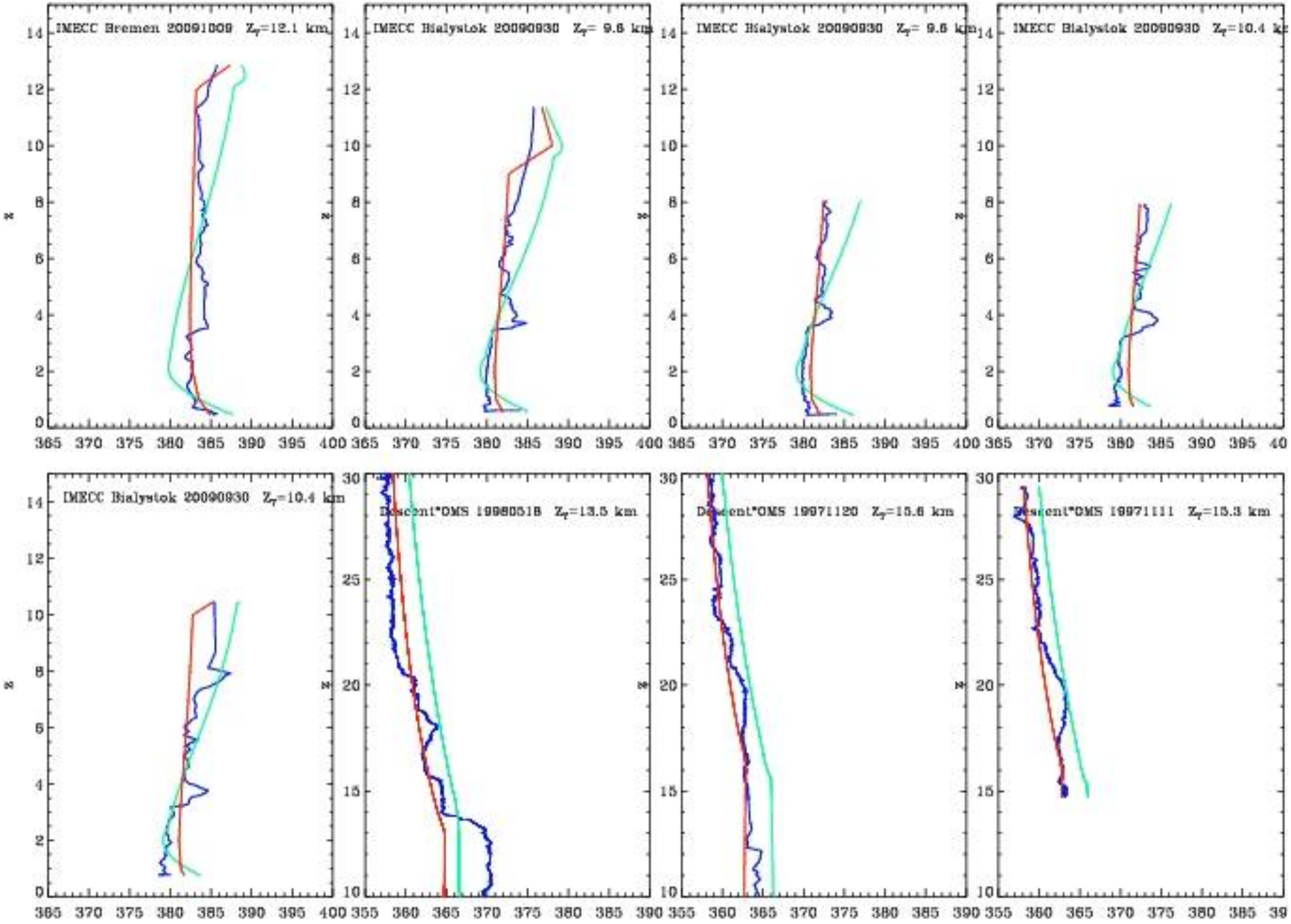
IMECC Bremen 20091009 Z_T=12.1 km
IMECC Bialystok 20090930 Z_T= 9.6 km
IMECC Bialystok 20090930 Z_T= 9.6 km
IMECC Bialystok 20090930 Z_T=10.4 km
IMECC Bialystok 20090930 Z_T=10.4 km
Descent*OMS 19980518 Z_T=13.5 km
Descent*OMS 19971120 Z_T=15.6 km
Descent*OMS 19971111 Z_T=15.3 km
z

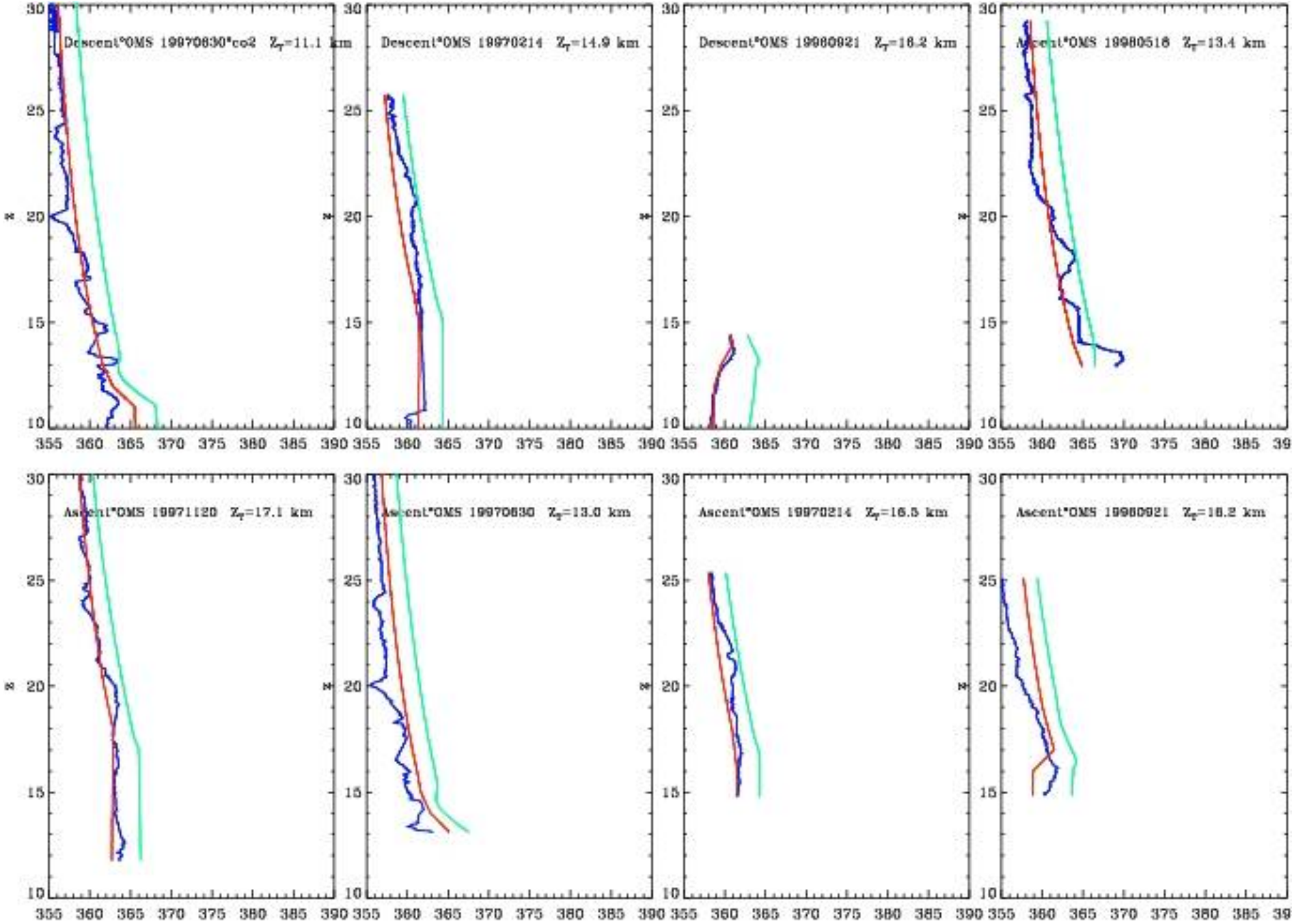
Descent*OMS 19970630*co2 Z_T=11.1 km
Descent*OMS 19970214 Z_T=14.9 km
Descent*OMS 19980921 Z_T=16.2 km
Ascent*OMS 19980516 Z_T=13.4 km
Ascent*OMS 19971120 Z_T=17.1 km
Ascent*OMS 19970630 Z_T=13.0 km
Ascent*OMS 19970214 Z_T=16.5 km
Ascent*OMS 19980921 Z_T=16.2 km
z
355 360 365 370 375 380 385 390
10 15 20 25 30

CH_4 Comparison Table

1	intex_parkfalls_20040712_CH4.atm	1.0310 +- 0.0102	1.0141 +- 0.0078
2	start08_parkfalls_20080512_CH4.atm	0.9987 +- 0.0063	0.9960 +- 0.0062
3	beechcraft_tsukuba_20090115_CH4.atm	0.9856 +- 0.0083	0.9828 +- 0.0068
4	hippo_lauder_20090121_CH4.atm	1.0584 +- 0.0078	1.0045 +- 0.0089
5	hippo_lamont_20090130_CH4.atm	1.0037 +- 0.0179	1.0004 +- 0.0131
6	learjet_lamont_20090731_CH4.atm	1.0037 +- 0.0111	1.0060 +- 0.0063
7	learjet_lamont_20090802_CH4.atm	1.0082 +- 0.0109	1.0105 +- 0.0085
8	learjet_lamont_20090803_CH4.atm	1.0083 +- 0.0073	1.0111 +- 0.0072
9	hippo_wgong_descent_20091115_CH4.atm	1.0423 +- 0.0050	0.9876 +- 0.0036
10	hippo_wgong_ascent_20091115_CH4.atm	1.0405 +- 0.0060	0.9891 +- 0.0051
11	aircore_20071027_ch4.dat.head	1.0033 +- 0.0214	0.9991 +- 0.0175
12	aircore_20090509_ch4.dat.head	1.0015 +- 0.0254	0.9957 +- 0.0286
13	aircore_20101016_ch4.dat.head	0.9966 +- 0.0129	0.9991 +- 0.0183
14	aircore_20110312_ch4.dat.head	1.0087 +- 0.0213	1.0065 +- 0.0119
15	Orleans20091002.23764secUT_ch4.dat	0.9984 +- 0.0072	1.0013 +- 0.0043
16	Orleans20091002.25299secUT_ch4.dat	0.9963 +- 0.0064	1.0011 +- 0.0037
17	Orleans20091002.38115secUT_ch4.dat	1.0001 +- 0.0083	1.0032 +- 0.0037
18	Orleans20091002.39447secUT_ch4.dat	0.9977 +- 0.0092	1.0020 +- 0.0045
19	Karlsruhe20091002.34251secUT_ch4.dat	0.9932 +- 0.0140	0.9994 +- 0.0083
20	Jena20091005.28541secUT_ch4.dat	1.0017 +- 0.0105	1.0048 +- 0.0057
21	Jena20091005.29303secUT_ch4.dat	0.9980 +- 0.0104	1.0027 +- 0.0062
22	Jena20091009.36713secUT_ch4.dat	0.9991 +- 0.0090	1.0022 +- 0.0064
23	Jena20091009.38125secUT_ch4.dat	0.9977 +- 0.0088	1.0014 +- 0.0064
24	Garmisch20091005.31598secUT_ch4.dat	1.0092 +- 0.0041	1.0111 +- 0.0038
25	Bremen20091009.39920secUT_ch4.dat	0.9961 +- 0.0090	1.0000 +- 0.0051
26	Bremen20091005.42336secUT_ch4.dat	0.9995 +- 0.0131	1.0033 +- 0.0075
27	Bialystok20090930.34740secUT_ch4.dat	0.9927 +- 0.0166	0.9944 +- 0.0121
28	Bialystok20090930.36217secUT_ch4.dat	0.9861 +- 0.0081	0.9899 +- 0.0044
29	Bialystok20090930.49693secUT_ch4.dat	0.9868 +- 0.0068	0.9908 +- 0.0041
30	Bialystok20090930.50975secUT_ch4.dat	0.9875 +- 0.0076	0.9903 +- 0.0046
	Overall	**1.0041 +- 0.0212**	**1.0017 +- 0.0181**

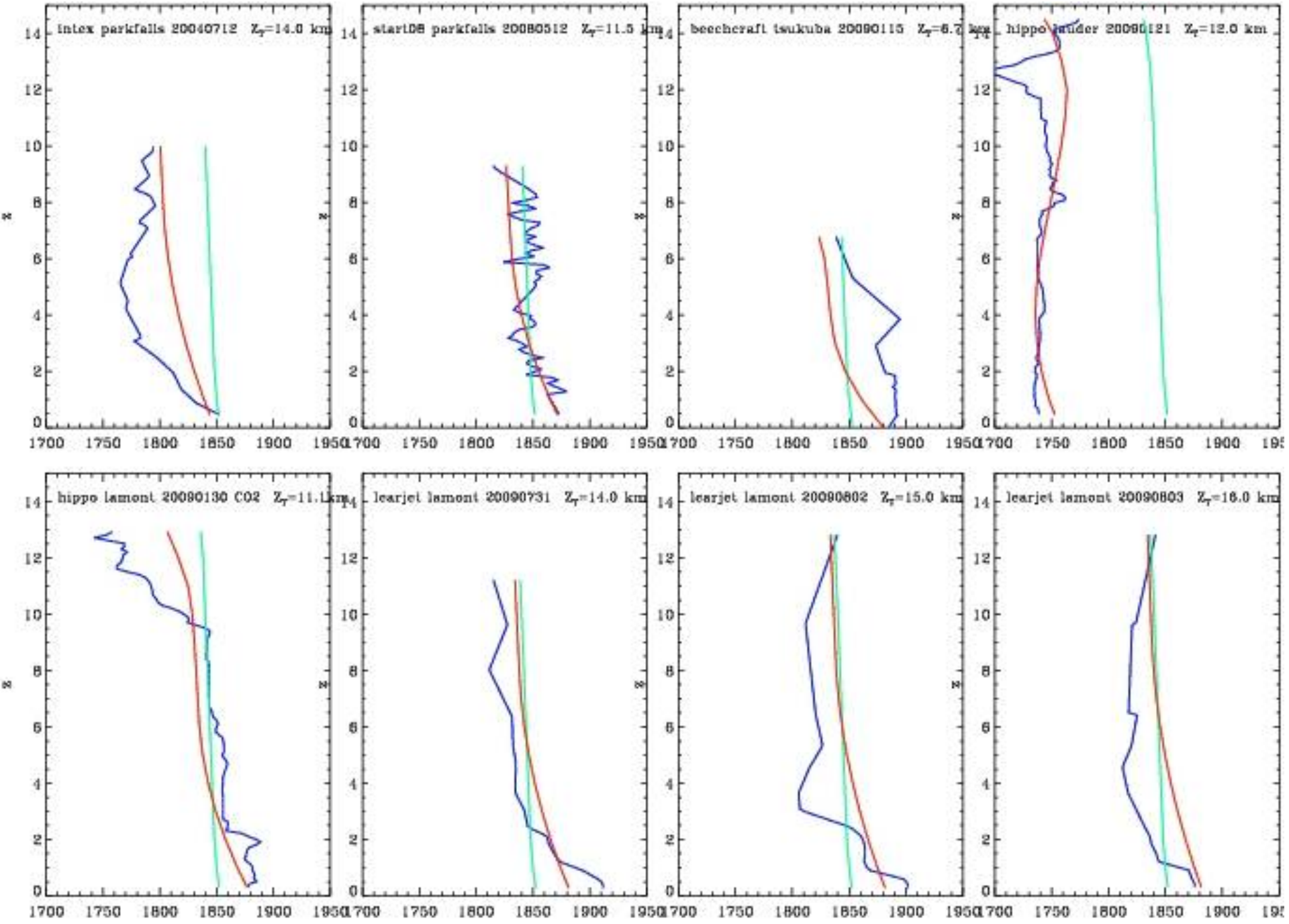
intex parkfalls 20040712 Z_T=14.0 km
start08 parkfalls 20080512 Z_T=11.5 km
beechcraft tsukuba 20090115 Z_T=6.7 km
hippo lauder 20090121 Z_T=12.0 km
hippo lamont 20090130 CO2 Z_T=11.1km
learjet lamont 20090731 Z_T=14.0 km
learjet lamont 20090802 Z_T=15.0 km
learjet lamont 20090803 Z_T=16.0 km
z
0 2 4 6 8 10 12 14
1700 1750 1800 1850 1900 1950

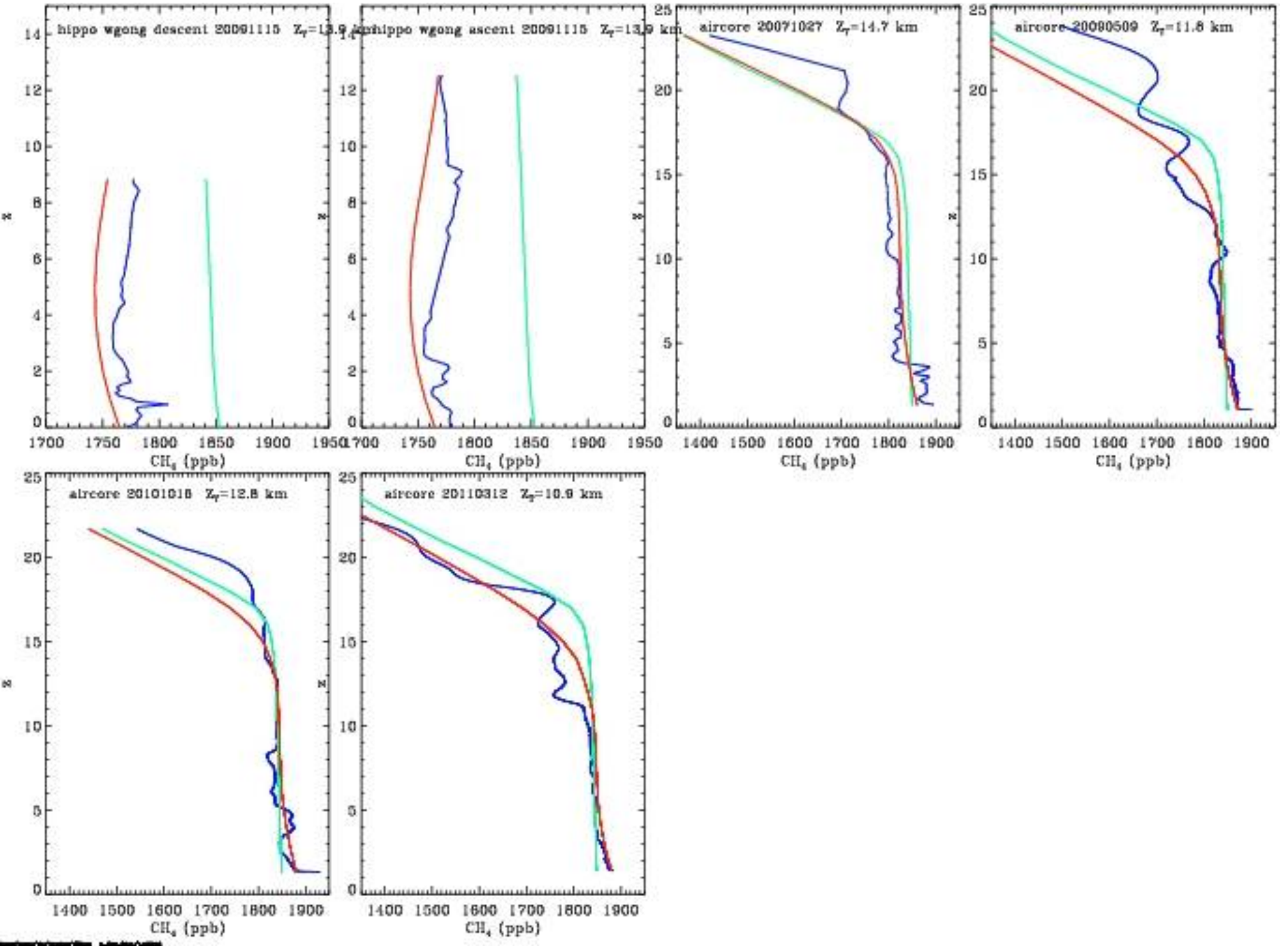
hippo wgong descent 20091115 Z_T=13.9 km
hippo wgong ascent 20091115 Z_T=13.9 km
aircore 20071027 Z_T=14.7 km
aircore 20080509 Z_T=11.8 km
aircore 20101016 Z_T=12.8 km
aircore 20110312 Z_T=10.9 km
z
CH4 (ppb)

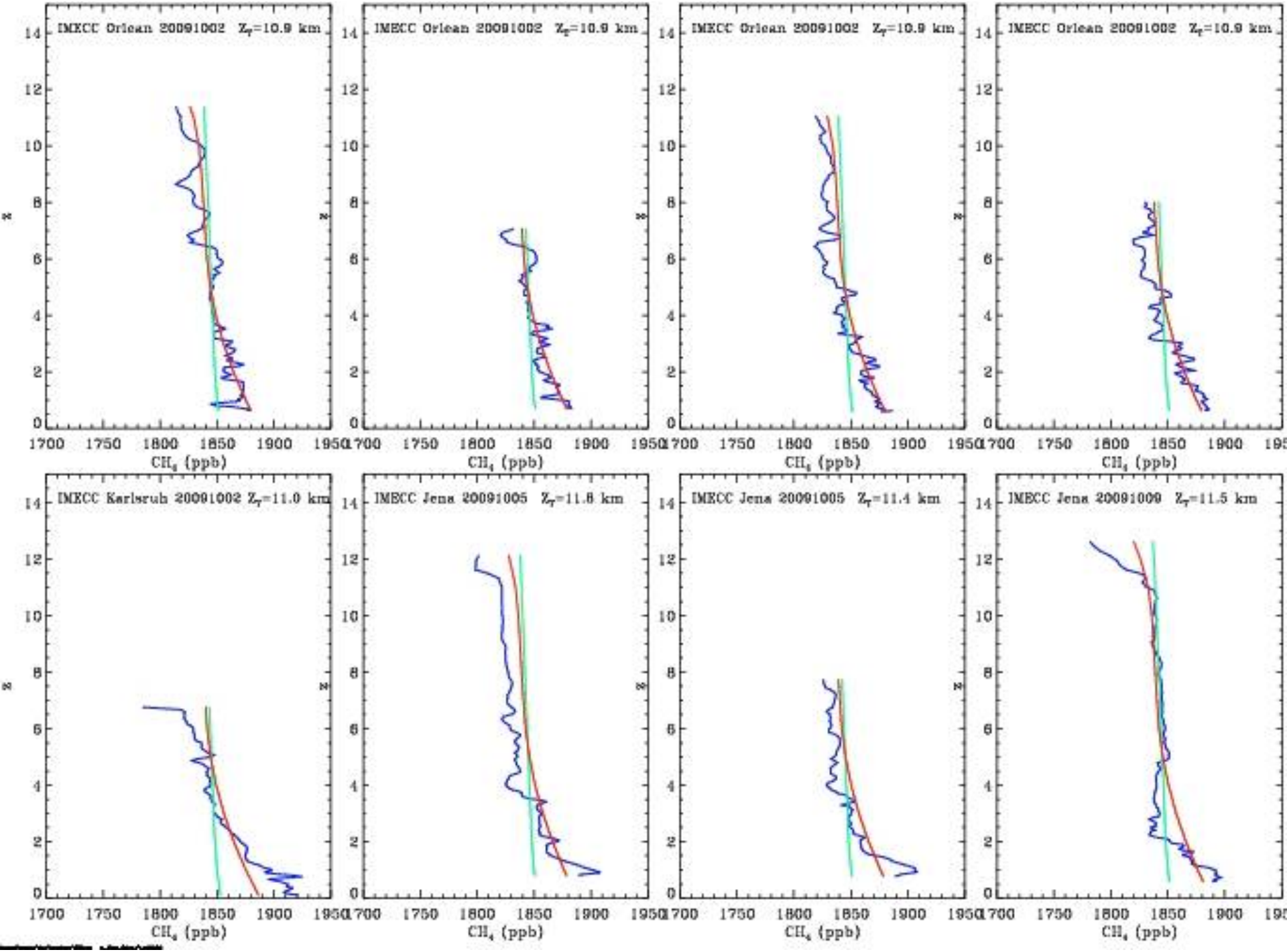
IMECC Orleans 20091002 Z_T=10.9 km
IMECC Orleans 20091002 Z_T=10.9 km
IMECC Orleans 20091002 Z_T=10.9 km
IMECC Orleans 20091002 Z_T=10.9 km
IMECC Karlsruhe 20091002 Z_T=11.0 km
IMECC Jena 20091005 Z_T=11.8 km
IMECC Jena 20091005 Z_T=11.4 km
IMECC Jena 20091009 Z_T=11.5 km
z
CH_4 (ppb)
0
2
4
6
8
10
12
14
1700
1750
1800
1850
1900
1950

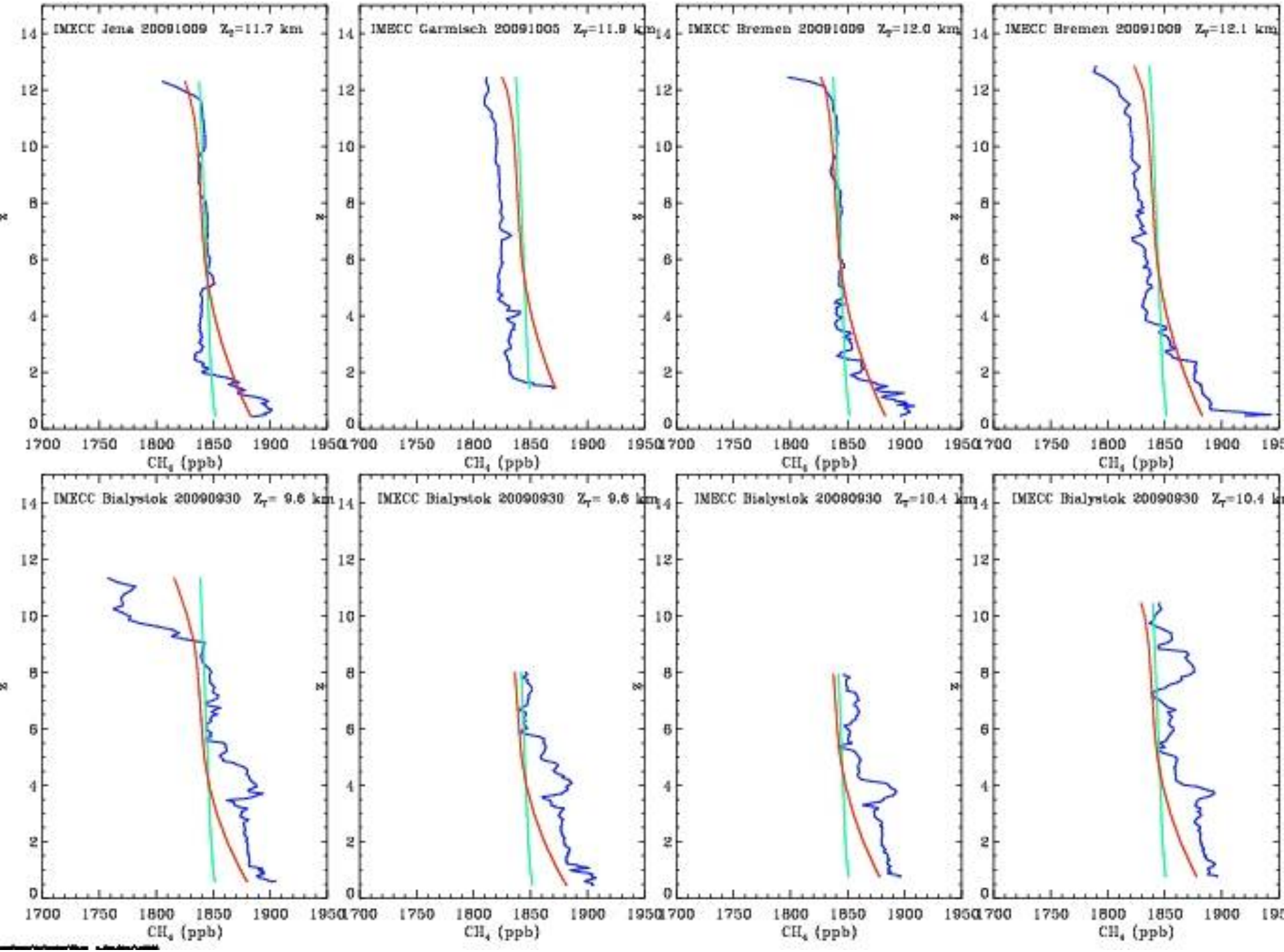
IMECC Jena 20091009 Z_T=11.7 km
IMECC Garmisch 20091005 Z_T=11.9 km
IMECC Bremen 20091009 Z_T=12.0 km
IMECC Bremen 20091009 Z_T=12.1 km
IMECC Bialystok 20090930 Z_T= 9.6 km
IMECC Bialystok 20090930 Z_T= 9.6 km
IMECC Bialystok 20090930 Z_T=10.4 km
IMECC Bialystok 20090930 Z_T=10.4 km
z
CH4 (ppb)
0
2
4
6
8
10
12
14
1700
1750
1800
1850
1900
1950

CO Comparison Table

#	Site/Date/Gas	2010 Priors	2011 Priors
1	cobra_parkfalls_20040715_CO.atm	0.9667 +- 0.2377	0.8256 +- 0.2163
2	cobra_parkfalls_20040815_CO.atm	1.0837 +- 0.1826	0.8747 +- 0.1492
3	start08_parkfalls_20080512_CO.atm	0.7958 +- 0.0343	0.8324 +- 0.0434
4	hippo_lauder_20090121_CO.atm	1.8953 +- 0.4165	1.0374 +- 0.1940
5	hippo_lamont_20090130_CO.atm	1.0396 +- 0.3116	1.0847 +- 0.1286
6	learjet_lamont_20090731_CO.atm	1.0107 +- 0.1284	0.8391 +- 0.1142
7	learjet_lamont_20090802_CO.atm	1.1385 +- 0.1825	0.9627 +- 0.1424
8	learjet_lamont_20090803_CO.atm	1.1611 +- 0.1818	0.9923 +- 0.1112
9	hippo_wgong_descent_20091115_CO.atm	1.3538 +- 0.1474	0.9344 +- 0.0847
10	hippo_wgong_ascent_20091115_CO.atm	1.1973 +- 0.2157	0.8562 +- 0.1098
11	Orleans20091002.23764secUT_co.dat	1.3150 +- 0.1028	1.0591 +- 0.1351
12	Orleans20091002.25299secUT_co.dat	1.2780 +- 0.0680	1.0732 +- 0.0425
13	Orleans20091002.38115secUT_co.dat	1.2278 +- 0.0821	0.9948 +- 0.1229
14	Orleans20091002.39447secUT_co.dat	1.1975 +- 0.0666	1.0011 +- 0.0602
15	Karlsruhe20091002.34251secUT_co.dat	1.1400 +- 0.1189	0.9582 +- 0.1147
16	Jena20091005.28541secUT_co.dat	1.2807 +- 0.1534	1.0617 +- 0.1583
17	Jena20091005.29303secUT_co.dat	1.2747 +- 0.1272	1.0860 +- 0.1184
18	Jena20091009.36713secUT_co.dat	1.2071 +- 0.1138	0.9999 +- 0.1467
19	Jena20091009.38125secUT_co.dat	1.1948 +- 0.1052	1.0020 +- 0.1445
20	Garmisch20091005.31598secUT_co.dat	1.4389 +- 0.0968	1.1962 +- 0.1597
21	Bremen20091009.39920secUT_co.dat	1.1763 +- 0.0948	0.9938 +- 0.1315
22	Bremen20091005.42336secUT_co.dat	1.2792 +- 0.1116	1.0614 +- 0.1253
23	Bialystok20090930.34740secUT_co.dat	1.2392 +- 0.2858	0.9233 +- 0.1250
24	Bialystok20090930.36217secUT_co.dat	1.1510 +- 0.1020	0.9364 +- 0.1036
25	Bialystok20090930.49693secUT_co.dat	1.1397 +- 0.1049	0.9408 +- 0.0852
26	Bialystok20090930.50975secUT_co.dat	1.1083 +- 0.0945	0.8854 +- 0.1269
	Overall	**1.4083 +- 0.4323**	**1.0007 +- 0.1688**

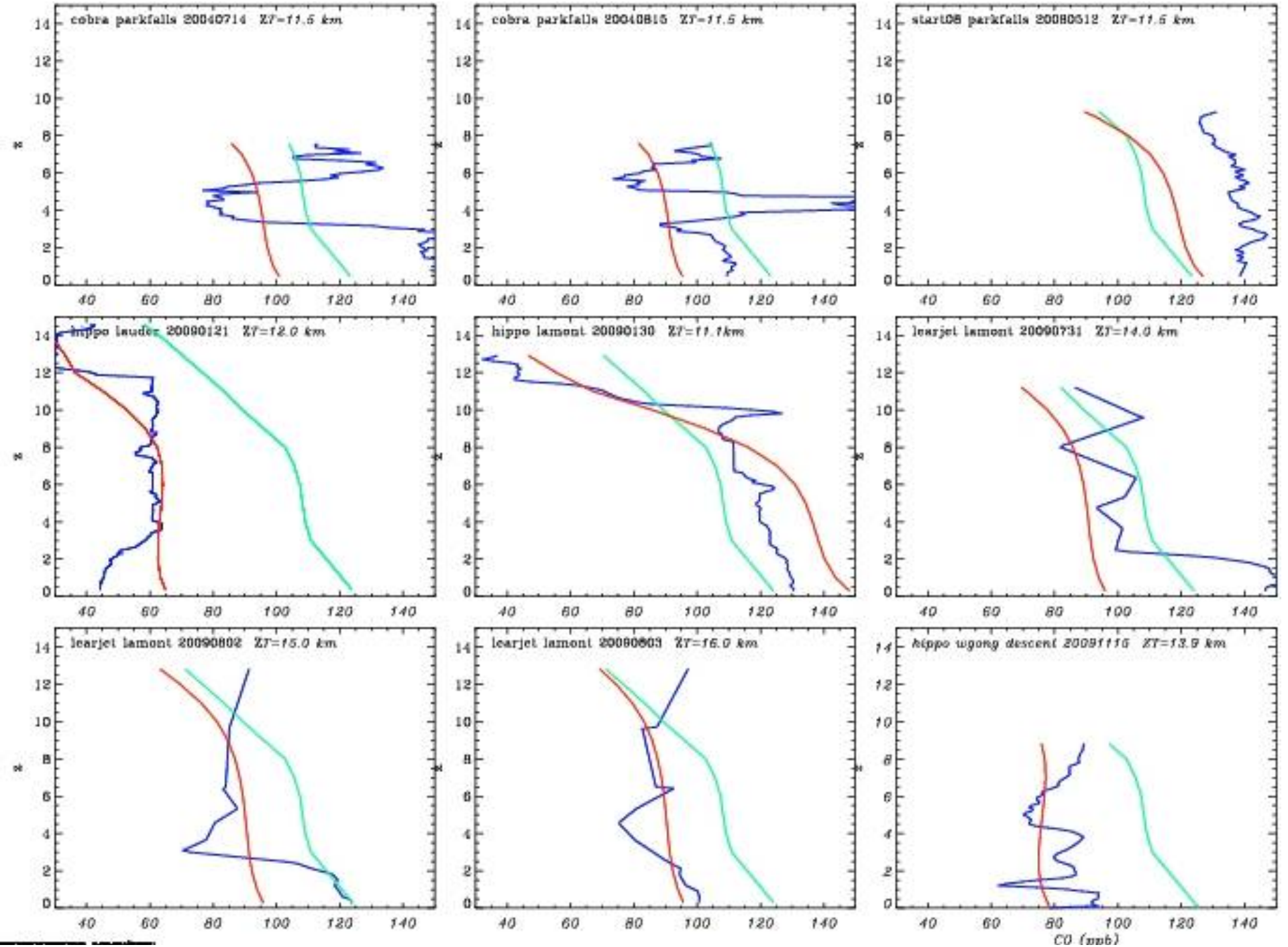
cobra parkfalls 20040714 ZT=11.5 km
cobra parkfalls 20040815 ZT=11.5 km
start08 parkfalls 20080512 ZT=11.5 km
hippo lauder 20090121 ZT=12.0 km
hippo lamont 20090130 ZT=11.1km
learjet lamont 20090731 ZT=14.0 km
learjet lamont 20090802 ZT=15.0 km
learjet lamont 20090803 ZT=16.0 km
hippo wgong descent 20091116 ZT=13.9 km
z
CO (ppb)

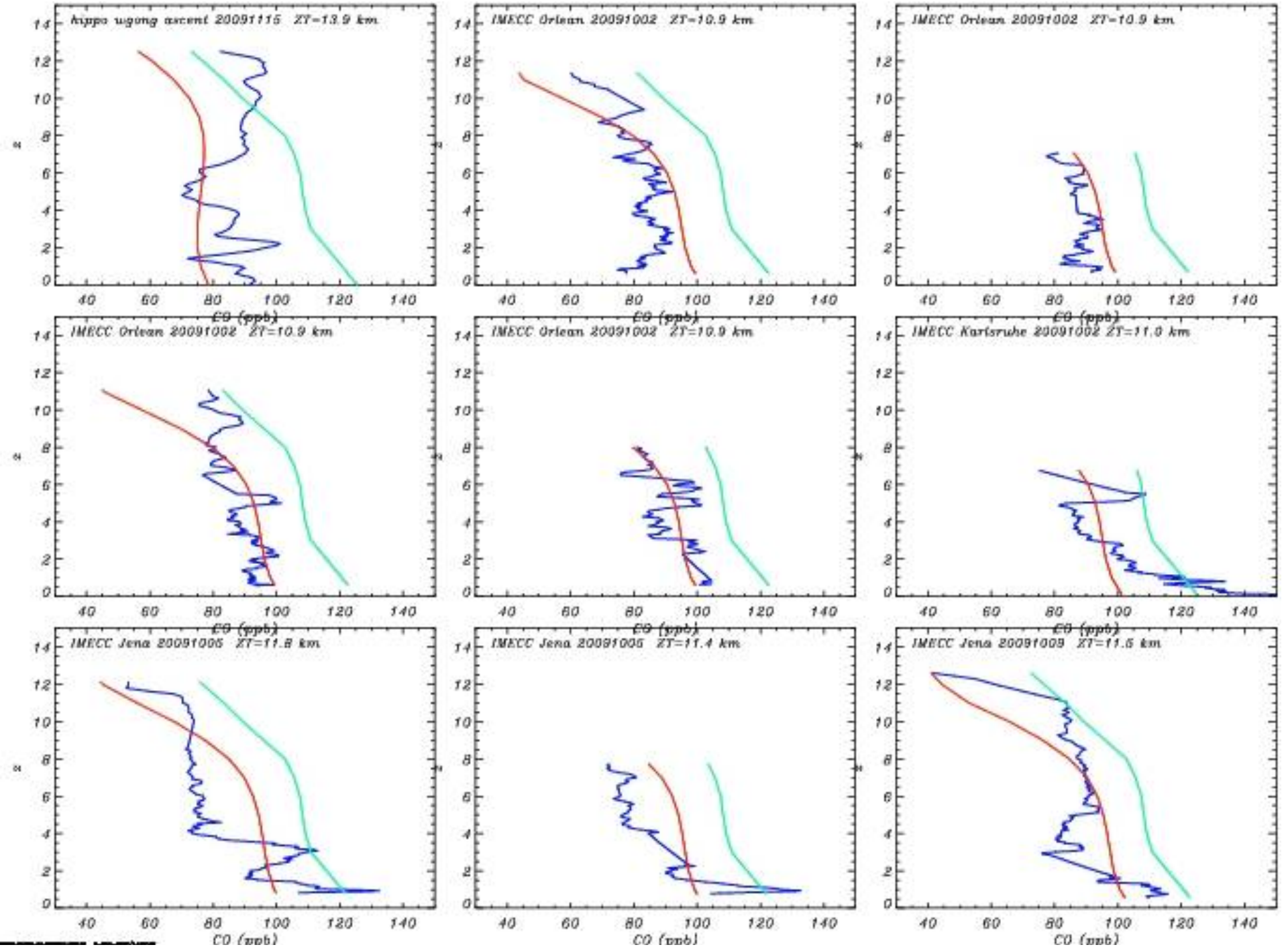
hippo wgong ascent 20091115 ZT=13.9 km
IMECC Orleans 20091002 ZT=10.9 km
IMECC Orleans 20091002 ZT=10.9 km
IMECC Orleans 20091002 ZT=10.9 km
IMECC Orleans 20091002 ZT=10.9 km
IMECC Karlsruhe 20091002 ZT=11.0 km
IMECC Jena 20091006 ZT=11.8 km
IMECC Jena 20091006 ZT=11.4 km
IMECC Jena 20091009 ZT=11.5 km
CO (ppb)
z

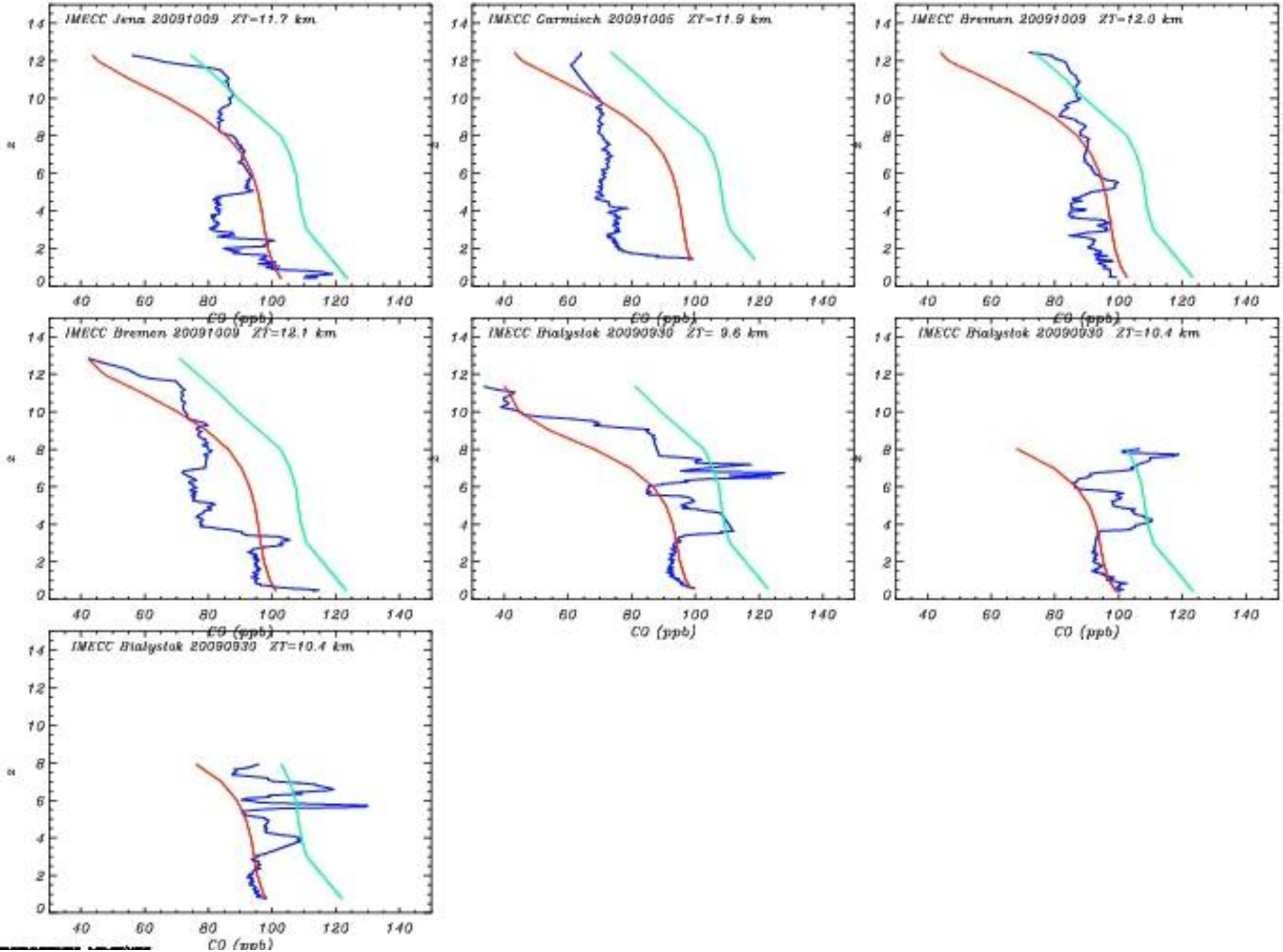
IMECC Jena 20091009 ZT=11.7 km
IMECC Garmisch 20091005 ZT=11.9 km
IMECC Bremen 20091009 ZT=12.0 km
IMECC Bremen 20091009 ZT=12.1 km
IMECC Bialystok 20090930 ZT= 9.6 km
IMECC Bialystok 20090930 ZT=10.4 km
IMECC Bialystok 20090930 ZT=10.4 km
CO (ppb)

Comparison with MkIV and ACE VMR profiles

Red Line is latest A priori (2011-10-31)

Plots made with the script: mkiv_ace.log

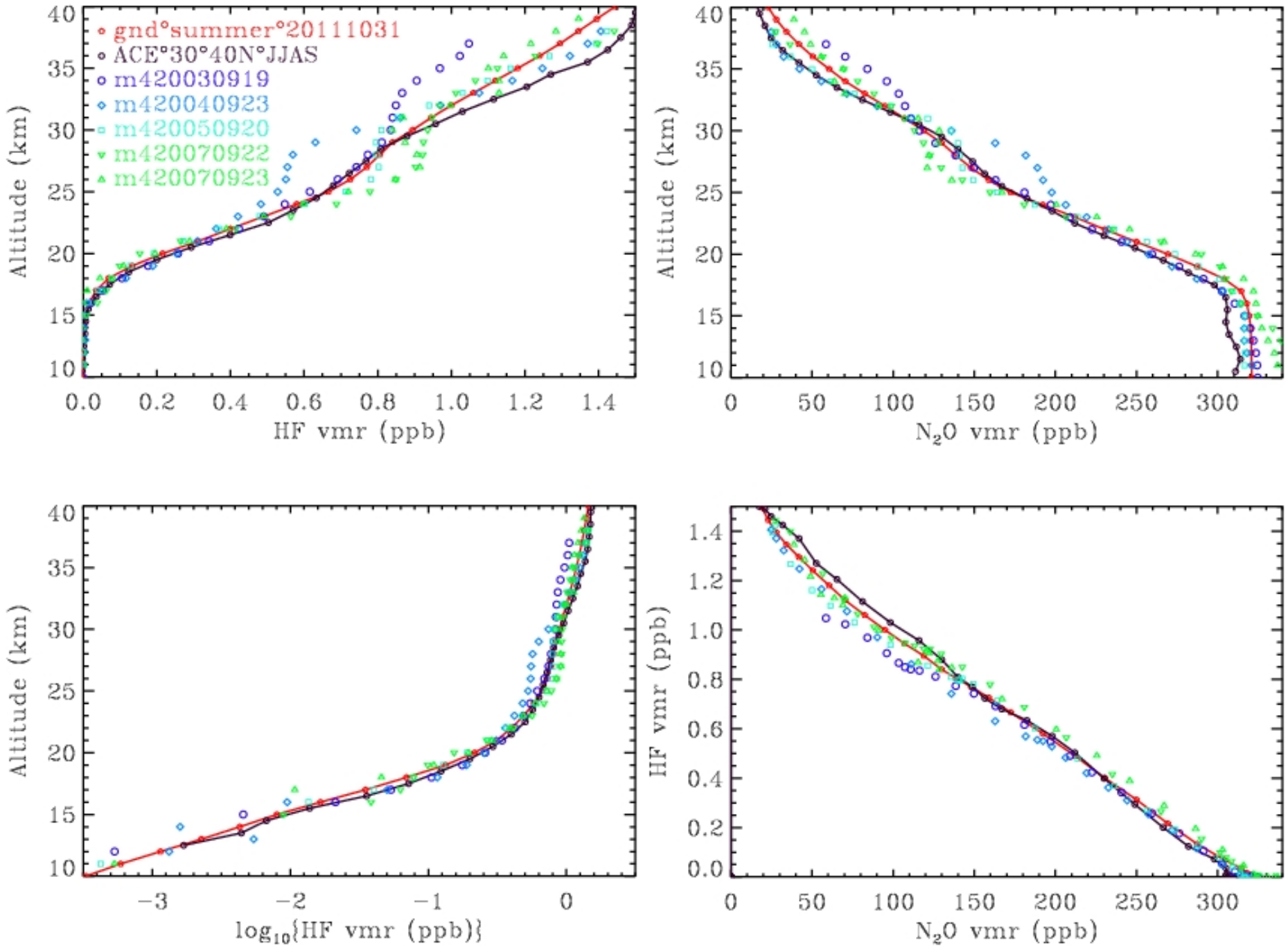
gnd°summer°20111031
ACE°30°40N°JJAS
m420030919
m420040923
m420050920
m420070922
m420070923
Altitude (km)
HF vmr (ppb)
N2O vmr (ppb)
log10{HF vmr (ppb)}
HF vmr (ppb)

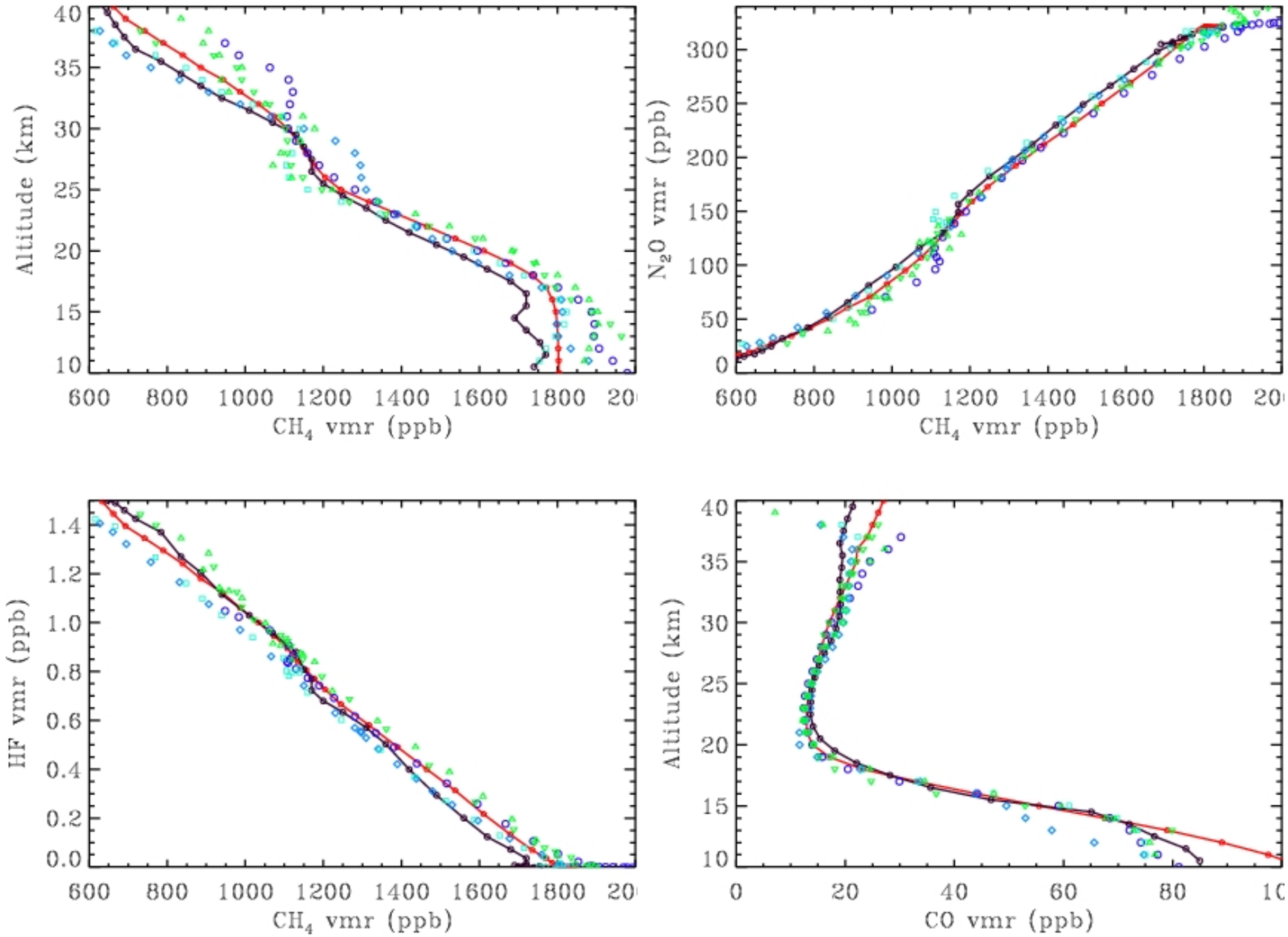
Altitude (km)
CH4 vmr (ppb)
N2O vmr (ppb)
CH4 vmr (ppb)
HF vmr (ppb)
CH4 vmr (ppb)
Altitude (km)
CO vmr (ppb)

Summary

2011 a priori profiles agree better with validation measurements than 2009 priors

To achieve this, tropopause altitude assignment for gnd_summer.vmr set was reduced from 16 to 15 km

Also, interhemispheric differences were introduced for CO, CH_4, and CO.